Strength and Fresh Properties of Cemented Paste Backfill with a Low-Carbon Binder

Soya Bathily

A thesis submitted to the University of Ottawa in partial
fulfillment of the requirements for the
degree of Master of Applied Science
In Civil Engineering

Under the supervision of
Dr. Mamadou Fall

Department of Civil Engineering
Faculty of Engineering
University of Ottawa

ABSTRACT

Cemented paste backfill (CPB) is widely used in underground mining to provide ground support and enable the safe disposal of tailings. Ordinary Portland cement (OPC), commonly employed as the binder in CPB, is associated with high energy consumption and significant CO_2 emissions, motivating the development of low-carbon alternative binders. Among these, alkali-activated slag (AAS) systems have shown strong potential; however, their application in CPB remains limited, particularly with respect to the coupled evolution of fresh properties, strength development, and hydration mechanisms.

This thesis investigates the performance of CPB incorporating ground granulated blast furnace slag activated by a blended sodium carbonate-sodium hydroxide (Na_2CO_3-NaOH) system. An experimental program was conducted to evaluate the influence of activator composition and dosage on both fresh-state behavior and hardened properties. Rheological parameters, setting time, electrical conductivity (EC), volumetric water content (VWC), and matric suction were monitored to characterize early-age structuration and hydration kinetics. Unconfined compressive strength (UCS) was measured at multiple curing ages, and microstructural analyses, including X-ray diffraction were performed to link phase assemblage and pore structure to macroscopic performance.

The results demonstrate that the Na_2CO_3-NaOH co-activation system governs CPB behavior through a two-stage hydration process, consisting of an initial ionization regime followed by accelerated gel formation and pore refinement. Fresh-state properties and early-age kinetics were found to be strongly coupled with long-term strength development. Compared to OPC-based CPB, the AAS systems exhibited competitive strength performance while offering significant potential for reducing the carbon footprint of backfill operations. Overall, this research provides an integrated understanding of the mechanisms controlling fresh and hardened behavior of AAS-based CPB and highlights the feasibility of sodium carbonate-sodium hydroxide activated slag as a low-carbon binder for underground mine backfill applications.

DEDICATION

To my parents, Issa and Fatimata, for their unconditional love, sacrifices, and unwavering support throughout my journey.

To my sisters, Fatimata, Aissatou, and Awa, whose support, patience, and guidance made this work possible.

All praise is due to Allah.

Acknowledgments

I would like to sincerely thank my supervisor, Dr. Mamadou Fall, for his constant guidance, support, and trust throughout this research. His expertise, scientific insight, and thoughtful feedback were fundamental to the development and completion of this thesis and guided me through all stages of my graduate studies.

I am particularly grateful to Abdurrahman Suleiman Mohammed for his substantial support and insightful contributions throughout both the experimental work and the writing process of this research.

I would like to express my sincere appreciation to Jean-Claude Célestin for his significant assistance with laboratory work, as well as for his continuous support in addressing technical challenges throughout the experimental program.

I would also like to acknowledge my close friends, Godlove Sengoma Kabuyanga, Souleman Baba Eya, Yacine Ibrahim Djido, and Michel Ange Folefack Tegomo, for their constant encouragement, moral support, and presence throughout this academic journey. Their support played an important role in helping me stay motivated and focused during challenging periods of my studies.

Finally, I wish to express my gratitude to my family for their patience, understanding, and continued support throughout this academic journey.

Table of Contents

ABSTRACT ii

DEDICATION iii

Acknowledgments iv

List of Figures x

List of Tables xii

List of Symbols and Abbreviations xiii

Chapter 1: General Introduction 1

1.1 Background 1

1.1.1 Importance of the Mining Industry 1

1.1.2 Waste Generated by Mining and Its Management 1

1.1.3 Cemented Paste Backfill Technology 2

1.2 Motivation for Low-Carbon Binders in CPB and Problem Statement 3

1.2.1 Limitations of Portland Cement 3

1.2.2 Alkali-Activated Slag (AAS) as a Low-Carbon Alternative 3

1.2.3 Knowledge Gap 3

1.3 Research Objectives 4

1.3.1 General Objective 4

1.3.2 Specific Objectives (SO) 4

1.4 Research Approach and Methodology 5

1.4.1 Phase 1: Material Characterization 5

1.4.2 Phase 2: Mix Design and Fresh-State Testing 5

1.4.3 Phase 3: Strength and Microstructural Evaluation 6

1.4.4 Phase 4: Data Integration and Interpretation 6

1.5 Thesis Organization 7
1.6 References 9
Chapter 2: Theoretical and Technical Background 12
2.1 Introduction 12
2.2 Overview of Cemented Mine Backfill Technologies 12
2.2.1 Cemented Rockfill (CRF) 12
2.2.2 Cemented Hydraulic Backfill (CHF) 13
2.2.3 Cemented Paste Backfill (CPB) 14
2.3 Fundamentals of Cemented Paste Backfill (CPB) and Mix Design 16
2.3.1 Tailings Characteristics 16
2.3.2 Binder Types and Proportions 16
2.3.3 CPB Preparation, Transport, and Placement 17
2.3.4 Key Design Criteria 17
2.4 Rheology of CPB 19
2.4.1 Flow Behavior Models 19
2.4.2 Yield Stress 20
2.4.3 Viscosity 20
2.4.4 Setting Time and Rheological Structuration 21
2.4.5 Measurement Methods 21
2.5 Setting of CPB 23
2.6 Strength Development in CPB 24
2.6.1 UCS as a Key Geotechnical Design Parameter 24
2.6.2 Geotechnical Design Considerations 26
2.7 Hydration Processes in Portland Cement-Based CPB 27
2.7.1 Cement Hydration Reactions and Products 27

2.7.2 Effect of Curing Conditions 27
2.7.3 Transition from Portland cement to alkali-activated binders 28
2.8 Alkali-Activated Slag Chemistry (AAS) with SC/SH Activators 29
2.8.1 Activation Mechanisms 29
2.8.2 Key Parameters Influencing AAS Reactivity 29
2.8.3 Expected Hydration Products 31
2.8.4 Effects of Binary Binder Blends on the Rheology and Strength Development of CPB 31
2.9 Conclusion 33
2.10 References 34
Chapter 3: Literature Review on Fresh and Strength Properties of CPB with Low-Carbon Binders 38
3.1 Introduction and Scope 38
3.2 Previous Studies on Rheological Properties and Setting Times of CPB with AAS Systems 39
3.2.1 Reported Rheological Behaviors and Controlling Variables 39
3.2.2 Reported Setting Times and Controlling Variables 42
3.3 Previous Studies on Strength of CPB with Alkali-Activated Slag (AAS) . 43
3.3.1 UCS Evolution in AAS-Based Systems 43
3.3.2 Factors Affecting UCS Evolution in AAS-Based CPB 44
3.4 Knowledge Gaps and Research Needs 46
3.5 Summary and Conclusions 48
3.6 References 49
Chapter 4: Technical Paper 1: Hydration Mechanisms and Strength Development in Slag-Based Cemented Paste Backfill Activated by Blended Sodium Carbonate–Sodium Hydroxide 52

Abstract 52
4.1 Introduction 53
4.2 Material and experimental program 57
4.2.1 Materials 57
4.2.2 Mixture design 59
4.2.3 Specimen Preparation and curing 60
4.2.4 Test methods 61
4.3 Results 63
4.3.1 Hydration Kinetics from Coupled Monitoring 63
4.3.2 Microstructural Evolution (XRD) 68
4.3.3 Physical Property Evolution 73
4.3.4 Strength Development (UCS) 77
4.4. Integrated Mechanistic Discussion 80
4.5. Conclusions 83
4.6 References 86
Chapter 5: Technical Paper 2: Fresh properties of cemented paste backfill with slag activated by a blend of sodium carbonate and sodium hydroxide 89
Abstract 89
5.1 Introduction 90
5.2 Experimental program 92
5.2.1 Materials and mixture proportioning 92
5.2.2 Test methods 97
5.3. Results and discussions 99
5.3.1 Evolution of the rheological properties of alkali-activated ternary CPB, AA-TC-CPB 99
5.3.2 Development of initial and final setting times of AA-TC-CPBs 112

5.4 Conclusions 115
5.5 References 117
Chapter 6: Synthesis of the Findings and Discussion 120
6.1 Introduction 120
6.2 Synthesis and Integrated Interpretation of Fresh and Strength Results 121
6.2.1 Role of activator chemistry on early-age kinetics and fresh-state behavior 121
6.2.2 Transition from early structuration to hydrate development and pore refinement 122
6.2.3 Coupling between fresh-state behavior and long-term strength development 122
6.3 Practical Implications for CPB Design 123
6.4 Novel Research Contributions of the Thesis 125
6.5 Limitations 126
6.6 References 128
Chapter 7: Conclusions and Recommendations for Future Studies 130
7.1 Key Conclusions Aligned with the Objectives 130
7.2 Recommendations for Future Research 131

List of Figures

Figure 1.1 Overall research approach and experimental program 7

Figure 2.1 Brookfield digital viscometer (DV-E model) used to measure the viscosity of CPB samples. Source: LABOMAT ESSOR SA (n.d.). 22

Figure 2.2 Laboratory vane shear apparatus (Wykeham-Farrance) used to determine the yield stress of CPB. Source: VJ Tech Limited (n.d.). 23

Figure 2.3 Vicat apparatus used to determine the initial and final setting times of CPB. Source: Forney CMT Equipment (n.d.)..... 24

Figure 2.4 Uniaxial compressive strength (UCS) testing machine used to measure the compressive strength of CPB specimens. 25

Figure 4.1: Grain size distribution of the silica tailings (ST) as well as average grain size distribution of tailings from nine mines in Eastern Canada. 58

Figure 4.2. Evolution of electrical conductivity (EC) of CPB mixtures over 28 days of curing. 65

Figure 4.3. Evolution of volumetric water content (VWC) of CPB mixtures over 28 days of curing. 66

Figure 4.4. Evolution of matric suction (ψ), expressed as the absolute value of negative pore water pressure, in CPB mixtures over 28 days of curing. 67

Figure 4.5. XRD patterns after 150 days: (a) OPC control; (b) SC/SH (20/80)-15%; (c) SC/SH (50/50)-20%; (d) SC/SH (50/50)-15%; (e) SC/SH (50/50)-10%. Main phases: calcite ($CaCO_3$), hydrotalcite (LDH), zeolite A (LTA). OPC reference shows AFt and CH. 73

Figure 4.6. Evolution of dry density (ρd) of CPB mixtures with curing time. 74

Figure 4.7. Evolution of void ratio (e) and porosity (n) of CPB mixtures with curing time. 75

Figure 4.8. Evolution of water content (w) of CPB mixtures with curing time ... 76

Figure 4.9. Evolution of unconfined compressive strength (UCS) of CPB mixtures with curing time 77

Figure 5.1: Grain size distribution of the silica tailings (ST) as well as average grain size distribution of tailings from nine mines in Eastern Canada 93

Figure 5.2. Time-dependent evolution of yield stress for CPB prepared with Slag activated by sodium carbonate (SC) and sodium hydroxide (SH) and for CPB with Portland cement. 100

Figure 5.3. Time-dependent evolution of viscosity for CPB prepared with Slag activated by sodium carbonate (SC) and sodium hydroxide (SH) and for CPB with Portland cement. 102

Figure 5.4. XRD patterns of cement pastes prepared with ternary binder after 4 h of curing: (a) OPC control, (b) SC-SH (20/80)-15 %, (c) SC-SH (50/50)-20 %, (d) SC-SH (50/50)-15 %, (e) SC-SH (50/50)-10 %. 105

Figure 5.5. Zeta potential of AA-TC-CPB and Portland cement-CPB mixtures after 4 h of curing. 108

Figure 5.6. Electrical conductivity of AA-TC-CPBs and Portland cement CPB mixtures during the first 24 h of curing. 110

Figure 5.7. Volumetric water content (VWC) of AA-TC-CPBs and Portland cement-CPB mixtures during the first 24 h of curing. 112

Figure 5.8. Initial and final setting times of AA-TC-CPBs and Portland cement-CPB mixtures 113

List of Tables

Table 4.1: Physical and grain-size characteristics of the silica tailings (ST) used in the CPB mixtures. 57

Table 4.2: Mineralogical composition of the silica tailings (ST) determined by X-ray diffraction (wt.%)..... 57

Table 4.3: Chemical composition and physical properties of Portland cement type I and ground granulated blast-furnace slag (GGBFS). 58

Table 4.4: Mix design of CPB mixtures for uniaxial compressive strength testing, physical property determination, electrical conductivity (EC), volumetric water content (VWC), and matric suction (ψ) monitoring. 59

Table 4.5: Composition of cement paste mixtures (without tailings) prepared for XRD analysis after 150 days of curing. 60

Table 5.1: Physical and grain-size characteristics of the silica tailings (ST) used in the CPB mixtures. 93

Table 5.2: Mineralogical composition of the silica tailings (ST) determined by X-ray diffraction (wt.%)..... 93

Table 5.3: Chemical composition and physical properties of Portland cement type I and ground granulated blast-furnace slag (GGBFS). 94

Table 5.4: Mix design of CPB samples used for rheological, setting time, and zeta potential tests as well as for monitoring volumetric water content (VWC) and electrical conductivity (EC). 95

Table 5.5: Composition of cement paste mixtures prepared for XRD analysis after 4 h of curing*. 96

List of Symbols and Abbreviations

AA-TC-CPB: Alkali-Activated Ternary Cemented Paste Backfill

AAS: Alkali-Activated Slag

AFm: Aluminate Ferrite Monosulfate Phase

AFt: Aluminate Ferrite Trisulfate (Ettringite)

ASTM: American Society for Testing and Materials

C-(A)-S-H: Calcium-(Alumino)-Silicate-Hydrate

C-S-H: Calcium Silicate Hydrate

CH: Calcium Hydroxide (Portlandite)

CHF: Cemented Hydraulic Fill

CO_2: Carbon Dioxide

CPB: Cemented Paste Backfill

CRF: Cemented Rockfill

e: Void Ratio

EC: Electrical Conductivity

EDS: Energy Dispersive Spectroscopy

GGBFS: Ground Granulated Blast Furnace Slag

Gs: Specific Gravity

L/S: Liquid-to-Solid Ratio

LDH: Layered Double Hydroxide

n: Porosity

Na_2CO_3: Sodium Carbonate

Na_2Oeq: Sodium Oxide Equivalent

NaOH: Sodium Hydroxide

NMR: Nuclear Magnetic Resonance

OPC: Ordinary Portland Cement

PALS: Phase Analysis Light Scattering

PC: Portland Cement

PCI: Portland Cement Type I

pH: Potential of Hydrogen

SC: Sodium Carbonate

SEM: Scanning Electron Microscopy

SH: Sodium Hydroxide

ST: Silica Tailings

TSF: Tailings Storage Facility

UCS: Unconfined Compressive Strength

VWC: Volumetric Water Content

w: Water Content

W/B: Water-to-Binder Ratio

wt.%: Weight Percent

XRD: X-ray Diffraction

XRF: X-ray Fluorescence

μ_p: Plastic Viscosity (Pa·s)

ρd: Dry Density (kg/m^3)

τ_γ: Yield Stress (Pa)

ψ: Matric Suction (kPa)

Chapter 1: General Introduction

1.1 Background

1.1.1 Importance of the Mining Industry

The mining industry plays a critical role in global economic development by providing essential raw materials for construction, energy, transportation, and manufacturing. Metals such as gold, copper, nickel, and zinc are indispensable for infrastructure, renewable energy systems, and modern technologies (Ali et al., 2017). Despite its importance, mining is also among the most resource and energy-intensive industries, generating vast quantities of solid waste and posing significant environmental challenges (Lottermoser, 2010). With the growing demand for metals and the depletion of high-grade ores, sustainable waste management and resource efficiency have become central to responsible mining practices (Adiansyah et al., 2015).

1.1.2 Waste Generated by Mining and Its Management

Ore extraction and mineral processing produce enormous volumes of waste materials, including tailings and waste rocks. Globally, it is estimated that approximately 14 billion tonnes of tailings were generated in 2010 alone (Adiansyah et al., 2015), with current annual production estimates ranging from 8.85 to 14.4 billion tonnes (Oberle et al., 2019). Traditionally, these tailings are disposed of in surface impoundments or tailings storage facilities (TSFs). However, the long-term stability and environmental risks associated with TSFs such as dam failures, seepage, acid mine drainage, and dust emissions, have raised serious concerns (Kossoff et al., 2014; Rico et al., 2008).

To mitigate these risks, backfilling technologies have been increasingly adopted in underground mining. Among these, CPB stands out as one of the most sustainable solutions, allowing tailings to be reused as structural material for mine voids, thereby reducing surface disposal while enhancing ground stability and worker safety (Belem & Benzaazoua, 2008; Yilmaz et al., 2014).

1.1.3 Cemented Paste Backfill Technology

Overview of CPB in Underground Mining

Cemented paste backfill is produced by mixing dewatered tailings with a hydraulic or pozzolanic binder, traditionally ordinary Portland cement (OPC), water, and, where needed, admixtures. The paste is pumped into underground stopes to provide mechanical support and to minimize surface environmental footprints (Fall et al., 2008; Belem & Benzaazoua, 2008). Typical mixtures contain 70-85% solids by weight with 3-7% binder, depending on operational requirements and tailings properties (Yilmaz et al., 2014; Belem and Benzaazoua, 2008). After placement, CPB undergoes hydration and consolidation, progressively gaining stiffness and strength.

Key Performance Criteria: Fresh and Hardened Properties

At the fresh state, CPB must maintain sufficient flowability and pumpability to ensure pipeline transport and uniform stope filling without segregation or blockage (Belem & Benzaazoua, 2008; Qi & Fourie, 2019). Flowability is commonly characterized by the yield stress (τ_γ) and the plastic viscosity (μ_p), which together describe the rheological response (Ouattara et al., 2018). The setting time is a second critical parameter because it governs the turnaround between placement and subsequent mining activities; a shorter setting time can improve productivity but must not compromise workability during transport and placement (Carnogursky & Fall, 2023).

At the hardened state, the unconfined compressive strength (UCS) is the primary performance indicator. Depending on stope geometry, sequencing, and binder content, UCS at 28 days typically ranges from 0.3 to 1.5 MPa (Yilmaz et al., 2014; Kesimal et al., 2005). Adequate strength is required to maintain stope stability, withstand blast-induced stresses, and prevent structural failure. Accordingly, understanding and controlling both fresh- and hardened-state properties is essential for safe, cost-effective, and sustainable CPB design.

1.2 Motivation for Low-Carbon Binders in CPB and Problem Statement

1.2.1 Limitations of Portland Cement

Despite its widespread use, ordinary Portland cement (OPC) presents notable economic and environmental drawbacks. Its manufacture contributes roughly 7–8% of global CO_2 emissions when considering both process emissions from limestone calcination and energy emissions from fossil-fuel combustion (Scrivener et al., 2018; Andrew, 2019). In parallel, persistent price volatility and supply constraints in remote mining districts elevate operational costs. The dual pressure to cut greenhouse-gas emissions and stabilize binder costs has therefore accelerated efforts to adopt low-carbon alternatives for CPB (Provis, 2018; Bernal and Provis, 2014).

1.2.2 Alkali-Activated Slag (AAS) as a Low-Carbon Alternative

Among cement-free binders, alkali-activated slag (AAS), produced by activating ground granulated blast-furnace slag (GGBFS) with alkaline solutions such as sodium hydroxide (NaOH), sodium silicate (Na_2SiO_3), or sodium carbonate (Na_2CO_3), can achieve mechanical and durability performance comparable to or exceeding OPC (Provis and Bernal, 2014; Ke et al., 2016). Because AAS valorizes an industrial by-product and avoids carbonate decomposition, its carbon footprint has been reported to be up to 40–80% lower than that of OPC, depending on the type of activator used and the system boundaries considered (Habert et al., 2020; Juenger et al., 2019). Additional benefits reported for mining environments include improved chemical resistance and long-term stability under aggressive pore waters (Bakharev et al., 2002; Bernal et al., 2015).

1.2.3 Knowledge Gap

Although previous studies have demonstrated the potential of alkali-activated slag (AAS) as a low-carbon binder for CPB, major knowledge gaps remain regarding the coupled evolution of fresh-state rheology, setting behavior, and mechanical performance, particularly in hybrid Na_2CO_3–NaOH activated systems. While Na_2CO_3 offers advantages in terms of safety, cost, and sustainability, its use is commonly associated with slow

reaction kinetics and poor early-age strength development (Bernal and Provis, 2016; Walkley et al., 2021). Recent evidence suggests that introducing controlled amounts of NaOH can markedly enhance pore-solution alkalinity, accelerate slag dissolution, and promote rapid gel formation (Dai et al., 2023; Akturk et al., 2022). However, to date, no comprehensive and systematic study has elucidated how the Na_2CO_3–NaOH activation balance governs CPB rheological parameters, specifically yield stress (τ_γ) and plastic viscosity (μ_p), in conjunction with setting kinetics and unconfined compressive strength (UCS) under realistic tailings compositions and practical mix-design constraints. More critically, the fundamental linkage between early-age fresh properties and long-term hardened performance in such hybrid-activated CPB systems remains largely unexplored.

This lack of integrated understanding currently limits the rational design and field-scale implementation of low-carbon CPB using hybrid alkali activation. Addressing these unresolved mechanisms is therefore essential not only for advancing the scientific basis of AAS-CPB systems but also for enabling the development of high-performance, environmentally sustainable backfill formulations for modern deep mining operations.

1.3 Research Objectives

1.3.1 General Objective

The overarching objective of this research is to experimentally quantify the effects of a low-carbon alkali-activated slag (AAS) binder, activated by a blend of sodium carbonate (Na_2CO_3) and sodium hydroxide (NaOH) on the fresh state and mechanical properties of CPB.

1.3.2 Specific Objectives (SO)

SO1. To evaluate the rheological behavior, specifically yield stress (τ_γ) and plastic viscosity (μ_p), of CPB prepared with Na_2CO_3-NaOH-activated ground granulated blast-furnace slag (GGBFS) binders.

SO2. To investigate the setting time and early hydration characteristics of CPB containing low-carbon AAS binders.

SO3. To analyze the unconfined compressive strength (UCS) development of AAS-based CPB over multiple curing ages (1, 3, 7, 28, 90, 150, and 210 days) to capture both early- and long-term strength evolution.

SO4. To establish correlations between fresh-state parameters (rheology, setting) and mechanical performance, thereby clarifying the link between activation chemistry, hydration kinetics, and structural build-up in AAS-based CPB systems.

Together, these objectives aim to develop a comprehensive understanding of how blended Na_2CO_3-NaOH activation governs CPB performance, thereby contributing to the advancement of sustainable, low-carbon mining backfill practices.

1.4 Research Approach and Methodology

To accomplish the research objectives presented in Section 1.3, a systematic experimental framework was developed to investigate the influence of Na_2CO_3-NaOH activation on the fresh and hardened behavior of CPB. The study combines laboratory testing, instrumented monitoring, and microstructural analyses to establish quantitative relationships between activation chemistry, hydration kinetics, and mechanical performance. The overall experimental sequence and its interconnections are summarized in Figure 1.1.

1.4.1 Phase 1: Material Characterization

Comprehensive chemical, mineralogical and physical characterizations were conducted on both tailings and binder materials to establish baseline parameters prior to mix preparation. Tests included grain-size distribution (PSD), specific gravity, oxide composition (XRF), and mineralogical analysis (XRD). These data were used to assess the suitability of the materials and to guide the subsequent mix-design process.

1.4.2 Phase 2: Mix Design and Fresh-State Testing

A series of CPB mixtures were formulated using varying Na_2CO_3-NaOH ratios and activator dosages, while maintaining a constant water-to-binder ratio (W/B) and

target solids content. The rheological behavior, characterized by yield stress (τ_γ) and plastic viscosity (μ_p), was evaluated using rotational and vane-shear methods. The setting time was determined using a Vicat apparatus, and complementary monitoring of electrical conductivity (EC) and volumetric water content (VWC) was performed during the early hydration period to assess the evolution of workability and structuration.

1.4.3 Phase 3: Strength and Microstructural Evaluation

The unconfined compressive strength (UCS) was measured at multiple curing ages (1, 3, 7, 28, 90, 150, and 210 days) to capture both early and long-term strength development. Microstructural evolution was analyzed through X-ray diffraction (XRD) to identify hydration products and relate phase assemblage to mechanical and physical performance. These data provided insight into the mechanisms governing strength gain and binder densification in low-carbon CPB systems.

1.4.4 Phase 4: Data Integration and Interpretation

All results from the previous phases were integrated to establish quantitative and qualitative correlations among rheological, setting, and mechanical responses. This step focused on understanding how activation chemistry and hydration mechanisms jointly control microstructural development and overall mechanical stability. The resulting correlations support the development of optimized, low-carbon binder formulations for sustainable CPB design.

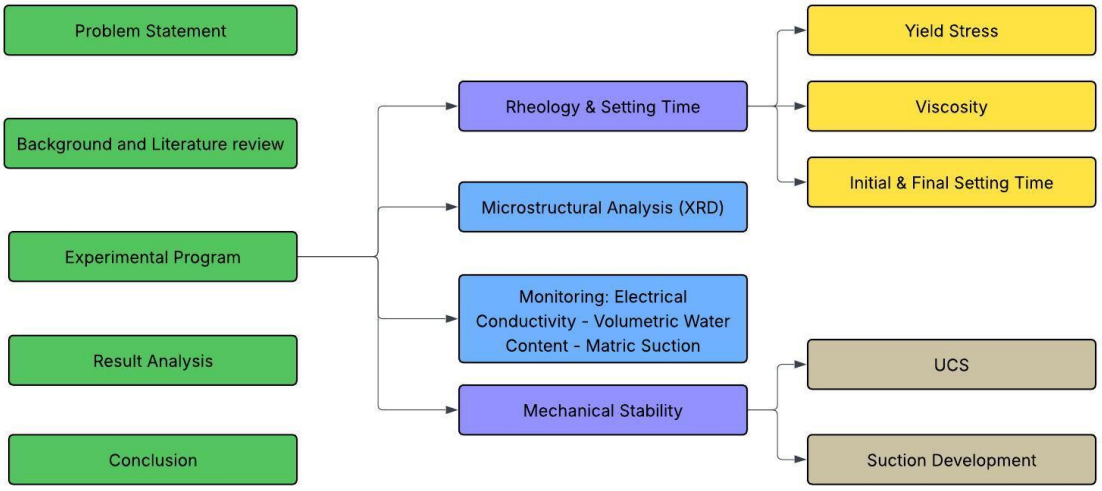

Figure 1.1 Overall research approach and experimental program

1.5 Thesis Organization

This thesis is organized into seven chapters, structured to provide a logical progression from the research background to the experimental investigations and concluding synthesis and two research papers.

Chapter 1: General Introduction presents the overall context and motivation of the study. It introduces the importance of the mining industry, the challenges of mine waste management, and the fundamentals of CPB technology. The chapter defines the problem statement, highlights the need for low-carbon binders, formulates the research objectives, and outlines the experimental approach and methodology.

Chapter 2: Theoretical and Technical Background provides a concise overview of cemented mine backfill technologies and details the fundamental concepts of CPB design, rheology, setting behavior, and strength development. The chapter also reviews key previous studies relevant to CPB and binder chemistry in order to establish the theoretical framework of the research and to highlight the fundamental differences between conventional ordinary Portland cement (OPC) systems and alkali-activated slag (AAS) binders activated with sodium carbonate (Na_2CO_3) and sodium hydroxide (NaOH).

Chapter 3: Literature Review on Fresh and Strength Properties of CPB with Low-Carbon Binders presents a critical and focused review of previous research on the rheological, setting, and mechanical behavior of CPB prepared with alkali-activated slag systems. This chapter identifies the specific knowledge gaps associated with the combined use of Na_2CO_3-NaOH activators in CPB and clearly positions the original contribution of the present study relative to existing work, thereby establishing the basis for the experimental investigations described in the subsequent chapters.

Chapter 4: Technical Paper 1: Hydration Mechanisms and Strength Development in Slag-Based Cemented Paste Backfill Activated by Blended Sodium Carbonate–Sodium Hydroxide focuses on the mechanical and microstructural evolution of CPB**.** It analyzes the UCS development up to 210 days of curing, interprets the corresponding hydration mechanisms, and discusses the in-mold monitoring data (EC, VWC, and suction).

Chapter 5: Technical Paper 2: Fresh Properties of Cemented Paste Backfill with Slag Activated by a Blend of Sodium Carbonate and Sodium Hydroxide presents the experimental results on rheology, setting time, and early-age structuration of AAS-based CPB mixtures. The findings are linked to microstructural observations to explain how activator chemistry governs early paste behavior and pumpability.

Chapter 6: Synthesis of the Findings and Discussion integrates the results from the two technical papers. It examines the interrelationships between fresh-state and hardened-state properties, develops a conceptual understanding of the underlying activation mechanisms, and outlines the practical implications for the design of sustainable CPB formulations. The chapter also synthesizes the key novelties of this research and critically discusses its limitations.

Chapter 7: Conclusions and Recommendations for Future Studies summarizes the key findings of the research in relation to the stated objectives. It also presents practical recommendations for industrial application and proposes future research directions to further optimize low-carbon binder systems for CPB.

1.6 References

Adiansyah, J. S., M. Rosano, S. Vink, and G. Keir. 2015. “A framework for a sustainable approach to mine tailings management: disposal strategies.” *Journal of Cleaner Production*, 108: 1050–1062.

Akturk, B., A. B. Kizilkanat, and N. Kabay. 2019. “Effect of calcium hydroxide on fresh state behavior of sodium carbonate activated blast furnace slag pastes.” *Construction and Building Materials*, 212: 388–399.

Alexandra Carnogursky, E., M. Fall, and S. Haruna. 2023. “Rheology and setting time of saline cemented paste backfill.” *Minerals Engineering*, 202: 108258.

Ali, S. H., D. Giurco, N. Arndt, E. Nickless, G. Brown, A. Demetriades, R. Durrheim, M. A. Enriquez, J. Kinnaird, A. Littleboy, L. D. Meinert, R. Oberhänsli, J. Salem, R. Schodde, G. Schneider, O. Vidal, and N. Yakovleva. 2017. “Mineral supply for sustainable development requires resource governance.” *Nature*, 543 (7645): 367–372. Nature Publishing Group.

Andrew, R. M. 2019. “Global CO_2 emissions from cement production, 1928–2018.” *Earth System Science Data*, 11 (4): 1675–1710. Copernicus GmbH.

Bakharev, T., J. G. Sanjayan, and Y.-B. Cheng. 2002. “Sulfate attack on alkali-activated slag concrete.” *Cement and Concrete Research*, 32 (2): 211–216.

Belem, T., and M. Benzaazoua. 2008. “Design and Application of Underground Mine Paste Backfill Technology.” *Geotechnical and Geological Engineering*, 26 (2): 147–174.

Bernal, S. A., and J. L. Provis. 2014. “Durability of Alkali-Activated Materials: Progress and Perspectives.” *Journal of the American Ceramic Society*, 97 (4): 997–1008.

Bernal, S. A., J. L. Provis, R. J. Myers, R. San Nicolas, and J. S. J. van Deventer. 2015. “Role of carbonates in the chemical evolution of sodium carbonate-activated slag binders.” *Materials and Structures*, 48 (3): 517–529.

Dai, X., Q. Ren, S. Aydin, M. Y. Yardimci, and G. De Schutter. 2023. “Accelerating the reaction process of sodium carbonate-activated slag mixtures with the incorporation of a small addition of sodium hydroxide/sodium silicate.” *Cement and Concrete Composites*, 141: 105118.

Fall, M., M. Benzaazoua, and E. G. Saa. 2008. “Mix proportioning of underground cemented tailings backfill.” *Tunnelling and Underground Space Technology*, 23 (1): 80–90.

Habert, G., S. A. Miller, V. M. John, J. L. Provis, A. Favier, A. Horvath, and K. L. Scrivener. 2020. “Environmental impacts and decarbonization strategies in the cement and concrete industries.” *Nature Reviews Earth & Environment*, 1 (11): 559–573. Nature Publishing Group.

Juenger, M. C. G., R. Snellings, and S. A. Bernal. 2019. “Supplementary cementitious materials: New sources, characterization, and performance insights.” *Cement and Concrete Research*, 122: 257–273.

Ke, X., S. A. Bernal, and J. L. Provis. 2016. “Controlling the reaction kinetics of sodium carbonate-activated slag cements using calcined layered double hydroxides.” *Cement and Concrete Research*, 81: 24–37.

Kesimal, A., E. Yilmaz, B. Ercikdi, I. Alp, and H. Deveci. 2005. “Effect of properties of tailings and binder on the short-and long-term strength and stability of cemented paste backfill.” *Materials Letters*, 59 (28): 3703–3709.

Kossoff, D., W. E. Dubbin, M. Alfredsson, S. J. Edwards, M. G. Macklin, and K. A. Hudson-Edwards. 2014. “Mine tailings dams: Characteristics, failure, environmental impacts, and remediation.” *Applied Geochemistry*, 51: 229–245.

Lottermoser, B. 2010. *Mine Wastes*. Berlin, Heidelberg: Springer.

Oberle, B., S. Bringezu, S. Hatfield-Dodds, S. Hellweg, H. Schandl, and J. Clement. 2019. *Global Resources Outlook: 2019*. Nairobi, Kenya: International Resource Panel, United Nations Envio, Paris, France.

Ouattara, D., M. Mbonimpa, A. Yahia, and T. Belem. 2018. “Assessment of rheological parameters of high density cemented paste backfill mixtures incorporating superplasticizers.” *Construction and Building Materials*, 190: 294–307.

Provis, J. L. 2018. “Alkali-activated materials.” *Cement and Concrete Research*, Report of UNEP SBCI working group on low-co2 eco-efficient cement-based materials, 114: 40–48.

Provis, J. L., and S. A. Bernal. 2014. “Geopolymers and Related Alkali-Activated Materials.” *Annual Review of Materials Research*, 44 (Volume 44, 2014): 299–327. Annual Reviews.

Qi, C., and A. Fourie. 2019. “Cemented paste backfill for mineral tailings management: Review and future perspectives.” *Minerals Engineering*, 144: 106025.

Rico, M., G. Benito, A. R. Salgueiro, A. Díez-Herrero, and H. G. Pereira. 2008. “Reported tailings dam failures: A review of the European incidents in the worldwide context.” *Journal of Hazardous Materials*, 152 (2): 846–852.

Scrivener, K. L., V. M. John, and E. M. Gartner. 2018. “Eco-efficient cements: Potential economically viable solutions for a low-CO2 cement-based materials industry.” *Cement and Concrete Research*, Report of UNEP SBCI working group on low-co2 eco-efficient cement-based materials, 114: 2–26.

Shi, C., D. Roy, and P. Krivenko. 2003. *Alkali-Activated Cements and Concretes*. London: CRC Press.

Walkley, B., X. Ke, J. L. Provis, and S. A. Bernal. 2021. “Activator Anion Influences the Nanostructure of Alkali-Activated Slag Cements.” *The Journal of Physical Chemistry C*, 125 (37): 20727–20739. American Chemical Society.

Yilmaz, E., T. Belem, and M. Benzaazoua. 2014. “Effects of curing and stress conditions on hydromechanical, geotechnical and geochemical properties of cemented paste backfill.” *Engineering Geology*, 168: 23–37.

Chapter 2: Theoretical and Technical Background

2.1 Introduction

This chapter provides the theoretical and technical framework required to understand the development, performance, and behavior of cemented paste backfill (CPB), with particular emphasis on systems incorporating alkali-activated slag (AAS) binders. It first presents an overview of the evolution of cemented mine backfill technologies and the principles governing the design and performance of CPB. The discussion then highlights the key parameters that control both the fresh properties, such as rheology, flowability, and setting time, and the hardened properties, including strength and microstructural development.

In addition, this chapter examines the chemical mechanisms and hydration processes associated with alkali-activated slag systems, particularly those activated by sodium carbonate (Na_2CO_3) and sodium hydroxide (NaOH). Understanding these mechanisms is essential for interpreting the results obtained in the experimental chapters that follow. The concepts, models, and background information presented herein therefore form the scientific foundation for the experimental program and the subsequent analyses discussed in Chapters 4 and 5, as well as for the synthesis and conclusions provided in Chapter 6.

2.2 Overview of Cemented Mine Backfill Technologies

2.2.1 Cemented Rockfill (CRF)

Cemented Rockfill (CRF) is a backfilling technique that involves the placement of coarse waste rock mixed with a cementitious slurry to form a rigid, self-supporting mass. It is mainly employed in large stopes and open stoping operations where the availability of coarse rock material is abundant. The rock skeleton provides the primary structural framework, while the injected cemented slurry fills the voids and bonds the particles together, thereby enhancing overall stability (Archibald et al., 2000).

Typical CRF mixtures contain low binder dosages, generally between 3% and 8% by weight of the fine fraction, resulting in a relatively economical solution for high-volume stopes. The coarse nature of the aggregate contributes to its high load-bearing capacity and rapid drainage, making CRF particularly suitable for applications requiring early exposure or secondary blasting. However, the heterogeneous particle size distribution can lead to non-uniform strength development and localized stress concentrations. In addition, the need for large rock fragments limits its applicability in mines where suitable waste rock is unavailable or where finer tailings must be managed (Potvin et al., 2005).

2.2.2 Cemented Hydraulic Backfill (CHF)

Cemented Hydraulic Backfill (CHF) consists of a slurry prepared from hydraulically classified mill tailings, water, and a cementitious binder, most commonly Ordinary Portland Cement (OPC). The mixture typically contains between 55% and 65% solids by weight and is pumped underground in a highly diluted form (Potvin et al., 2005). Once placed in the stope, the excess water drains or evaporates, leading to consolidation and subsequent strength gain as cement hydration proceeds.

CHF is well established in the mining industry due to its excellent transportability through gravity flow or low-pressure pipelines, which enables long-distance delivery with relatively low pumping energy. The use of classified tailings improves flowability and drainage; however, this approach requires additional dewatering and classification infrastructure at the surface plant. Moreover, the removal of fines may increase the volume of surface tailings requiring disposal (Sivakugan et al., 2006).

Despite its operational simplicity, CHF is susceptible to segregation and bleeding during placement, which can result in non-uniform strength and potential instability at the stope interface (Liu et al., 2017). In addition, CHF is prone to liquefaction, which may lead to barricade failures associated with casualties, reputational damage, and financial losses for mining operations. Consequently, while CHF remains effective for mines equipped with classification circuits and moderate backfill strength requirements, it is progressively being replaced by CPB systems, which offer improved material homogeneity, enhanced stability, and better environmental performance.

2.2.3 Cemented Paste Backfill (CPB)

CPB is produced by mixing unclassified tailings with a hydraulic or alternative binder and water to obtain a homogeneous, non-segregating paste typically containing 70-85% solids by weight. In contrast to Cemented Hydraulic Backfill (CHF), CPB exhibits minimal drainage and negligible segregation after placement, which promotes uniform strength development throughout the filled stope (Belem and Benzaazoua, 2008; Fall et al., 2008).

The high solids content and controlled rheology of CPB allow it to be pumped using positive-displacement pumps and transported through dedicated pipelines directly to underground stopes. Once placed, the paste gradually hardens through binder hydration or activation reactions, providing structural support while enabling safer and more efficient ore extraction (Belem and Benzaazoua, 2008).

CPB technology offers several advantages over conventional backfill methods. It allows the direct use of unclassified tailings, thereby reducing the volume of surface tailings storage and improving water recovery. Its non-segregating nature minimizes bleed water and enhances stability during curing. Moreover, the technique supports continuous backfilling operations and is adaptable to complex mine geometries (Qi and Fourie, 2019). However, these benefits are balanced by challenges such as higher pumping pressures, increased binder consumption, and the need for precise control of rheological properties to avoid pipeline blockage or stope instability (Fall et al., 2008).

Comparative Advantages and Limitations

Compared with CRF and CHF, CPB offers greater versatility in the use of fine, unclassified tailings and provides improved control over both mechanical and geochemical performance (Belem and Benzaazoua, 2008). The higher solids content and non-segregating nature of CPB ensure more uniform strength development (Fall et al., 2008), while its capacity to incorporate all tailings fractions significantly reduces the volume of surface tailings storage and associated environmental risks (Benzaazoua et al., 2008). These features make CPB particularly attractive for modern underground mining operations seeking enhanced safety, environmental compliance, and efficient resource

utilization (Qi and Fourie, 2019). A comparative summary of the key differences between CRF, CHF, and CPB is presented in Table 2.1.

Table 2.1 Comparison of cemented mine backfill technologies (CRF, CHF, CPB).

Criterion	CRF	CHF	CPB
Physical characteristics	Coarse rock fragments with cemented slurry; heterogeneous skeleton	Classified tailings with high water content; drainage after placement	Homogeneous paste of unclassified tailings, binder, and water; minimal drainage
Rheology	Not a paste flow; gravity placement/injection of slurry	Low yield stress slurry; segregation/bleeding potential	Viscoplastic paste with measurable yield stress and viscosity; requires rheological control
Environmental impact	Depends on waste rock availability; limited tailings reuse	Requires classification and significant water management	Maximizes tailings reuse and reduces surface disposal and environmental risks
Cost	Lower binder demand but operational constraints	Moderate binder; added costs for dewatering systems	Higher binder and pumping energy costs; potential offset by improved safety/environmental benefits

Source: Compiled by the author based on Belem and Benzaazoua (2008), Fall et al. (2008), Potvin et al. (2005), Qi and Fourie (2019)

However, the CPB technology also presents notable challenges. The reliance on high binder dosages, most commonly Ordinary Portland Cement (OPC), can substantially increase operating costs and carbon emissions (Qi and Fourie, 2019). In addition, the high-density paste requires careful rheological control to maintain an optimal balance between pumpability and in-stope stability (Belem and Benzaazoua, 2008). Excessive yield stress can lead to pipeline blockages, whereas insufficient viscosity may result in segregation or incomplete filling (Fall et al., 2008). Consequently, optimizing binder composition and rheological behavior is essential to ensure the technical and economic viability of CPB systems (Fall et al., 2008).

2.3 Fundamentals of Cemented Paste Backfill (CPB) and Mix Design

2.3.1 Tailings Characteristics

The physical, mineralogical, and chemical properties of tailings play a decisive role in the behavior of CPB. Key parameters include particle size distribution (PSD), specific surface area, particle shape, and mineralogical composition, all of which directly influence the rheology, setting behavior, and strength development of the backfill (Kesimal et al., 2005).

Fine-grained and angular tailings generally exhibit higher water demand and yield stress due to increased surface area and interparticle friction, which reduce flowability and pumpability. In contrast, coarser or more rounded particles decrease the specific surface area and promote better particle packing, thereby improving flow characteristics and reducing the viscosity of the paste (Fall et al., 2005a).

From a chemical standpoint, tailings often contain reactive silicate, aluminosilicate, oxide, and sulfide minerals that can interact with the binder during hydration. The oxidation of sulfide-bearing phases such as pyrite or pyrrhotite may generate acidic conditions, which can alter binder hydration products, delay setting, or compromise long-term durability (Fall and Benzaazoua, 2005b). Understanding the geochemical reactivity of tailings is therefore critical for selecting an appropriate binder type and dosage and for ensuring chemical compatibility within the CPB system (Benzaazoua et al., 2004).

2.3.2 Binder Types and Proportions

The binder is the most critical component in CPB, as it provides mechanical integrity and cohesion through hydration or pozzolanic reactions (Benzaazoua et al., 2004). Conventional CPB systems primarily rely on Ordinary Portland Cement (OPC), either used alone or blended with supplementary materials such as ground granulated blast-furnace slag (GGBFS), fly ash, or limestone. These blended cements are commonly adopted to reduce binder cost, moderate heat generation, and improve workability and long-term performance (Fall et al., 2008). Typical binder contents in conventional CPB range from approximately 3% to 7% by weight of the total dry solids, depending on the required strength, stope geometry, and curing conditions (Belem and Benzaazoua, 2008).

2.3.3 CPB Preparation, Transport, and Placement

The preparation of CPB involves proportioning the main constituents (tailings, binder, water, and, when applicable, chemical activators) to achieve the desired rheological and mechanical performance. Mix design requires the careful selection of solids concentration, binder type and dosage, and activator composition, as these parameters collectively determine the paste's flowability, pumpability, and strength development (Belem and Benzaazoua, 2008).

In practice, the constituents are mechanically blended to form a homogeneous, non-segregating paste. The resulting mixture is typically characterized by a solids content ranging from 70% to 85% by weight (Fall et al., 2008; Belem and Benzaazoua, 2008), which ensures sufficient cohesiveness while maintaining pumpability. The water-to-binder ratio (W/B) exerts a dominant influence on the workability and strength of CPB: higher ratios enhance flowability but may reduce final strength, whereas lower ratios yield stiffer pastes that are more difficult to pump (Fall et al., 2008). In the present research, a constant W/B of 7.4 was adopted to maintain consistent rheological conditions across all mixtures and to reflect realistic operational practices in mine backfilling systems.

Once prepared, the paste is conveyed underground using positive-displacement or peristaltic pumps and distributed through dedicated pipeline networks (Belem and Benzaazoua, 2008). Proper design of the transport system is essential to ensure stable laminar flow, prevent segregation or blockage, and minimize energy losses during pumping. The paste is then discharged into mined-out stopes, where it gradually hardens to form a self-supporting mass that provides ground stability and facilitates subsequent mining operations (Ghirian and Fall, 2013). Ensuring adequate curing conditions, uniform filling, and controlled placement rates are critical to achieving consistent strength development and long-term structural integrity of the backfill (Belem and Benzaazoua, 2008; Ghirian and Fall, 2013).

2.3.4 Key Design Criteria

The design of CPB must satisfy several interrelated performance requirements to ensure safe, efficient, and cost-effective underground operations. These criteria encompass

the fresh-state, early-age, and long-term behaviors of the material and directly influence both operational feasibility and structural stability (Belem and Benzaazoua, 2008; Fall et al., 2008).

Flowability is a critical parameter governing the ability of the paste to be pumped through pipelines and to fill underground stopes uniformly without segregation or blockage. Adequate flowability ensures stable transport and consistent placement, directly affecting the overall efficiency of mine backfilling operations (Roshani and Fall, 2020; Haruna and Fall, 2020).

Setting time must be controlled to allow sequential mining and barricade removal while preventing premature stiffening during transport. This parameter depends on binder chemistry, temperature, and water content, and is particularly sensitive in alkali-activated systems where reaction kinetics differ from those of Portland cement (Sagade and Fall, 2024; Haruna and Fall, 2020).

Unconfined Compressive Strength (UCS) is the primary mechanical design criterion for CPB. The backfill must develop sufficient strength to support mine openings and withstand stress redistribution following ore extraction.

Typical UCS targets, ranging from 0.3 to 1.5 MPa after 28 days, are determined by stope geometry, exposure conditions, and operational safety requirements (Kesimal et al., 2005; Belem and Benzaazoua, 2008).

Finally, **durability** under chemical and thermal influences is essential for the long-term performance of CPB. Underground conditions often expose the material to varying temperatures, humidity, and potentially aggressive porewater chemistry. Maintaining low permeability and stable hydration or activation products is key to ensuring chemical and structural stability (Fall and Pokharel, 2010; Bernal and Provis, 2014).

Together, these design criteria form the basis for optimizing CPB mixture composition and backfilling practices to achieve the desired balance between pumpability, strength, and long-term stability.

2.4 Rheology of CPB

2.4.1 Flow Behavior Models

The rheological behavior of CPB is commonly described using viscoplastic models that account for both yield stress and shear-dependent viscosity. The most frequently applied constitutive models are the Bingham plastic and the Herschel-Bulkley models (Ouattara et al., 2018; Xiapeng et al., 2019).

The Bingham model assumes a linear relationship between shear stress (τ) and shear rate ($\dot{\gamma}$) once a critical yield stress (τ_0) is exceeded:

$$\tau = \tau_0 + \mu_p \dot{\gamma}$$

where τ_0 is the yield stress (Pa), representing the minimum stress required to initiate flow, and μ_p is the plastic viscosity (Pa·s), describing the resistance to flow once motion begins. This model is widely used in CPB studies because it provides a reasonable approximation for many paste-like materials with near-linear shear behavior at moderate shear rates (Ouattara et al., 2018; Wu et al., 2013).

The Herschel-Bulkley model extends the Bingham formulation by introducing a power-law term to capture non-linear flow behavior:

$$\tau = \tau_0 + K\dot{\gamma}^n$$

where K is the consistency index (Pa·s^n) and n is the flow index. When $n < 1$, the material exhibits shear-thinning behavior (viscosity decreases with increasing shear rate), whereas $n > 1$ corresponds to shear-thickening. This model provides greater flexibility in representing the complex rheological responses of CPB containing varying solid concentrations, tailings types, and binder systems (Xiapeng et al., 2019; Yang et al., 2019).

Both models have been successfully applied to characterize the flowability and pumping behavior of CPB mixtures. In practice, the choice between them depends on the experimental data fitting and the degree of non-linearity observed in the shear stress-shear rate relationship.

2.4.2 Yield Stress

Yield stress (τ_0) is a fundamental rheological parameter governing the flow initiation of cemented paste backfill (Belem and Benzaazoua, 2008; Ouattara et al., 2017). It represents the minimum shear stress required to overcome interparticle forces and initiate deformation of the paste (Ouattara et al., 2017). In CPB systems, yield stress is primarily controlled by solids concentration, particle size distribution, particle shape, and interparticle interactions within the tailings-binder matrix (Wu et al., 2013; Ouattara et al., 2018).

A sufficiently high yield stress is required to prevent segregation and bleeding after placement, thereby ensuring uniform filling and early-age stability within underground stopes (Belem and Benzaazoua, 2008). However, excessive yield stress may lead to increased pumping pressures and a higher risk of pipeline blockage (Ouattara et al., 2018; Haruna and Fall, 2020). Consequently, the optimization of yield stress is critical to achieving a balance between pumpability during transport and stability after placement (Ouattara et al., 2018; Haruna and Fall, 2020).

2.4.3 Viscosity

Plastic viscosity (μ_p) describes the resistance of cemented paste backfill to flow once the yield stress has been exceeded (Ouattara et al., 2017; Wu et al., 2013). It governs the energy required to maintain flow during pumping and has a direct influence on pressure losses along pipeline systems (Haruna and Fall, 2020). In CPB, viscosity is affected by the water-to-binder ratio, fines content, binder type, and the degree of particle dispersion within the paste (Wu et al., 2013; Ouattara et al., 2018).

Low viscosity facilitates pumping and reduces energy demand, but excessively low values may increase the risk of segregation or incomplete stope filling (Ouattara et al., 2017; Ouattara et al., 2018). Conversely, high viscosity enhances cohesiveness and homogeneity but increases pumping energy requirements (Haruna and Fall, 2020; Xiapeng et al., 2019). Effective control of viscosity is therefore essential to ensure reliable transport while maintaining adequate in-stope performance (Wu et al., 2013; Haruna and Fall, 2020).

2.4.4 Setting Time and Rheological Structuration

Setting time is closely linked to the time-dependent evolution of rheological properties in cemented paste backfill (Haruna and Fall, 2020; Wu et al., 2013). As hydration or activation reactions progress, the formation of solid reaction products leads to gradual structuration of the paste, manifested by increases in yield stress and viscosity with time (Wu et al., 2013; Xiapeng et al., 2019). This rheological structuration marks the transition from a fluid or workable state to a rigid, self-supporting material (Sagade and Fall, 2024; Ouattara et al., 2018).

In operational terms, setting time defines the workable window available for transport and placement of CPB, as well as the timing of early-age stability development within the stope (Sagade and Fall, 2024; Haruna and Fall, 2020). Excessively rapid structuration may compromise pumpability, whereas delayed setting can prolong stope exposure and reduce early-age stability (Wu et al., 2013; Ouattara et al., 2018). The control of setting time is therefore a critical design consideration, linking rheological behavior during transport to mechanical performance after placement (Sagade and Fall, 2024; Haruna and Fall, 2020).

2.4.5 Measurement Methods

Rheological characterization of CPB is typically performed using laboratory rotational rheometers equipped with geometries such as vane spindles or coaxial cylinder systems (Ouattara et al., 2018; Wu et al., 2013). These devices measure the relationship between shear stress and shear rate, enabling the determination of key viscoplastic parameters including yield stress (τ_0) and plastic viscosity (μ_p). Vane geometries are particularly suited for coarse or highly structured materials like CPB, as they minimize wall-slip effects and provide more reliable results for high-solids pastes (Ouattara et al., 2018; Haruna and Fall, 2020).

In addition to laboratory rheometry, several complementary field-oriented tests are commonly employed to validate mixture performance under operational conditions. Flow table tests and Marsh cone flow times provide rapid assessments of workability at the plant scale (Ouattara et al., 2017; Belem and Benzaazoua, 2008), while pipeline loop tests

simulate pumping behavior over realistic distances and pressures (Belem and Benzaazoua, 2008). These field proxies are essential for translating laboratory-derived rheological parameters into practical guidelines for pipeline transport, pump selection, and stope filling.

Together, laboratory rheometry and field tests provide a comprehensive evaluation of CPB flow behavior, ensuring that mixtures exhibit both the fundamental rheological properties, and the operational performance required for reliable underground backfilling (Wu et al., 2013; Haruna and Fall, 2020). The Brookfield digital viscometer (DV-E model) used in this study to measure the viscosity of CPB samples is shown in Figure 2.1. The laboratory vane shear apparatus (Wykeham-Farrance) used to determine the yield stress of CPB samples is presented in Figure 2.2.

Figure 2.1 Brookfield digital viscometer (DV-E model) used to measure the viscosity of CPB samples. Source: LABOMAT ESSOR SA (n.d.).

Figure 2.2 Laboratory vane shear apparatus (Wykeham-Farrance) used to determine the yield stress of CPB. Source: VJ Tech Limited (n.d.).

2.5 Setting of CPB

The setting process describes the transition of CPB from a fluid material to a rigid, self-supporting structure (Haruna and Fall, 2020; Sagade and Fall, 2024). This evolution is driven by binder hydration or activation reactions and by the progressive formation of an interconnected solid skeleton at early age (Sagade and Fall, 2024; Wu et al., 2013). Initial and final setting times are commonly determined using standardized penetration-based methods such as the Vicat needle (ASTM C191) or the concrete penetration resistance test (ASTM C403/C403M). More recently, ultrasonic pulse velocity (UPV) techniques have been employed as non-destructive tools to monitor stiffness gain and structural development continuously over time (Ercikdi et al., 2014).

Control of setting behavior is essential for ensuring both operational efficiency and underground stability. Rapid setting can shorten the mining cycle by enabling earlier barricade removal and faster stope turnover (Belem and Benzaazoua, 2008), but excessive stiffening during transport may hinder pumpability or cause pipeline blockage (Haruna and Fall, 2020; Ouattara et al., 2018). Conversely, delayed setting prolongs stope exposure and may compromise early-age stability, particularly in water-saturated or weakly confined stopes (Sagade and Fall, 2024; Belem and Benzaazoua, 2008).

The setting characteristics of CPB also play a key role in its liquefaction resistance and early-age structural integrity (Ghirian and Fall, 2016; Sagade and Fall, 2024).

Adequate structuration during the first hours after placement reduces the risk of deformation or instability under self-weight, blasting-induced vibrations, or drainage-related pore pressure changes (Ghirian and Fall, 2016; Belem and Benzaazoua, 2008). Achieving an appropriate balance between workability during transport and rapid early stiffening is therefore critical for safe and efficient backfilling operations (Haruna and Fall, 2020; Sagade and Fall, 2024). The Vicat apparatus used in this study to determine the initial and final setting times of CPB samples is shown in Figure 2.3.

Figure 2.3 Vicat apparatus used to determine the initial and final setting times of CPB. Source: Forney CMT Equipment (n.d.).

2.6 Strength Development in CPB

2.6.1 UCS as a Key Geotechnical Design Parameter

The Unconfined Compressive Strength (UCS) is the primary mechanical design criterion used to evaluate the performance of CPB. It provides a direct measure of the backfill's capacity to support mine openings, resist stress redistribution, and maintain structural integrity under operational and post-mining conditions. Required UCS values vary depending on mine geometry, stope height, extraction sequence, and exposure to blasting-induced loads, but typical design targets range from approximately 0.3 to 1.5 MPa at 28 days (Belem and Benzaazoua, 2008; Yilmaz et al., 2014).

Strength development in CPB is strongly influenced by several interdependent factors, including binder type, binder dosage, curing time, temperature, tailings mineralogy, and the chemical environment within the pore solution (Belem and Benzaazoua, 2008; Benzaazoua et al., 2004). Higher binder contents and elevated curing temperatures generally accelerate hydration or activation reactions (Fall and Pokharel, 2010), while reactive tailings containing silicates or aluminosilicates can enhance gel formation and contribute positively to early-age strength (Benzaazoua et al., 2004). Conversely, sulfide-rich or chemically aggressive tailings may interfere with binder hydration, delay strength gain, or reduce long-term durability (Kesimal et al., 2005).

Given these sensitivities, UCS testing is essential for validating mixture designs, calibrating binder dosages, and ensuring that backfill performance meets the operational requirements of underground mining. The uniaxial compressive strength (UCS) testing machine used in this study to measure the compressive strength of CPB specimens is shown in Figure 2.4.

Figure 2.4 Uniaxial compressive strength (UCS) testing machine used to measure the compressive strength of CPB specimens. Source: Laboratory of Dr. Fall, University of Ottawa.

2.6.2 Geotechnical Design Considerations

Geotechnical design of CPB focuses on ensuring that the backfill provides adequate structural support to the surrounding rock mass and maintains stability throughout the mining cycle. In practice, CPB must withstand horizontal and vertical stress redistribution following ore extraction, and it must resist potential failure mechanisms such as wall sloughing, stope closure, and post-blast instability (Belem and Benzaazoua, 2008).

Empirical or semi-empirical relationships between UCS and the in-situ stress state are commonly used to determine the minimum strength required for safe stope design (Belem and Benzaazoua, 2008). These relationships help establish UCS envelopes for various stope geometries, exposure heights, and blasting sequences. They also guide decisions related to binder dosage and curing time to ensure that the backfill reaches its target strength before being subjected to mining-induced loads (Belem and Benzaazoua, 2008).

Beyond short-term stability, long-term geotechnical performance requires that CPB maintain sufficient cohesion and stiffness under chemical, hydraulic, or mechanical disturbances (Ghirian and Fall, 2013). Degradation mechanisms such as sulfate attack, acid generation from sulfide oxidation, and cyclic loading from repeated blasting operations can alter the microstructure and reduce strength over time (Fall and Pokharel, 2010; Kesimal et al., 2005). Ensuring durability therefore requires careful selection of binder type, optimization of mixture proportions, and control of curing and environmental conditions (Belem and Benzaazoua, 2008; Benzaazoua et al., 2004).

Overall, robust geotechnical design integrates UCS targets, stress analyses, and durability considerations to ensure that CPB performs reliably throughout the mine's operational life.

2.7 Hydration Processes in Portland Cement-Based CPB

2.7.1 Cement Hydration Reactions and Products

In Ordinary Portland Cement (OPC)-based CPB, hydration is driven by the reaction of the main clinker phases (alite (C_3S), belite (C_2S), tricalcium aluminate (C_3A), and tetracalcium aluminoferrite (C_4AF)) with water. These reactions produce calcium silicate hydrate (C-S-H) and calcium hydroxide (CH), which together form the primary binding phases responsible for strength development and stiffness in CPB (Taylor, 1997).

C-S-H is the dominant hydration product and provides most of the mechanical strength due to its cohesive, gel-like structure and ability to refine the pore network (Taylor, 1997). CH, although structurally weaker, contributes to high alkalinity in the pore solution and promotes continued hydration of silicate phases at early age (Taylor, 1997).

Secondary reaction products also form during hydration. Ettringite, produced from the reaction between C_3A, gypsum, and water, contributes to early stiffening and influences setting behavior. As sulfate availability decreases, ettringite may convert to monosulfate, which can influence dimensional stability and long-term chemical behavior (Taylor, 1997). The combined formation of C-S-H, CH, and sulfate-bearing phases governs the evolution of microstructure and mechanical performance in OPC-based CPB systems (Taylor, 1997; Benzaazoua et al., 2004).

2.7.2 Effect of Curing Conditions

Curing conditions, particularly temperature and moisture, play a critical role in controlling hydration kinetics and the resulting mechanical performance of Portland cement-based CPB. Elevated temperatures generally accelerate the hydration of silicate phases and promote faster formation of calcium silicate hydrate (C-S-H), leading to increased early-age strength. However, excessively high temperatures may induce thermal microcracking or contribute to delayed ettringite formation (DEF), both of which can compromise long-term durability and dimensional stability (Fall and Pokharel, 2010; Taylor, 1997).

Moisture availability is equally important. Hydration reactions require continuous access to water, and premature moisture loss reduces the degree of hydration, yielding

lower UCS, higher porosity, and a more heterogeneous microstructure. Unsaturated curing environments can also lead to shrinkage-induced cracking, further weakening the CPB matrix. For these reasons, maintaining a high relative humidity, typically around 95%, and preventing moisture evaporation during early curing are essential to ensure consistent strength development and long-term performance (Ghirian and Fall, 2013; Yilmaz et al., 2014).

Optimal curing practices therefore balance temperature and moisture control to maximize hydration, refine the pore structure, and minimize the risk of early-age damage or degradation (Fall and Pokharel, 2010; Yilmaz et al., 2014).

2.7.3 Transition from Portland cement to alkali-activated binders

In recent years, alternative binders have been developed to address the high carbon footprint associated with Portland cement in cemented paste backfill applications. Among these alternatives, alkali-activated slag (AAS) and geopolymer-based systems have attracted considerable attention as sustainable substitutes. These binders can achieve comparable or superior mechanical strength and durability while significantly reducing CO_2 emissions compared with OPC-based systems (Bernal and Provis, 2014; Habert et al., 2020).

The activation of industrial by-products such as ground granulated blast-furnace slag (GGBFS) using alkaline solutions typically containing sodium hydroxide, sodium carbonate, or sodium silicate produces cementitious gels analogous to the calcium-aluminosilicate-hydrate (C-A-S-H) phases formed in OPC systems (Bernal and Provis, 2014). The increasing interest in such low-carbon binders aligns with the global transition toward more sustainable mine backfilling practices and provides the motivation for the detailed discussion of alkali-activated slag systems presented in the following section (Qi and Fourie, 2019).

2.8 Alkali-Activated Slag Chemistry (AAS) with SC/SH Activators

2.8.1 Activation Mechanisms

Alkali-activated slag (AAS) systems develop their binding properties through the dissolution of the amorphous phases of granulated blast furnace slag followed by the precipitation of calcium-aluminosilicate-hydrate (C-(A)-S-H) gels. These reaction products form the primary binding matrix and are broadly analogous to those observed in Portland cement hydration, although they exhibit distinct chemistry and nanostructure (Provis and Bernal, 2014; Myers et al., 2013).

The reaction pathway and kinetics of AAS strongly depend on the nature of the alkaline activator. Hydroxide-activated systems, typically using sodium hydroxide (NaOH), promote rapid slag dissolution due to their high initial pH. This leads to early gel formation and accelerated strength development. However, high hydroxide concentrations can generate significant heat release and may pose handling and safety challenges (Provis et al., 2015; Shi et al., 2011).

In contrast, carbonate-activated systems based on sodium carbonate (Na_2CO_3) exhibit slower reaction kinetics. Carbonate ions initially buffer the pore solution pH, delaying the dissolution of slag and the precipitation of calcium-rich phases. Early-age reaction products often include intermediate phases such as hydrotalcite-like compounds or calcium carbonate polymorphs before the system transitions toward C-(A)-S-H formation (Ke et al., 2016; Bernal et al., 2014).

Blending sodium carbonate with sodium hydroxide (SC/SH) has emerged as an effective strategy to balance activation rate, safety, and workability. The NaOH component increases early alkalinity and accelerates dissolution, while Na_2CO_3 moderates pH, reduces efflorescence, and lowers handling risks (Abdalqader et al., 2016). This combination results in improved activation efficiency and more controlled reaction kinetics compared with the use of either activator alone (Akturk et al., 2019; Akturk and Kizilkanat, 2020).

2.8.2 Key Parameters Influencing AAS Reactivity

The performance of alkali-activated slag (AAS) systems is governed by several key parameters that control dissolution kinetics, gel formation, and early-age rheology. Among

these, the most influential are the overall activator concentration, the sodium carbonate-to-sodium hydroxide (Na_2CO_3: NaOH) ratio, the liquid-to-solid (L/S) ratio, and curing temperature (Provis and Bernal, 2014).

The total alkalinity, commonly expressed as Na_2O equivalent (Na_2Oeq), dictates the rate of slag dissolution and the subsequent precipitation of C-(A)-S-H gels. Higher Na_2Oeq values generally enhance reactivity and accelerate strength development but may compromise workability by increasing early-age viscosity or promoting rapid structuration (Gebregziabiher et al., 2016). The proportion between Na_2CO_3 and NaOH plays a central role in balancing these effects: NaOH increases initial pH and dissolution rate, whereas Na_2CO_3 moderates pH, improves handling safety, and reduces efflorescence. Optimizing the SC/SH ratio is therefore critical for achieving favourable rheological properties while maintaining sufficient activation efficiency.

The liquid-to-solid (L/S) ratio also influences both workability and mechanical performance (Fall et al., 2008). Lower L/S ratios yield denser matrices and higher long-term strength but can reduce pumpability and hinder homogeneity in CPB applications (Jiang et al., 2022). Conversely, higher L/S ratios increase flowability but may slow down gel formation or result in more porous hardened structures (Fall et al., 2008; Jiang et al., 2022).

Curing temperature further affects reaction kinetics. Higher curing temperatures generally accelerate slag dissolution and enhance early-age strength development of AAS-based CPB, while lower temperatures significantly suppress hydration kinetics (Jiang et al., 2022). However, excessively elevated temperatures can accelerate reactions beyond the optimal regime, potentially leading to a coarser gel microstructure and reduced long-term performance.

Overall, the interplay between activator composition, alkalinity, L/S ratio, and curing temperature defines the rheological response and mechanical evolution of AAS-based CPB mixtures.

2.8.3 Expected Hydration Products

Alkali-activated slag (AAS) systems generate a suite of reaction products that collectively govern the mechanical and durability performance of the material. The primary binding phase is the calcium-aluminosilicate-hydrate (C-(A)-S-H) gel, which forms through the dissolution of slag glassy phases and subsequent precipitation of a cross-linked, low-Ca gel structure. This phase provides the main contribution to stiffness and strength in AAS-based materials (Myers et al., 2013; Walkley et al., 2021).

In addition to C-(A)-S-H, AAS systems commonly produce hydrotalcite-like phases (Mg-Al layered double hydroxides), which incorporate magnesium and aluminum released from slag dissolution. These phases contribute to chemical stability, chloride binding, and long-term performance (Bernal et al., 2014; Myers et al., 2013). Secondary carbonates, such as calcite or hydromagnesite, may also form through reactions involving carbonate ions, atmospheric CO_2, or dissolution-precipitation processes within the pore solution. The presence of carbonates can refine the pore structure by filling capillary voids and enhancing matrix density (Ke et al., 2016).

The activator composition plays a direct role in determining the abundance and chemistry of these products. The addition of NaOH increases initial alkalinity, promotes faster slag dissolution, and enhances cross-linking within C-(A)-S-H gels, resulting in improved early-age strength (Myers et al., 2015; Provis et al., 2015). Conversely, carbonate-rich systems produce reaction products more gradually but may yield denser long-term microstructures due to secondary carbonate formation.

Overall, the interplay between C-(A)-S-H gel formation, hydrotalcite precipitation, and carbonate stabilization influences rheology, setting behavior, and strength evolution in AAS-based CPB systems.

2.8.4 Effects of Binary Binder Blends on the Rheology and Strength Development of CPB

Several studies have investigated the use of binary binder systems in cemented paste backfill with the objective of improving mechanical performance while reducing binder cost and environmental footprint (Fall et al., 2008; Qi and Fourie, 2019). These

systems typically involve the combination of two cementitious or alkali-activated components, such as Portland cement blended with supplementary cementitious materials or alkali-activated slag activated using mixed alkaline solutions.

From a rheological perspective, previous studies have shown that binary blends can significantly influence yield stress and viscosity through changes in particle interactions and early-age reaction kinetics (Jiang et al., 2020). In alkali-activated systems, the combination of sodium carbonate and sodium hydroxide has been reported to provide improved workability compared with single-activator systems, as carbonate ions moderate early alkalinity while hydroxide ions enhance slag dissolution (Ke et al., 2016; Dai et al., 2023). This balance can result in a wider operational window for transport and placement. However, most of these studies were conducted on paste systems or mortars, rather than on full CPB mixtures incorporating real tailings.

Regarding strength development, binary alkali-activated systems have been shown to promote more controlled early-age reactions and improved long-term strength through the formation of dense C-(A)-S-H gels and secondary reaction products such as hydrotalcite-like phases (Myers et al., 2015; Akturk et al., 2019). While enhanced mechanical performance has been reported, the majority of these investigations focus on standardized curing conditions and simplified material matrices, which do not fully capture the complex physical and chemical environment encountered in underground mine backfilling.

Overall, the existing literature demonstrates the potential of binary binder blends to improve the rheological behavior and strength development of cemented paste backfill. Nevertheless, clear gaps remain regarding the coupled evolution of rheology, setting, and strength in CPB systems produced with real tailings and subjected to realistic curing conditions. In particular, limited attention has been given to the simultaneous monitoring of early-age physicochemical processes and mechanical performance in SC/SH-activated slag-based CPB, which constitutes the primary focus of the present research.

2.9 Conclusion

This chapter established the theoretical and technical background required to analyse the behavior of CPB, with emphasis on the transition from conventional Portland cement-based systems to low-carbon binders such as alkali-activated slag (AAS). It first reviewed the main mine backfill technologies (CRF, CHF, and CPB) and highlighted the specific advantages of CPB in terms of tailings management, environmental performance, and mechanical behavior. The discussion then focused on the fundamentals of CPB design, including tailings characteristics, binder types and proportions, mixture preparation, rheology, setting behavior, and Unconfined Compressive Strength (UCS) as the principal design parameter.

The chapter also examined the hydration processes in OPC-based systems and the distinct activation mechanisms governing AAS binders, particularly those activated with blended sodium carbonate/sodium hydroxide (Na_2CO_3-NaOH, SC/SH). The literature indicates that SC/SH-activated slag systems can offer a promising, lower-carbon alternative to Portland cement, with the potential to deliver adequate strength and durability for mine backfilling applications. However, the rheological behavior, setting kinetics, and strength development of these systems within real tailings matrices are still not fully understood.

These knowledge gaps motivate the experimental program developed in this thesis. The following chapters build on the concepts introduced here to investigate, in detail, the fresh properties (rheology and setting) and hardened properties (UCS, microstructure, and pore structure) of SC/SH-activated slag-based CPB, and to assess their suitability as sustainable binders for underground mine backfill.

2.10 References

Abdalqader, A. F., F. Jin, and A. Al-Tabbaa. 2016. "Development of greener alkali-activated cement: utilisation of sodium carbonate for activating slag and fly ash mixtures." *Journal of Cleaner Production*, 113: 66–75.

Akturk, B., and A. B. Kizilkanat. 2020. "Improvement of durability and drying shrinkage of sodium carbonate activated slag through the incorporation of calcium hydroxide and sodium hydroxide." *Construction and Building Materials*, 243: 118260.

Akturk, B., S. Nayak, S. Das, and A. B. Kizilkanat. 2019. "Microstructure and Strength Development of Sodium Carbonate–Activated Blast Furnace Slags." *Journal of Materials in Civil Engineering*, 31 (11): 04019283. American Society of Civil Engineers.

Archibald, J. F., F. Hassani, J. Nantel, and D. O. DeGagne,. 2000. *Mine Backfill, an Operator's Guide. an Interactive Cd-rom for Mine Operators and Engineers*. Montreal, Canada: Canadian Institute of Mining, Metallurgy and Petroleum.

ASTM International. 2016. *Standard Test Method for Time of Setting of Concrete Mixtures by Penetration Resistance*. C403/C403M-16. West Conshohocken, PA: ASTM International.

ASTM International. 2021. *Standard Test Methods for Time of Setting of Hydraulic Cement by Vicat Needle*. C191-21. West Conshohocken, PA: ASTM International.

Belem, T., and M. Benzaazoua. 2008. "Design and Application of Underground Mine Paste Backfill Technology." *Geotechnical and Geological Engineering*, 26 (2): 147–174.

Benzaazoua, M., B. Bussière, I. Demers, M. Aubertin, É. Fried, and A. Blier. 2008. "Integrated mine tailings management by combining environmental desulphurization and cemented paste backfill: Application to mine Doyon, Quebec, Canada." *Minerals Engineering*, Selected Papers from Processing and Disposal of Minerals Industry Wastes '07, Falmouth, UK, June 2007, 21 (4): 330–340.

Benzaazoua, M., M. Fall, and T. Belem. 2004. "A contribution to understanding the hardening process of cemented pastefill." *Minerals Engineering*, Processing and Disposal of Minerals Industry Waste '03, 17 (2): 141–152.

Bernal, S. A., and J. L. Provis. 2014. "Durability of Alkali-Activated Materials: Progress and Perspectives." *Journal of the American Ceramic Society*, 97 (4): 997–1008.

Bernal, S. A., R. San Nicolas, R. J. Myers, R. Mejía de Gutiérrez, F. Puertas, J. S. J. van Deventer, and J. L. Provis. 2014. "MgO content of slag controls phase evolution and structural changes induced by accelerated carbonation in alkali-activated binders." *Cement and Concrete Research*, 57: 33–43.

Dai, X., Q. Ren, S. Aydin, M. Y. Yardimci, and G. De Schutter. 2023. “Accelerating the reaction process of sodium carbonate-activated slag mixtures with the incorporation of a small addition of sodium hydroxide/sodium silicate.” *Cement and Concrete Composites*, 141: 105118.

“Digital Viscometer Model DV-E.” n.d. Accessed March 20, 2026.

Ercikdi, B., T. Yılmaz, and G. Külekci. 2014. “Strength and ultrasonic properties of cemented paste backfill.” *Ultrasonics*, 54 (1): 195–204.

Fall, M., and M. Benzaazoua. 2005. “Modeling the effect of sulphate on strength development of paste backfill and binder mixture optimization.” *Cement and Concrete Research*, 35 (2): 301–314.

Fall, M., M. Benzaazoua, and S. Ouellet. 2005. “Experimental characterization of the influence of tailings fineness and density on the quality of cemented paste backfill.” *Minerals Engineering*, 18 (1): 41–44.

Fall, M., M. Benzaazoua, and E. G. Saa. 2008. “Mix proportioning of underground cemented tailings backfill.” *Tunnelling and Underground Space Technology*, 23 (1): 80–90.

Fall, M., and M. Pokharel. 2010. “Coupled effects of sulphate and temperature on the strength development of cemented tailings backfills: Portland cement-paste backfill.” *Cement and Concrete Composites*, 32 (10): 819–828.

Forney CMT Equipment. n.d. “Modified Vicat Apparatus.” *Forney CMT Equipment*. Accessed March 20, 2026.

Gebregziabiher, B. S., R. J. Thomas, and S. Peethamparan. 2016. “Temperature and activator effect on early-age reaction kinetics of alkali-activated slag binders.” *Construction and Building Materials*, 113: 783–793.

Ghirian, A., and M. Fall. 2013. “Coupled thermo-hydro-mechanical–chemical behaviour of cemented paste backfill in column experiments. Part I: Physical, hydraulic and thermal processes and characteristics.” *Engineering Geology*, 164: 195–207.

Ghirian, A., and M. Fall. 2016. “Strength evolution and deformation behaviour of cemented paste backfill at early ages: Effect of curing stress, filling strategy and drainage.” *International Journal of Mining Science and Technology*, 26 (5): 809–817.

Habert, G., S. A. Miller, V. M. John, J. L. Provis, A. Favier, A. Horvath, and K. L. Scrivener. 2020. “Environmental impacts and decarbonization strategies in the cement and concrete industries.” *Nature Reviews Earth & Environment*, 1 (11): 559–573. Nature Publishing Group.

Haruna, S., and M. Fall. 2020. “Time- and temperature-dependent rheological properties of cemented paste backfill that contains superplasticizer.” *Powder Technology*, 360: 731–740.

Jiang, H., M. Fall, E. Yilmaz, Y. Li, and L. Yang. 2020. “Effect of mineral admixtures on flow properties of fresh cemented paste backfill: Assessment of time dependency and thixotropy.” *Powder Technology*, 372: 258–266.

Jiang, H., L. Ren, Q. Zhang, J. Zheng, and L. Cui. 2022. “Strength and microstructural evolution of alkali-activated slag-based cemented paste backfill: Coupled effects of activator composition and temperature.” *Powder Technology*, 401: 117322.

Ke, X., S. A. Bernal, and J. L. Provis. 2016. “Controlling the reaction kinetics of sodium carbonate-activated slag cements using calcined layered double hydroxides.” *Cement and Concrete Research*, 81: 24–37.

Kesimal, A., E. Yilmaz, B. Ercikdi, I. Alp, and H. Deveci. 2005. “Effect of properties of tailings and binder on the short-and long-term strength and stability of cemented paste backfill.” *Materials Letters*, 59 (28): 3703–3709.

“Laboratory Vane Apparatus.” n.d. *VJ Tech Limited*. Accessed March 20, 2026.

Liu, G., L. Li, M. Yao, D. Landry, F. Malek, X. Yang, and L. Guo. 2017. “An Investigation of the Uniaxial Compressive Strength of a Cemented Hydraulic Backfill Made of Alluvial Sand.” *Minerals*, 7 (1). Multidisciplinary Digital Publishing Institute.

Myers, R. J., S. A. Bernal, J. D. Gehman, J. S. J. van Deventer, and J. L. Provis. 2015. “The Role of Al in Cross-Linking of Alkali-Activated Slag Cements.” *Journal of the American Ceramic Society*, 98 (3): 996–1004.

Myers, R. J., S. A. Bernal, R. San Nicolas, and J. L. Provis. 2013. “Generalized Structural Description of Calcium–Sodium Aluminosilicate Hydrate Gels: The Cross-Linked Substituted Tobermorite Model.” *Langmuir*, 29 (17): 5294–5306. American Chemical Society.

Ouattara, D., M. Mbonimpa, A. Yahia, and T. Belem. 2018. “Assessment of rheological parameters of high density cemented paste backfill mixtures incorporating superplasticizers.” *Construction and Building Materials*, 190: 294–307.

Ouattara, D., A. Yahia, M. Mbonimpa, and T. Belem. 2017. “Effects of superplasticizer on rheological properties of cemented paste backfills.” *International Journal of Mineral Processing*, 161: 28–40.

Potvin, Y., E. Thomas, and A. Fourie. 2005. *Handbook on Mine Fill*. Nedlands, Western Australia, Australia: Australian Centre for Geomechanics.

Provis, J. L., and S. A. Bernal. 2014. “Geopolymers and Related Alkali-Activated Materials.” *Annual Review of Materials Research*, 44: 299–327. Annual Reviews.

Provis, J. L., A. Palomo, and C. Shi. 2015. “Advances in understanding alkali-activated materials.” *Cement and Concrete Research*, Keynote papers from 14th International Congress on the Chemistry of Cement (ICCC 2015), 78: 110–125.

Qi, C., and A. Fourie. 2019. “Cemented paste backfill for mineral tailings management: Review and future perspectives.” *Minerals Engineering*, 144: 106025.

Roshani, A., and M. Fall. 2020. “Flow ability of cemented pastefill material that contains nano-silica particles.” *Powder Technology*, 373: 289–300.

Sagade, A., and M. Fall. 2024. “Study of fresh properties of cemented paste backfill material with ternary cement blends.” *Construction and Building Materials*, 411: 134287.

Shi, C., A. F. Jiménez, and A. Palomo. 2011. “New cements for the 21st century: The pursuit of an alternative to Portland cement.” *Cement and Concrete Research*, Special Issue: 13th International Congress on the Chemistry of Cement, 41 (7): 750–763.

Sivakugan, N., R. M. Rankine, K. J. Rankine, and K. S. Rankine. 2006. “Geotechnical considerations in mine backfilling in Australia.” *Journal of Cleaner Production*, Improving Environmental, Economic and Ethical Performance in the Mining Industry. Part 2. Life cycle and process analysis and technical issues, 14 (12): 1168–1175.

Taylor, H. F. W. 1997. *Cement Chemistry*. 2nd Edition. London: Thomas Telford.

Walkley, B., X. Ke, J. L. Provis, and S. A. Bernal. 2021. “Activator Anion Influences the Nanostructure of Alkali-Activated Slag Cements.” *The Journal of Physical Chemistry C*, 125 (37): 20727–20739. American Chemical Society.

Wu, D., M. Fall, and S. J. Cai. 2013. “Coupling temperature, cement hydration and rheological behaviour of fresh cemented paste backfill.” *Minerals Engineering*, 42: 76–87.

Xiapeng, P., M. Fall, and S. Haruna. 2019. “Sulphate induced changes of rheological properties of cemented paste backfill.” *Minerals Engineering*, 141: 105849.

Yang, L., H. Wang, A. Wu, H. Li, A. B. Tchamba, and T. A. Bier. 2019. “Shear thinning and thickening of cemented paste backfill.” *Applied Rheology*, 29 (1): 80–93. De Gruyter Open Access.

Yilmaz, E., T. Belem, and M. Benzaazoua. 2014. “Effects of curing and stress conditions on hydromechanical, geotechnical and geochemical properties of cemented paste backfill.” *Engineering Geology*, 168: 23–37.

Chapter 3: Literature Review on Fresh and Strength Properties of CPB with Low-Carbon Binders

3.1 Introduction and Scope

CPB is increasingly used in underground mining due to its combined geotechnical and environmental benefits (Belem and Benzaazoua, 2008). However, the conventional reliance on ordinary Portland cement (OPC) as the primary binder leads to high CO_2 emissions and significant binder-related costs. In recent years, low-carbon binders, particularly alkali-activated materials (AAMs), have emerged as promising alternatives for CPB, as they can reduce the carbon footprint while maintaining satisfactory mechanical and durability performance (Provis, 2018; Cihangir et al., 2012). In the context of stricter environmental regulations and growing societal expectations, the integration of such sustainable binders into backfill technology is becoming increasingly important for the mining industry (Habert et al., 2020).

Among the various AAMs, alkali-activated slag (AAS) systems have attracted considerable attention because they allow the valorization of industrial by-products while potentially achieving mechanical performance comparable to OPC-based binders (Cihangir et al., 2012). When used in CPB, these binders must satisfy multiple, sometimes conflicting, requirements. The fresh-state properties, including rheological behavior (yield stress, plastic viscosity) and setting time, must ensure pumpability through long pipelines and adequate stability after placement (Kou et al., 2020). At the same time, the hardened properties, typically evaluated through unconfined compressive strength (UCS), must meet design criteria for stope stability and safe mining operations (Belem and Benzaazoua, 2008).

Alkali-activated slag binders activated with sodium carbonate (Na_2CO_3) and sodium hydroxide (NaOH) are of particular interest, as their combined use offers opportunities to control hydration kinetics, rheological evolution, and strength development (Bernal et al., 2015a). However, despite growing research on AAS-based systems, the specific behavior of CPB incorporating these blended activators under realistic conditions remains insufficiently understood (Jiang et al., 2023). A critical synthesis of

existing studies is therefore required to identify the main trends, governing parameters, and remaining uncertainties.

This chapter provides a critical review of the literature on the fresh and mechanical behavior of CPB produced with low-carbon binders, with emphasis on alkali-activated slag systems activated by Na_2CO_3 and NaOH. The review focuses on rheological properties, setting kinetics, and UCS development, and examines how binder type, activator chemistry, and mixture design influence these key performance criteria.

The chapter is organized as follows:

Section 3.2 summarizes previous studies on the rheological properties and setting times of CPB incorporating alkali-activated slag binders.

Section 3.3 discusses strength development mechanisms and the main factors influencing UCS in AAS-based CPB systems.

Section 3.4 identifies the existing knowledge gaps and outlines the motivation for the present research.

Section 3.5 concludes the chapter by linking the main findings of the literature review to the overall objectives of this thesis.

3.2 Previous Studies on Rheological Properties and Setting Times of CPB with AAS Systems

3.2.1 Reported Rheological Behaviors and Controlling Variables

The rheological behavior of CPB is a fundamental design parameter because it governs flowability, pumpability, and overall handling during transport and placement in underground stopes. Fresh CPB mixtures typically exhibit yield-pseudoplastic behavior that can be described using viscoplastic models such as the Bingham or Herschel-Bulkley formulations, where the response is mainly characterized by the yield stress (τ_0) and plastic viscosity (μ_p) (Ouattara et al., 2018; Kou et al., 2020; Haruna and Fall, 2020). These parameters are influenced by several interacting factors, including solid concentration, particle size distribution and morphology, binder chemistry, activator composition, temperature, and the evolution of early-age hydration products (Kou et al., 2020).

For OPC-based CPB, numerous studies have shown that both τ_0 and μ_p increase with higher solid content, more angular tailings, and elapsed time after mixing, due to the progressive formation of hydration products that promote particle bridging and structuration (Ouattara et al., 2018; Cheng et al., 2020). In alkali-activated slag (AAS) systems, rheology is additionally influenced by the formation rate and nature of early reaction products such as calcium-(alumino)-silicate-hydrate (C-(A)-S-H) gels and hydrotalcite-like phases (Bernal et al., 2015a). When highly alkaline activators such as NaOH or sodium silicate are used, slag dissolution proceeds rapidly, leading to early gel formation and a correspondingly faster increase in yield stress and viscosity (Dai et al., 2022a; Lu et al., 2022).

Sodium carbonate (Na_2CO_3) activation results in a distinctly different rheological evolution, because Na_2CO_3 produces a slower rise in pore-solution pH and involves the formation of transient carbonate-bearing intermediates before the development of a stable C-(A)-S-H gel network. As a result, stiffening tends to be delayed, and mixtures often exhibit extended workability during the first minutes after mixing (Ke et al., 2016; Bernal et al., 2016; Yuan et al., 2017). However, purely Na_2CO_3-activated slag systems can show slow reaction kinetics and poor early mechanical performance if no additional source of alkalinity is provided.

Several studies have attempted to quantitatively describe these behaviors. Ouattara et al. (2018) demonstrated that the Bingham model adequately represents CPB rheology across a wide range of mixture compositions and reported an exponential-type increase in τ_0 with increasing solids content and binder dosage. For CPB incorporating alkali-activated slag, Kou et al. (2020) also reported that the Bingham formulation captures the time-dependent evolution of τ_0 and μ_p, while showing that activator modulus and curing temperature strongly influence rheological parameters. In AAS pastes and mortars, Walkley et al. (2021) showed that the nature of the activator anion (e.g., OH^-, CO_3^{2-}, SO_4^{2-}) significantly affects the nanostructure and local hydration environment of the binding gel, which in turn influences early-age rheology and structural build-up.

In Na_2CO_3-based systems, increasing the carbonate dosage may initially improve flowability by delaying extensive gel formation, but as carbonate-containing phases

precipitate, both τ_0 and μ_p tend to increase (Yuan et al., 2017; Kiiashko et al., 2021). For this reason, blended activation with Na_2CO_3 and NaOH (or with sodium silicate) has been proposed as a promising strategy to balance early workability with adequate reaction kinetics (Bernal et al., 2016). Dai et al. (2023) reported that adding a small amount of NaOH to Na_2CO_3-activated slag accelerates early hydration, shortens setting time, and increases early compressive strength, while maintaining the favourable rheological characteristics associated with carbonate activation. Similar trends have been observed in other hybrid-activator systems, where the combined presence of carbonate and hydroxide ions enhances slag dissolution and promotes earlier formation of a load-bearing gel network (Ke et al., 2016).

Beyond activator chemistry, the ionic strength and composition of the pore solution also play important roles in determining interparticle interactions. High concentrations of Na^+ and CO_3^{2-} ions can modify the electrical double layer around tailings particles, affecting the balance between flocculation and dispersion and influencing both yield stress and viscosity (Lu et al., 2022). Divalent cations such as Mg^{2+}, originating from slag or tailings, may contribute to the formation of hydrotalcite-like phases, which can enhance structuration and affect the thixotropic response of fresh mixtures (Bernal et al., 2015a).

From an experimental standpoint, rheological characterization of CPB is commonly performed using rotational rheometers fitted with vane geometries, which are well suited to the analysis of highly concentrated, yield-stress materials and allow accurate determination of τ_0 and μ_p from torque-shear-rate relationships (Ouattara et al., 2018; Kou et al., 2020). These measurements are often complemented by practical workability tests such as slump cone or flow spread measurements (Belem and Benzaazoua, 2008; Ouattara et al., 2018). Despite these advances, the majority of published work remains focused on OPC-based CPB or AAS systems activated with silicate or hydroxide solutions. Systematic rheological studies dedicated specifically to CPB produced with slag activated by blended Na_2CO_3-NaOH solutions remain limited, particularly under realistic solids contents and curing conditions, highlighting the need for further research in this area.

3.2.2 Reported Setting Times and Controlling Variables

Setting time is a critical operational parameter in CPB applications because it determines how soon subsequent mining activities can safely resume after filling (Nasir and Fall, 2010). It reflects the early hydration kinetics of the binder and the rate at which a continuous, load-bearing network forms within the paste. In OPC-based systems, setting behavior is primarily governed by the hydration of alite (C_3S) and tricalcium aluminate (C_3A), leading to the precipitation of ettringite and calcium-silicate-hydrate (C-S-H) phases that progressively increase stiffness (Taylor, 1997).

In alkali-activated slag (AAS) systems, the mechanisms underlying setting differ markedly from those in OPC. Setting is controlled by the dissolution of the amorphous slag phase and the subsequent precipitation of reaction products such as C-(A)-S-H gels and, depending on activator chemistry, carbonate-bearing phases (Bernal et al., 2016). The type, concentration, and alkalinity of the activator exert strong influence over early-age behavior (Ke et al., 2016). Activation with NaOH generally promotes rapid setting due to the high pH of the pore solution, which enhances slag dissolution and accelerates gel formation (Ke et al., 2016). In contrast, Na_2CO_3 activation is typically associated with significantly delayed setting, primarily because the initial pH is lower and intermediate carbonate phases form before the main binding gels appear (Ke et al., 2016; Bernal et al., 2015a).

Hybrid activation combining Na_2CO_3 and NaOH has been proposed as an effective strategy to balance these contrasting effects. By partially replacing Na_2CO_3 with NaOH, it is possible to increase pore-solution alkalinity, accelerate slag dissolution, and reduce setting times without completely sacrificing the improved workability associated with carbonate activation. Dai et al. (2023) reported that such hybrid mixtures can reduce setting times from several hours to less than one hour, depending on curing temperature and the overall Na_2Oeq content of the activator.

Other variables also influence early setting in AAS-based systems. Elevated curing temperatures tend to accelerate reaction kinetics and shorten setting time, while the chemical composition of tailings, particularly their sulfate, carbonate, or reactive mineral content, may either accelerate or delay the formation of a coherent gel network (Jiang et al., 2022a). Adequate moisture availability during early curing is also critical: premature

drying can interrupt the formation of hydration products, slow the stiffening process, and promote microcracking (Collins and Sanjayan, 2001).

Overall, while the setting behavior of AAS pastes, mortars, and concretes has been widely studied, dedicated investigations focusing on AAS-based CPB, with particular attention to mixtures activated using combined Na_2CO_3-NaOH solutions, remain limited. This lack of systematic data under realistic CPB mix designs and curing conditions highlights the need for further research, particularly to support operational decision-making in mining environments.

3.3 Previous Studies on Strength of CPB with Alkali-Activated Slag (AAS)

3.3.1 UCS Evolution in AAS-Based Systems

The UCS is the most commonly used indicator of the mechanical performance and in situ stability of CPB. In OPC-based CPB, UCS typically increases with curing time following a logarithmic-type trend, as progressive hydration refines the pore structure, reduces total porosity, and densifies the cementitious matrix (Fall et al., 2010). This behavior is relatively well understood and can often be related to classical cement hydration mechanisms and maturity concepts.

For alkali-activated slag (AAS) binders, the evolution of UCS is more sensitive to the chemistry of the activator, slag reactivity, and curing conditions (Bernal et al., 2016; Ke et al., 2016). In Na_2CO_3-activated slag systems, early-age strength is often limited because slag dissolution proceeds more slowly and transient carbonate phases form before a stable C-(A)-S-H network is established (Bernal et al., 2016; Ke et al., 2016). As hydration progresses and secondary C-(A)-S-H and related reaction products develop, the long-term strength can, however, approach or even exceed that of comparable OPC-based materials (Cihangir et al., 2018). In contrast, activation with NaOH or sodium silicate generally promotes faster dissolution of the slag glass and accelerates gel formation, which translates into significantly higher UCS at early ages (for example, 3-7 days), while still achieving comparable or superior strengths at longer curing times such as 28 or 56 days (Dai et al., 2022b; Jiang et al., 2022b).

The influence of curing conditions on strength development in AAS-based systems has also been emphasized. Jiang et al. (2022b) reported that curing temperature significantly affects the strength evolution of AAS-CPB, with higher temperatures consistently enhancing UCS development across all tested activator concentrations and silica moduli; the positive effect of temperature was more pronounced in AAS-CPB than in OPC-based systems, particularly at early curing ages. The availability of moisture during curing is also critical, as self-desiccation in AAS systems can limit slag hydration and reduce long-term strength gain (Ke et al., 2016).

Most of these findings, however, are based on paste or mortar specimens, and only a limited number of studies have examined full CPB mixtures incorporating actual tailings. In CPB, the interaction between tailings minerals and AAS hydration products can significantly modify strength evolution compared with pure slag systems. The MgO content of the slag, for instance, controls the formation of hydrotalcite-like phases alongside C-(A)-S-H, which in turn influences both the magnitude and durability of the developed strength (Walkley et al., 2021). When the tailings themselves contain appreciable amounts of Mg or Fe, additional secondary reactions may further modify the phase assemblage and strength evolution of AAS-CPB, though this remains an area requiring further systematic investigation. These observations highlight the need for additional systematic research on AAS-based CPB that explicitly considers the coupled effects of activator chemistry, curing conditions, and tailings mineralogy on UCS development.

3.3.2 Factors Affecting UCS Evolution in AAS-Based CPB

The evolution of UCS in alkali-activated slag (AAS)-based CPB is governed by a combination of chemical, physical, and environmental parameters. The main factors reported in the literature are outlined below.

Activator Concentration and Composition.

The concentration of the alkaline activator, usually expressed in terms of Na_2O equivalent (Na_2Oeq), is one of the most influential parameters controlling slag dissolution and early gel formation (Ke et al., 2016). Higher Na_2Oeq contents generally enhance the

rate of activation and promote early-age strength development, although excessively high concentrations may reduce workability and cause premature stiffening (Ke et al., 2016; Dai et al., 2022a). In blended activator systems, the balance between Na_2CO_3 and NaOH is particularly important. A larger fraction of NaOH tends to accelerate the initial dissolution of slag (Ke et al., 2016), while Na_2CO_3 contributes to a more gradual formation of secondary C-(A)-S-H gels, affecting both short-term and long-term strength (Dai et al., 2023).

Liquid-to-Solid (L/S) Ratio.

The L/S ratio affects both the rheology of the fresh mixture and the porosity of the hardened matrix (Ouattara et al., 2018). Lower ratios typically lead to denser microstructures and higher UCS due to reduced capillary porosity (Fall et al., 2010). However, overly low L/S ratios can compromise flowability and mixing efficiency, which are critical operational considerations in CPB placement (Ouattara et al., 2018). The optimal L/S ratio depends on the particle size distribution of the tailings as well as the fineness and reactivity of the slag binder (Ouattara et al., 2018; Dai et al., 2022b).

Curing Conditions.

Temperature and humidity exert strong control over hydration kinetics and gel development (Jiang et al., 2022b). Curing conditions around 20 to 25 °C and high relative humidity (typically above 90%) are commonly reported to favour consistent strength gain by ensuring continuous access to moisture (Ke et al., 2016). Higher temperatures accelerate early reactions but can induce thermal stresses in fresh CPB, while inadequate humidity may interrupt hydration and reduce UCS (Ke et al., 2016).

Tailings Mineralogy.

The chemical and mineralogical characteristics of the tailings also influence strength evolution. Reactive silica, alumina, and magnesia present in the tailings may participate in secondary hydration reactions, contributing to the formation of C-(A)-S-H and hydrotalcite-like phases (Walkley et al., 2021). In contrast, sulfide-rich tailings can undergo oxidation and generate acidic by-products that negatively affect long-term strength and durability (Cihangir et al., 2018).

Binder Dosage.

Increasing slag dosage typically enhances UCS by increasing the amount of hydration products capable of binding the matrix (Cihangir et al., 2018). However, higher binder contents also raise material costs and embodied energy (Belem and Benzaazoua, 2008). Determining an optimal binder dosage is therefore essential to balance mechanical performance with economic and environmental considerations (Belem and Benzaazoua, 2008).

Although significant research has been conducted on AAS mortars and concretes, relatively few studies have examined CPB systems activated with blended Na_2CO_3-NaOH solutions. In these mixtures, both rheological behavior and UCS development must meet operational requirements for underground backfilling. The limited data available underscore the need for systematic investigations under realistic CPB mix designs and curing conditions.

3.4 Knowledge Gaps and Research Needs

Although considerable progress has been made in understanding alkali-activated slag (AAS) binders, several key knowledge gaps remain regarding their application in CPB. These gaps limit the development of robust, low-carbon backfill systems capable of meeting operational requirements in mining environments.

Limited Data on Na_2CO_3-NaOH Co-Activation in CPB.

Most available studies on AAS systems are based on paste, mortar, or concrete formulations. Their direct application to CPB is challenging because CPB contains much higher water contents and large proportions of fine tailings, which influence ionic equilibria, dissolution rates, and overall reaction kinetics (Fall et al., 2010; Jiang et al., 2022b). As a result, the behavior of Na_2CO_3-NaOH co-activation observed in paste systems cannot be directly assumed for CPB mixtures (Dai et al., 2023).

Limited Transferability from Concrete to CPB.

Tailings differ significantly from conventional aggregates used in concrete in terms of mineralogy, particle size, and reactivity. Fine tailings with high specific surface areas

strongly affect rheology and setting behavior (Ouattara et al., 2018), while tailings rich in Fe, S, or Mg may participate in or disrupt hydration reactions (Walkley et al., 2021; Cihangir et al., 2018). Such interactions alter gel chemistry and subsequent strength (Walkley et al., 2021; Cihangir et al., 2018). Consequently, data from concrete-based studies have limited predictive value for CPB applications (Dai et al., 2023).

Insufficient Understanding of Early-Age Behavior.

The combined evolution of rheology, setting time, and early strength under the high-moisture, low-stress, and often variable temperature conditions typical of underground mines remains poorly documented. The lack of integrated early-age data prevents accurate modelling of CPB pumpability, placement behavior, and the timing of safe re-entry for mining operations.

Limited Insight into the Microstructural Impact of Activator Chemistry.

While Na_2CO_3-NaOH activation has been examined in simplified paste systems (Ke et al., 2016; Dai et al., 2023), its microstructural implications in CPB containing complex tailings matrices are not well understood. Interactions between tailings minerals and AAS hydration products may influence gel morphology, reaction pathways, and the formation of C-(A)-S-H and hydrotalcite-type phases (Walkley et al., 2021; Ke et al., 2016), but these effects have not been systematically studied.

Lack of Optimisation Frameworks for Practical Applications.

For field implementation, AAS-based CPB must meet specific operational requirements. Fresh mixtures must maintain adequate flowability for pipeline transport and placement, while hardened backfill must achieve sufficient strength to ensure stope stability and safe re-entry for mining personnel (Belem and Benzaazoua, 2008; Ouattara et al., 2018). Target UCS values typically range from 0.3 to 1.5 MPa depending on the intended application, with early-age strength development being particularly critical for mine scheduling (Belem and Benzaazoua, 2008; Fall et al., 2010). Current literature does not provide sufficient information to establish mix design guidelines for AAS-CPB with Na_2CO_3-NaOH co-activation that balance mechanical performance, cost, workability, and safety considerations.

Addressing these limitations through systematic laboratory studies on tailings-based CPB, particularly mixtures incorporating Na_2CO_3-NaOH co-activation, is essential for advancing reliable and sustainable alternatives to OPC-based binders for mine backfilling.

3.5 Summary and Conclusions

This chapter has reviewed the current state of knowledge on the fresh and hardened properties of CPB incorporating low-carbon binders, with particular emphasis on alkali-activated slag (AAS) systems. The main findings from the literature can be summarised as follows.

First, the rheological and setting behavior of CPB is primarily governed by solids concentration, particle morphology, and binder chemistry (Ouattara et al., 2018; Haruna and Fall, 2020). In AAS-based systems, the type, composition, and dosage of the activator play a dominant role in controlling flowability, thixotropy, and setting kinetics (Ke et al., 2016; Dai et al., 2022a). Activator chemistry therefore constitutes a key design variable for ensuring adequate pumpability and operationally acceptable setting times.

Second, Na_2CO_3 activation offers advantages in terms of handling safety, cost, and environmental impact compared with highly alkaline hydroxide or silicate solutions (Provis, 2018; Habert et al., 2020). However, it is generally associated with slower reaction kinetics and limited early-age strength (Ke et al., 2016; Dai et al., 2023). Partial replacement of Na_2CO_3 with NaOH has been shown to enhance slag dissolution, increase early reactivity, and provide a more favourable balance between workability and strength development, although the optimum Na_2CO_3-NaOH ratio remains mixture- and application-dependent (Dai et al., 2023; Haruna and Fall, 2020).

Third, strength evolution in AAS-based CPB is controlled by the combined effects of activator chemistry, curing conditions (temperature and humidity), and tailings mineralogy (Ke et al., 2016; Jiang et al., 2022b; Cihangir et al., 2018). The formation of C-(A)-S-H and hydrotalcite-type phases is widely recognised as the principal contributor to mechanical integrity and long-term performance (Walkley et al., 2021; Ke et al., 2016). At the same time, inappropriate curing regimes or adverse tailings compositions (for

example, high sulfide contents) can impair strength development and durability (Cihangir et al., 2018; Fall et al., 2010).

Fourth, the existing body of research on AAS binders in CPB remains relatively limited, particularly for systems activated with Na_2CO_3-NaOH blends. The specific characteristics of tailings, such as fineness, mineralogy, and sulfide or carbonate contents, combined with the high water and solids contents typical of CPB, mean that results obtained on pastes, mortars, or concretes cannot be directly extrapolated to backfill applications (Ouattara et al., 2018; Dai et al., 2023). Dedicated studies are required to optimize both rheological and mechanical performance under realistic CPB conditions.

In light of these gaps, the present research is designed to experimentally evaluate the fresh and strength properties of CPB produced with ground granulated blast furnace slag (GGBFS) activated by a blend of sodium carbonate and sodium hydroxide (SC+SH). The study focuses on key operational parameters such as flowability, setting time, and unconfined compressive strength at relevant curing ages, while explicitly accounting for the influence of activator composition, curing regime, and tailings characteristics.

By systematically investigating SC+SH-activated slag binders in tailings-based CPB, this work aims to provide data and insights that support the development of environmentally sustainable and technically reliable backfill materials for modern mining operations. The conclusions drawn from this literature review directly underpin the research objectives and experimental programme presented in the next chapter, where the materials, mix designs, and testing methodologies are described in detail.

3.6 References

Belem, T., and M. Benzaazoua. 2008. “Design and Application of Underground Mine Paste Backfill Technology.” *Geotechnical and Geological Engineering*, 26 (2): 147–174.

Bernal, S. A., J. L. Provis, R. J. Myers, R. San Nicolas, and J. S. J. van Deventer. 2015a. “Role of carbonates in the chemical evolution of sodium carbonate-activated slag binders.” *Materials and Structures*, 48 (3): 517–529.

Bernal, S. A., R. San Nicolas, J. S. J. van Deventer, and J. L. Provis. 2016. “Alkali-activated slag cements produced with a blended sodium carbonate/sodium silicate activator.” *Advances in Cement Research*, 28 (4): 262–273.

Cheng, H., S. Wu, H. Li, and X. Zhang. 2020. “Influence of time and temperature on rheology and flow performance of cemented paste backfill.” *Construction and Building Materials*, 231: 117117.

Cihangir, F., B. Ercikdi, A. Kesimal, S. Ocak, and Y. Akyol. 2018. “Effect of sodium-silicate activated slag at different silicate modulus on the strength and microstructural properties of full and coarse sulphidic tailings paste backfill.” *Construction and Building Materials*, 185: 555–566.

Cihangir, F., B. Ercikdi, A. Kesimal, A. Turan, and H. Deveci. 2012. “Utilisation of alkali-activated blast furnace slag in paste backfill of high-sulphide mill tailings: Effect of binder type and dosage.” *Minerals Engineering*, 30: 33–43.

Collins, F., and J. G. Sanjayan. 2001. “Microcracking and strength development of alkali activated slag concrete.” *Cement and Concrete Composites*, 23 (4): 345–352.

Dai, X., S. Aydin, M. Y. Yardimci, and G. De Schutter. 2022a. “Rheology and structural build-up of sodium silicate- and sodium hydroxide-activated GGBFS mixtures.” *Cement and Concrete Composites*, 131: 104570.

Dai, X., L. Ren, X. Gu, E. Yilmaz, K. Fang, and H. Jiang. 2022b. “Strength Analysis and Optimization of Alkali Activated Slag Backfills Through Response Surface Methodology.” *Frontiers in Materials*, 9: 844608. Frontiers.

Dai, X., Q. Ren, S. Aydin, M. Y. Yardimci, and G. De Schutter. 2023. “Accelerating the reaction process of sodium carbonate-activated slag mixtures with the incorporation of a small addition of sodium hydroxide/sodium silicate.” *Cement and Concrete Composites*, 141: 105118.

Fall, M., J. C. Célestin, M. Pokharel, and M. Touré. 2010. “A contribution to understanding the effects of curing temperature on the mechanical properties of mine cemented tailings backfill.” *Engineering Geology*, 114 (3): 397–413.

Habert, G., S. A. Miller, V. M. John, J. L. Provis, A. Favier, A. Horvath, and K. L. Scrivener. 2020. “Environmental impacts and decarbonization strategies in the cement and concrete industries.” *Nature Reviews Earth & Environment*, 1 (11): 559–573. Nature Publishing Group.

Haruna, S., and M. Fall. 2020. “Time- and temperature-dependent rheological properties of cemented paste backfill that contains superplasticizer.” *Powder Technology*, 360: 731–740.

Jiang, D., C. Shi, and Z. Zhang. 2022a. “Recent progress in understanding setting and hardening of alkali-activated slag (AAS) materials.” *Cement and Concrete Composites*, 134: 104795.

Jiang, H., L. Ren, X. Gu, J. Zheng, and L. Cui. 2023. “Synergistic effect of activator nature and curing temperature on time-dependent rheological behavior of cemented paste backfill containing alkali-activated slag.” *Environmental Science and Pollution Research*, 30 (5): 12857–12871.

Jiang, H., L. Ren, Q. Zhang, J. Zheng, and L. Cui. 2022b. “Strength and microstructural evolution of alkali-activated slag-based cemented paste backfill: Coupled effects of activator composition and temperature.” *Powder Technology*, 401: 117322.

Ke, X., S. A. Bernal, and J. L. Provis. 2016. “Controlling the reaction kinetics of sodium carbonate-activated slag cements using calcined layered double hydroxides.” *Cement and Concrete Research*, 81: 24–37.

Kiiashko, A., M. Chaouche, and L. Frouin. 2021. “Effect of phosphonate addition on sodium carbonate activated slag properties.” *Cement and Concrete Composites*, 119: 103986.

Kou, Y., H. Jiang, L. Ren, E. Yilmaz, and Y. Li. 2020. “Rheological Properties of Cemented Paste Backfill with Alkali-Activated Slag.” *Minerals*, 10 (3). Multidisciplinary Digital Publishing Institute.

Lu, C., Z. Zhang, J. Hu, QijunYu, and C. Shi. 2022. “Effects of anionic species of activators on the rheological properties and early gel characteristics of alkali-activated slag paste.” *Cement and Concrete Research*, 162: 106968.

Nasir, O., and M. Fall. 2010. “Coupling binder hydration, temperature and compressive strength development of underground cemented paste backfill at early ages.” *Tunnelling and Underground Space Technology*, 25 (1): 9–20.

Ouattara, D., M. Mbonimpa, A. Yahia, and T. Belem. 2018. “Assessment of rheological parameters of high density cemented paste backfill mixtures incorporating superplasticizers.” *Construction and Building Materials*, 190: 294–307.

Provis, J. L. 2018. “Alkali-activated materials.” *Cement and Concrete Research*, Report of UNEP SBCI working group on low-co2 eco-efficient cement-based materials, 114: 40–48.

Taylor, H. F. W. 1997. *Cement Chemistry*. 2nd Edition. London: Thomas Telford.

Walkley, B., X. Ke, J. L. Provis, and S. A. Bernal. 2021. “Activator Anion Influences the Nanostructure of Alkali-Activated Slag Cements.” *The Journal of Physical Chemistry C*, 125 (37): 20727–20739. American Chemical Society.

Yuan, B., Q. L. Yu, and H. J. H. Brouwers. 2017. “Time-dependent characterization of Na2CO3 activated slag.” *Cement and Concrete Composites*, 84: 188–197.

Chapter 4: Technical Paper 1: Hydration Mechanisms and Strength Development in Slag-Based Cemented Paste Backfill Activated by Blended Sodium Carbonate–Sodium Hydroxide

Soya Bathily, Mamadou Fall, Abdurrahman Suleiman Mohammed

Author Contributions

Soya Bathily: Formal analysis, Investigation, Methodology, Visualization, Writing – original draft. Mamadou Fall: Conceptualization, Methodology, Project administration, Resources, Supervision, Funding Acquisition; Writing – review & editing. Abdurrahman Suleiman: Analysis, Methodology, Writing – review & editing

(Submitted for publication)

Abstract

Slag-based alkali-activated binders have emerged as promising low-carbon alternatives to Portland cement for cemented paste backfill (CPB), offering significant potential to reduce the environmental footprint and CO_2 emissions associated with cement production while promoting the valorization of industrial by-products. However, sodium carbonate (SC) activation is commonly associated with pronounced early-age kinetic retardation, limiting its practical implementation in sustainable backfill systems. This study investigates the hydration mechanisms, microstructural evolution, physical property development, and strength performance of slag-based CPB activated with blended sodium carbonate and sodium hydroxide (SH) under realistic high water-to-binder CPB conditions. A systematic evaluation of SC/SH ratios and total activator dosages was conducted using an integrated monitoring framework combining electrical conductivity (EC), volumetric water content (VWC), and matric suction (ψ) to resolve hydration kinetics and matrix densification processes. X-ray diffraction analysis revealed the formation of environmentally stable hydration products dominated by amorphous C-(A)-S-H gels, calcite, and hydrotalcite-like phases. Hybrid SC–SH activation fundamentally altered

hydration pathways, reducing retardation effects and promoting accelerated gel formation and pore refinement. Balanced SC/SH ratios significantly enhanced matrix densification and strength development, with the SC/SH (50/50)–10% formulation achieving strength levels comparable to Portland cement-based CPB while maintaining lower environmental impact. The findings demonstrate that hybrid alkali activation provides an effective strategy to overcome kinetic limitations and enables the development of sustainable, low-carbon backfill materials. This approach supports cleaner production in mining by reducing cement consumption, promoting industrial waste utilization, and facilitating environmentally responsible underground infrastructure development.

Keywords: cemented paste backfill; alkali-activated slag; low-carbon binder; cleaner production; industrial by-product utilization; sustainable mining; sodium carbonate–sodium hydroxide activation

4.1 Introduction

CPB has become an essential ground support and tailings management technique in modern underground mining operations, providing improved ground stability, enhanced ore recovery, and reduced surface tailings disposal requirements (Fall et al., 2008; Wu et al. 2014; Grabinsky and Simms, 2006; Xiapeng et 2019). By incorporating tailings with binders and water to form a pumpable paste that hardens in situ, CPB contributes both to geotechnical safety and to more sustainable mining practices by enabling the in-situ reuse of mine waste, reducing surface tailings storage, and minimizing the environmental footprint associated with conventional tailings disposal methods (Cui and Fall, 2017). Portland cement (OPC) remains one of the most widely used binders in CPB systems due to its reliable strength development and well-established hydration mechanisms. However, its extensive use is associated with significant economic and environmental drawbacks. Cement production is highly energy-intensive and accounts for approximately 7–8% of global anthropogenic CO_2 emissions (Scrivener et al., 2018; Andrew, 2019), making it one of the largest industrial contributors to climate change. The replacement of Portland cement with lower-carbon alternatives therefore represents a critical priority for advancing cleaner production and improving the environmental sustainability of mining and construction

activities. In addition, cement costs represent a major operational expense in CPB operations, particularly in deep mines requiring large volumes of backfill. Durability concerns related to sulfate attack, acid mine drainage, and long-term chemical instability further limit the sustainability of OPC-based CPB in aggressive underground environments (Benzaazoua et al., 2004; Yilmaz et al., 2015a).

To address these limitations, slag-based alkali-activated binders have attracted growing attention as low-carbon alternatives to Portland cement. Ground granulated blast furnace slag (GGBFS), a by-product of the steel industry, possesses latent hydraulic properties that can be activated in alkaline environments to form cementitious gels with mechanical performance comparable to OPC (Provis and Bernal, 2015; Shi et al., 2003). The use of slag-based binders enables the valorization of industrial by-products that would otherwise require disposal, thereby supporting circular economy principles and reducing the environmental burden associated with industrial waste management. Alkali-activated slag binders offer substantially reduced CO_2 emissions, improved chemical resistance, and lower material costs, making them particularly attractive for sustainable CPB applications (Bakharev et al., 2002; Bernal et al., 2016). Previous studies have shown that alkali-activated slag systems can reduce CO_2 emissions by up to 40–80% compared to OPC, depending on activator type and formulation, highlighting their strong potential for enabling low-carbon underground infrastructure (e.g., Yang et al. 2013, Alsalman et al. 2021, Chottemada et al. 2023, Marathe et al. 2025). Among the various alkaline activators investigated, sodium carbonate (Na_2CO_3) has emerged as a promising option due to its lower environmental impact, safer handling, and reduced cost compared with conventional activators such as sodium hydroxide and sodium silicate (Duxson et al., 2007; Bernal and Provis, 2015). Sodium carbonate is non-corrosive and more suitable for large-scale industrial deployment, making it particularly attractive for cleaner production applications in large-volume backfilling operations.

Despite these advantages, sodium carbonate activation is widely reported to exhibit pronounced early-age kinetic retardation (Fernández-Jiménez et al., 2003; Bernal et al., 2015). The initial interaction between dissolved calcium species and carbonate ions promotes the formation of carbonate phases, which buffer pore-solution alkalinity and delay extensive slag dissolution. This buffering effect postpones the precipitation of

primary binding gels such as C-(A)-S-H, resulting in limited early-age strength development and slow matrix formation (Shi et al., 2003; Walkley et al., 2021). Such retardation is particularly problematic in CPB applications, where early structural development and timely stiffening are often required to ensure safe mining operations. Overcoming these limitations is essential to enable the practical implementation of carbonate-activated slag binders as viable low-carbon substitutes for Portland cement in sustainable backfilling systems.

To mitigate the limitations of sodium carbonate activation, hybrid activation strategies combining Na_2CO_3 with sodium hydroxide (NaOH) have recently been proposed (Bernal et al., 2015; Dai et al., 2023). In these systems, NaOH increases pore-solution alkalinity, enhances slag dissolution, and accelerates gel precipitation, while Na_2CO_3 provides buffering capacity and promotes secondary carbonate phase formation that may contribute to microstructural stability. The synergistic interaction between carbonate buffering and hydroxide-induced acceleration offers a mechanistic pathway for regulating hydration kinetics and microstructure evolution. By adjusting the SC/SH ratio, it becomes possible to tailor early-age reaction rates while maintaining the sustainability advantages associated with carbonate-based activation, thereby enabling the development of high-performance binders with reduced environmental impact and improved resource efficiency. However, most existing studies on hybrid activation have focused on cement pastes or mortars under conventional water-to-binder ratios. Very limited research has systematically investigated hybrid Na_2CO_3–NaOH activation under realistic CPB conditions characterized by extremely high water contents, complex tailings mineralogy, and long curing durations. Furthermore, the mechanistic understanding of hydration pathways, phase assemblage development, and densification processes in hybrid-activated CPB systems remains insufficient.

Previous investigations of alkali-activated CPB systems have largely relied on mechanical strength measurements to assess performance (Yilmaz et al., 2015b). While uniaxial compressive strength (UCS) provides valuable information on structural development, it does not capture the underlying physicochemical processes governing hydration and microstructure formation. Hydration in CPB systems involves complex coupled mechanisms including ionic dissolution, precipitation of reaction products, water

consumption, and pore-structure refinement. To resolve these processes, multi-parameter monitoring approaches are required. Electrical conductivity (EC) measurements provide a sensitive indicator of ionic mobility and dissolution–precipitation dynamics in the pore solution (Wang and Scrivener, 1995; Shi et al., 2003). Volumetric water content (VWC) reflects water consumption associated with hydration reactions and gel formation, while matric suction (ψ) captures capillary responses linked to pore refinement and matrix densification (Fredlund and Rahardjo, 1993; Fall et al., 2010). The coupled application of EC, VWC, and matric suction monitoring therefore offers a powerful framework to resolve hydration kinetics and structural evolution in CPB systems beyond conventional strength-based evaluations.

The objective of this study is to elucidate the hydration mechanisms and strength development of slag-based cemented paste backfill activated with blended sodium carbonate and sodium hydroxide under realistic CPB conditions. A systematic investigation of SC/SH ratios and total activator dosages is conducted to evaluate their influence on hydration kinetics, phase assemblage evolution, physical property development, and mechanical performance. The experimental program is performed under representative high water-to-binder ratios typical of field backfilling operations. A coupled EC–VWC–ψ monitoring framework is implemented to directly resolve ionic activity, water consumption, and pore-structure evolution during early hydration. Finally, an integrated interpretation linking hydration kinetics, microstructure development, matrix densification, and strength evolution is provided to establish a comprehensive mechanistic understanding of hybrid-activated CPB behavior. This work aims to provide a scientific basis for the rational design of low-carbon hybrid-activated binders for sustainable underground backfilling applications and to support the advancement of cleaner production technologies through reduced Portland cement consumption, enhanced utilization of industrial by-products, and improved environmental sustainability of mining infrastructure systems.

4.2 Material and experimental program

4.2.1 Materials

Silica tailings (ST) were used as the aggregate material for all CPB mixtures. The grain-size distribution and physical characteristics of the ST are summarized in Table 4.1. The particle-size distribution of the ST is representative of the average tailings produced by nine different mines in Eastern Canada, ensuring that the material used in this study is relevant to typical CPB applications.

Table 4.1: Physical and grain-size characteristics of the silica tailings (ST) used in the CPB mixtures.

Element	**G_s**	**D_{10}**	**D_{30}**	**D_{50}**	**D_{60}**
Unit	-	µm	µm	µm	µm
ST	2.7	1.9	9.0	22.5	31.5
Average of 9 types of tailings	-	1.8	9.1	20.0	30.8

ST: silica tailings; Gs: specific gravity; D10, D30, D50, D60: characteristic particle diameters

The mineralogical composition of the ST, determined by X-ray diffraction (XRD), is presented in Table 4.2. The tailings consist predominantly of quartz (dominant mineral in Canadian hard rock mine tailings), with only trace amounts of other mineral phases. This mineralogical simplicity limits potential chemical interactions between tailings and binders, allowing the effects of binder chemistry and activation to be more clearly isolated.

Table 4.2: Mineralogical composition of the silica tailings (ST) determined by X-ray diffraction (wt.%).

	Mineral											
Tailings	Quartz	Albite	Dolomite	Calcite	Chlorite	Magnetite	Pyrite	Talc	Pyrrhotite	Spinel	Others	Total
ST (wt.%)	99.8	-	-	-	-	-	-	-	-	-	0.2	100.0

ST: silica tailings; wt.: weight.

The grain-size distribution of the ST, together with the average grain-size distribution of tailings from nine mines in Eastern Canada, is shown in Fig. 4.1. The close

agreement between the two distributions confirms the representativeness of the tailings used in this study.

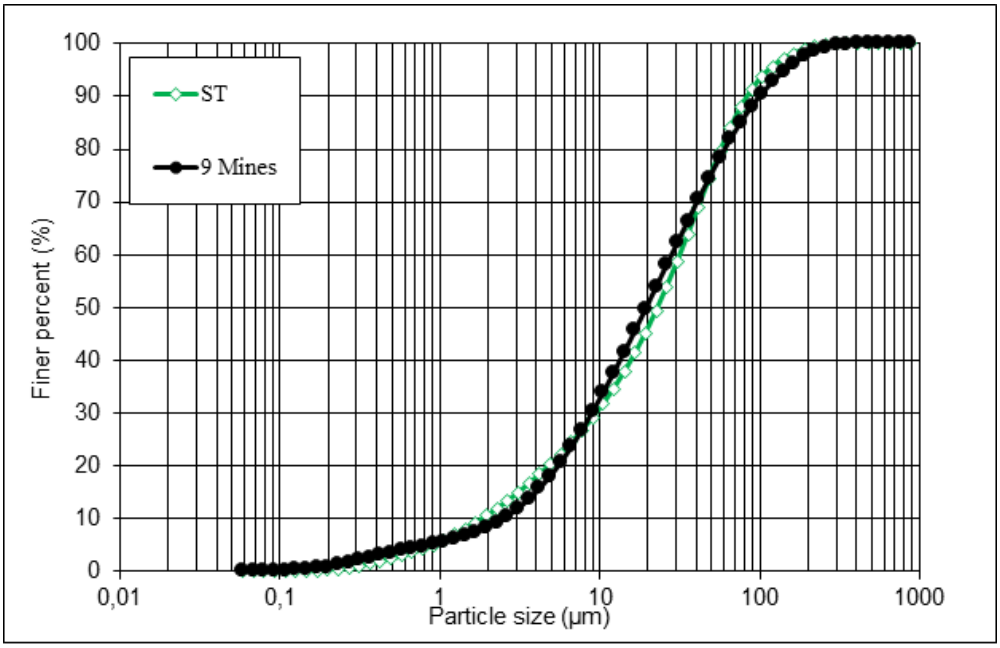

Figure 4.1: Grain size distribution of the silica tailings (ST) as well as average grain size distribution of tailings from nine mines in Eastern Canada.

Tap water was used as mixing water for all mixtures. Two binders were employed: (i) Portland cement type I (PCI), which served as the reference binder, and (ii) ground granulated blast-furnace slag (GGBFS). The chemical composition and physical properties of PCI and slag are reported in Table 4.3.

Table 4.3: Chemical composition and physical properties of Portland cement type I and ground granulated blast-furnace slag (GGBFS).

Binder	**MgO (wt.%)**	**CaO (wt. %)**	**SiO_2 (wt.%)**	**Al_2O_3 (wt.%)**	**Fe_2O_3 (wt.%)**	**SO_3 (wt.%)**	**Rel. Density (%)**	**Specific surface (m^2/g)**
PCI	2.65	62.82	18.03	4.53	2.70	3.82	3.15	1.3
Slag	10.98	41.14	34.23	9.54	-	3.87	2.90	2.2

wt.%: weight percent; PCI: Portland cement type I.

Alkali activation of slag was achieved using sodium carbonate (Na_2CO_3, >98%; SC) and sodium hydroxide (NaOH, >98%; SH). Both activators were added as anhydrous solids. Consequently, no correction was applied to the mixing water content.

4.2.2 Mixture design

The mixture proportions of the CPB specimens prepared for uniaxial compressive strength (UCS) testing, physical property determination, electrical conductivity (EC), volumetric water content (VWC), and matric suction (ψ) monitoring are summarized in Table 4.4. All CPB mixtures were prepared with a constant water-to-binder ratio (w/b) of 7.4 to ensure comparable rheology across formulations.

Table 4.4: Mix design of CPB mixtures for uniaxial compressive strength testing, physical property determination, electrical conductivity (EC), volumetric water content (VWC), and matric suction (ψ) monitoring.

Sample	PC (%)	Slag (%)	Activator content (%)	SC/SH* ratio	W/B**
Control	4.5	0	0	-	7.4
SC/SH (50/50) -15%	0	4.5	15	50/50	7.4
SC/SH (20/80) -15%	0	4.5	15	20/80	7.4
SC/SH (50/50) -20%	0	4.5	20	50/50	7.4
SC/SH (50/50) -10%	0	4.5	10	50/50	7.4

For alkali-activated systems, ground granulated blast-furnace slag (GGBFS) was used as the sole binder and activated using blended sodium carbonate (SC) and sodium hydroxide (SH). The SC/SH ratio denotes the mass ratio between sodium carbonate and sodium hydroxide, while the activator dosage is expressed as Na_2O equivalent percentage by mass of slag. Different SC/SH ratios and activator dosages were selected to investigate their combined effects on hydration kinetics and mechanical performance (Table 4.4).

In addition, cement paste mixtures without tailings were prepared for phase assemblage analysis by X-ray diffraction (XRD). The compositions of these paste mixtures are provided in Table 4.5. All paste mixtures were prepared with a water-to-binder ratio (w/b) of 1. Sodium carbonate (SC) and sodium hydroxide (SH) were added as anhydrous solids; therefore, no correction to the mixing water content was required.

Table 4.5: Composition of cement paste mixtures (without tailings) prepared for XRD analysis after 150 days of curing.

Sample	PC (g)	Slag (g)	Activator (%)	SC/SH* ratio	W/B
Control	100	0	0	-	1
SC/SH (50/50)-15%	0	100	15	50/50	1
SC/SH (20/80)-15%	0	100	15	20/80	1
SC/SH (50/50)-20%	0	100	20	50/50	1
SC/SH (50/50)-10%	0	100	10	50/50	1

4.2.3 Specimen Preparation and curing

All materials were weighed to the nearest 0.1 g prior to batching. The required quantities of binders (Portland cement type I and/or GGBFS), silica tailings, activators (SC and SH), and tap water were measured according to the mix designs presented in Tables 4.4-4.5. The constituents were blended using a household food mixer for approximately 10 min to obtain a homogeneous CPB slurry. For cement paste mixtures without tailings, the same protocol was followed, omitting the silica tailings. Fresh CPB was poured into rigid plastic cylindrical molds in a single lift. During casting, the slurry was gently stirred and the molds were tapped manually to release entrapped air; no external vibration was applied. Two specimen sizes were prepared: cylinders of 50 × 100 mm for mechanical and physical testing, and larger cylinders of 100 × 200 mm for instrumented monitoring to limit wall effects on embedded sensors. Immediately after casting, all molds were sealed to prevent moisture loss. A total of 120 cylinders (50 × 100 mm) were produced, corresponding to three specimens per CPB mixture and curing age listed in Table 4.4. In addition, five large cylinders (100 × 200 mm) were cast for the monitoring program described in Table 4.4.

Specimens were cured under sealed conditions at 20 ± 2 °C. Unless otherwise specified, samples remained in their molds until the scheduled testing or instrumentation stage in order to maintain internal moisture conditions. For UCS testing, specimens were

demolded immediately prior to loading. Specimens intended for XRD analysis were oven-dried at 45 °C for four days after curing and then stored in airtight containers until testing.

4.2.4 Test methods

Mechanical and physical tests were conducted on CPB specimens according to the experimental program summarized in Table 4.4. In addition, selected mixtures were instrumented to monitor electrical conductivity (EC), volumetric water content (VWC), and matric suction (ψ), as described in Table 4.4. X-ray diffraction (XRD) was performed on paste specimens without tailings (Table 4.5) to identify crystalline phases after long-term curing.

4.2.4.1 Mechanical testing (UCS)

Uniaxial compressive strength (UCS) tests were performed on cylindrical CPB specimens with dimensions of 50 × 100 mm after 1, 3, 7, 28, 90, 150, and 210 days of curing. Prior to testing, both ends of each specimen were trimmed to remove surface irregularities, and the exact diameter and height were measured to accurately determine the applied stress. UCS tests were carried out using a servo-controlled compression testing machine at a constant displacement rate of 2 mm/min, in accordance with ASTM C39/C39M. For each mixture and curing age, three specimens were tested, and the reported UCS value corresponds to the average of the three measurements. The UCS results were subsequently correlated with physical properties (void ratio, porosity, water content, and dry density), as well as with hydration indicators obtained from EC, VWC, and matric suction monitoring, in order to assess the influence of activator composition and curing time on mechanical performance.

4.2.4.2 Physical properties

The physical properties of the CPB specimens were determined to characterize the evolution of their internal structure with curing time. The properties investigated include water content (w), porosity (n), void ratio (e), degree of saturation (Sr), and dry density (ρ_d).

The specific gravity (Gs) of each specimen was measured individually at each curing age following ASTM D854 using the water pycnometer method. In this procedure, entrapped air was removed by gently boiling the sample in deaired water prior to recording the mass measurements required for the calculation of Gs. For each mixture and curing age, the average Gs value was used in subsequent calculations.

Water content, porosity, void ratio, degree of saturation, and dry density were calculated from the measured mass-volume relationships and the corresponding Gs values using standard geotechnical relationships. All measurements were conducted at a temperature of 20 ± 2 °C. The physical properties were later correlated with UCS and hydration indicators derived from EC, VWC, and matric suction monitoring to assess the influence of activator composition and curing time on matrix densification.

4.2.4.3 Coupled electrical conductivity (EC), volumetric water content (VWC), and matric suction monitoring

Electrical conductivity (EC), volumetric water content (VWC), and matric suction (ψ) were continuously monitored to track ionic activity, water consumption, and capillary behavior during the early curing of slag-based CPB. Measurements were performed on selected mixtures listed in Table 4.4 using 5TE and MPS-6 sensors (Decagon Devices, Inc., Pullman, WA, USA) connected to an Em50 data logger.

For each instrumented specimen, sensors were installed at the geometric centre of 100 × 200 mm cylindrical molds to minimize boundary effects and sensor-wall proximity. The 5TE sensor was used to measure EC and VWC, with measurement ranges of 0-23 dS/m for EC and 0-1 m^3/m^3 for VWC. EC measurements were obtained by applying an alternating electrical current between stainless-steel electrodes, while VWC was estimated from the dielectric permittivity of the material.

Matric suction was monitored using an MPS-6 dielectric water potential sensor installed adjacent to the 5TE probe. The MPS-6 sensor measures suction in the range of −9 to −100 kPa with an accuracy of ±10% following factory calibration. Installing both sensors in close proximity enabled the coupled interpretation of electrical, hydric, and capillary responses during hydration.

All signals were recorded automatically at 5-minute intervals over the first 28 days of curing. The temporal evolutions of EC, VWC, and ψ were used to interpret hydration kinetics, including ionization and deionization processes, water binding into reaction products, and pore-scale capillary effects associated with the formation and densification of hydration gels.

4.2.4.4 XRD analysis

X-ray diffraction (XRD) analysis was performed to identify the crystalline phases present in cement paste specimens prepared without tailings and cured for 150 days. Paste samples were used to avoid the interference of tailings minerals and to better resolve the phase assemblage associated with binder hydration.

After curing, samples were oven-dried at 45 °C for four days to minimize further hydration and carbonation. The dried specimens were then ground and sieved to obtain particles finer than 40 μm prior to analysis. XRD measurements were carried out using a diffractometer equipped with Cu Kα radiation (λ = 1.5406 Å), operated at 40 kV and 40 mA. Data were collected over a 2θ range of 2° to 90° with a step size of 0.02°.

Phase identification was conducted by comparing the measured diffraction patterns with reference data from the literature and standard databases. XRD results were used qualitatively to identify the dominant crystalline phases and to support the interpretation of hydration mechanisms and performance evolution discussed in Section 4.3.

4.3 Results

4.3.1 Hydration Kinetics from Coupled Monitoring

The coupled monitoring of electrical conductivity (EC), volumetric water content (VWC), and matric suction (ψ) provides direct insight into the hydration kinetics and microstructural evolution of slag-based CPB activated with blended sodium carbonate and sodium hydroxide. The simultaneous measurement of these parameters enables resolution of ionic activity, water consumption, and capillary effects during early curing, thereby capturing the temporal sequence of reaction processes governing matrix development.

4.3.1.1 Electrical conductivity evolution

The temporal evolution of electrical conductivity for the instrumented CPB mixtures is presented in Figure 4.2. All alkali-activated slag systems exhibit an initial stage characterized by high EC values or a slight increase during the first hours to days of curing, followed by a progressive decrease over time. This response reflects a two-stage hydration kinetic behavior.

(i) Ionization Stage

During the early curing period, EC remains high, indicating elevated ionic concentration within the pore solution. This stage corresponds to the dissolution of activators and the initial release of ions from the slag surface. In mixtures with higher sodium carbonate content, the ionization stage is prolonged due to the buffering action of carbonate species, which moderate the rise in pore-solution alkalinity. The delayed pH increase limits extensive slag dissolution and postpones the onset of rapid hydration reactions (Wang and Scrivener, 1995; Shi et al. 2003; Provis and Bernal, 2014). Consequently, ionic mobility remains high, and limited incorporation of ions into solid phases occurs.

(ii) Deionization–Acceleration Stage

Following the ionization stage, EC decreases markedly, signifying the onset of deionization associated with the precipitation of hydration products (Wang and Scrivener, 1995). This decrease reflects the consumption of dissolved ions during the formation of C-(A)-S-H gels and associated carbonate- and hydrotalcite-like phases (Bernal et al., 2011; Walkley et al., 2021). Hybrid Na_2CO_3–NaOH activated systems exhibit an earlier and more pronounced EC decline compared to Na_2CO_3-rich formulations, demonstrating that hydroxide addition effectively accelerates slag dissolution and gel formation (Bernal et al., 2015; Dai et al., 2023).

Among the formulations investigated, the SC/SH (50/50)–10% mixture shows the fastest transition from ionization to deionization, indicating the most rapid hydration kinetics. This behavior is consistent with its superior mechanical performance and matrix densification observed at later ages, as shown in Sections 4.3.3 and 4.3.4.

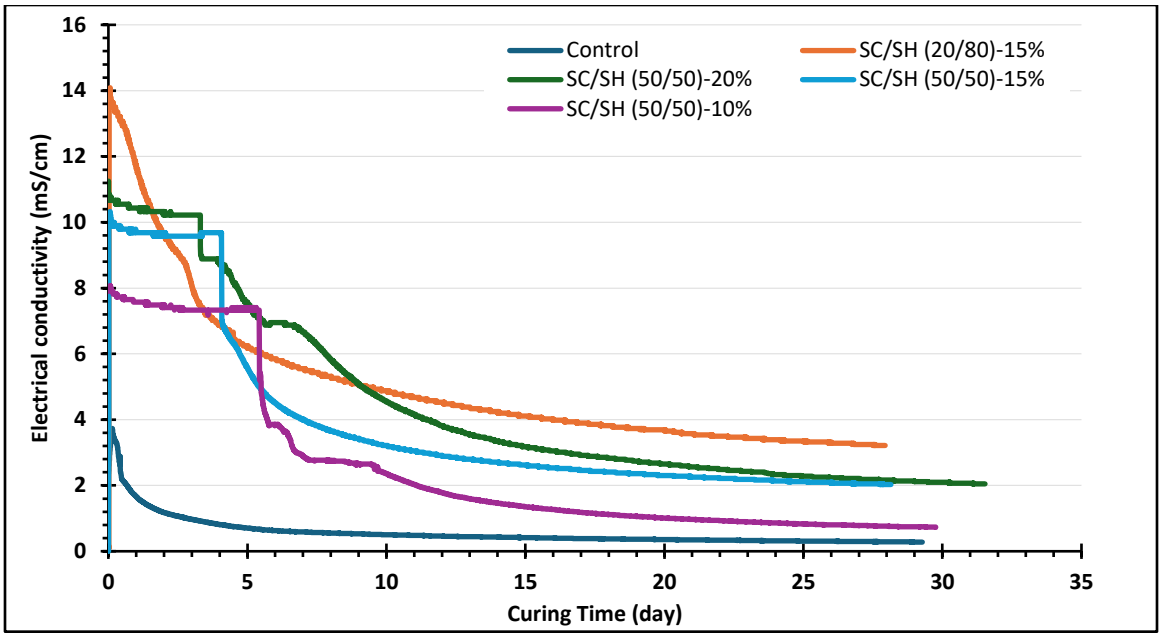

Figure 4.2. Evolution of electrical conductivity (EC) of CPB mixtures over 28 days of curing.

4.3.1.2 Volumetric water content evolution

The evolution of volumetric water content with curing time is illustrated in Figure 4.3. For all mixtures, VWC remains relatively stable during the initial ionization stage identified in the EC curves, followed by a substantial decrease coinciding with the deionization–acceleration phase.

(i) Water Consumption Trends

The initial plateau in VWC reflects limited incorporation of free water into hydration products during the early ionization period. As hydration reactions accelerate, VWC decreases sharply, indicating progressive consumption of pore water as it becomes chemically bound within newly formed reaction gels. Hybrid-activated mixtures exhibit more pronounced reductions in VWC compared to Na_2CO_3-dominated systems and the OPC control. The SC/SH (50/50)–10% mixture reaches the lowest stabilized VWC value (approximately 0.22 m^3/m^3), demonstrating the most extensive water binding and solid network development.

(ii) Link to Gel Formation

The synchronized decrease in EC and VWC confirms that water consumption is closely associated with the precipitation of hydration products. As ions are incorporated

into solid phases, free water is progressively consumed or redistributed within the evolving pore structure. This process directly reflects the formation and densification of C-(A)-S-H gels and associated phases that constitute the load-bearing skeleton of the CPB matrix (Myers et al., 2013; Walkley et al., 2021).

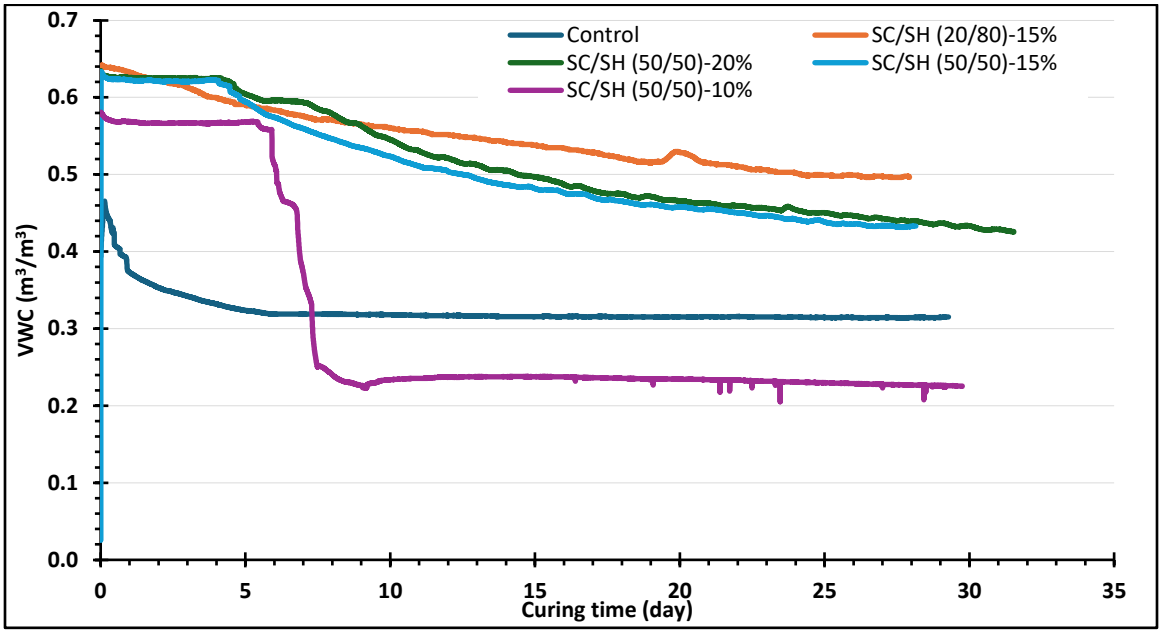

Figure 4.3. Evolution of volumetric water content (VWC) of CPB mixtures over 28 days of curing.

4.3.1.3 Matric suction development

The temporal evolution of matric suction is shown in Figure 4.4. All mixtures exhibit a gradual increase in the value of suction with curing time, reflecting progressive changes in pore structure and water distribution.

(i) Capillary Response

The rise in |ψ| occurs primarily after the onset of EC and VWC decreases, indicating that capillary effects become significant once hydration products begin filling pore spaces and reducing hydraulic connectivity. As free water is consumed and pore throats narrow, capillary stresses increase, resulting in higher matric suction values. Hybrid Na_2CO_3–NaOH activated mixtures develop substantially lower suction than the OPC control at early ages. At advanced ages (28 days), the SC/SH (50/50)–10% mixture reaches the highest stabilized suction of approximately 50 kPa, among the samples with Na_2CO_3–NaOH

activated slag, highlighting the extent of pore refinement achieved under balanced hybrid activation.

(ii) Pore Refinement Indicator

The evolution of matric suction serves as a sensitive indicator of microstructural densification, as increasing suction reflects progressive pore-size reduction and decreased pore connectivity within cemented matrices (Fredlund and Rahardjo, 1993). In CPB systems, suction development has been directly linked to hydration-driven pore refinement, increasing dry density, and decreasing porosity (Tian and Fall, 2021). The stronger suction observed in hybrid-activated systems therefore confirms enhanced matrix compaction relative to OPC-based CPB, consistent with improved microstructural development reported for alkali-activated binders (Walkley et al., 2021).

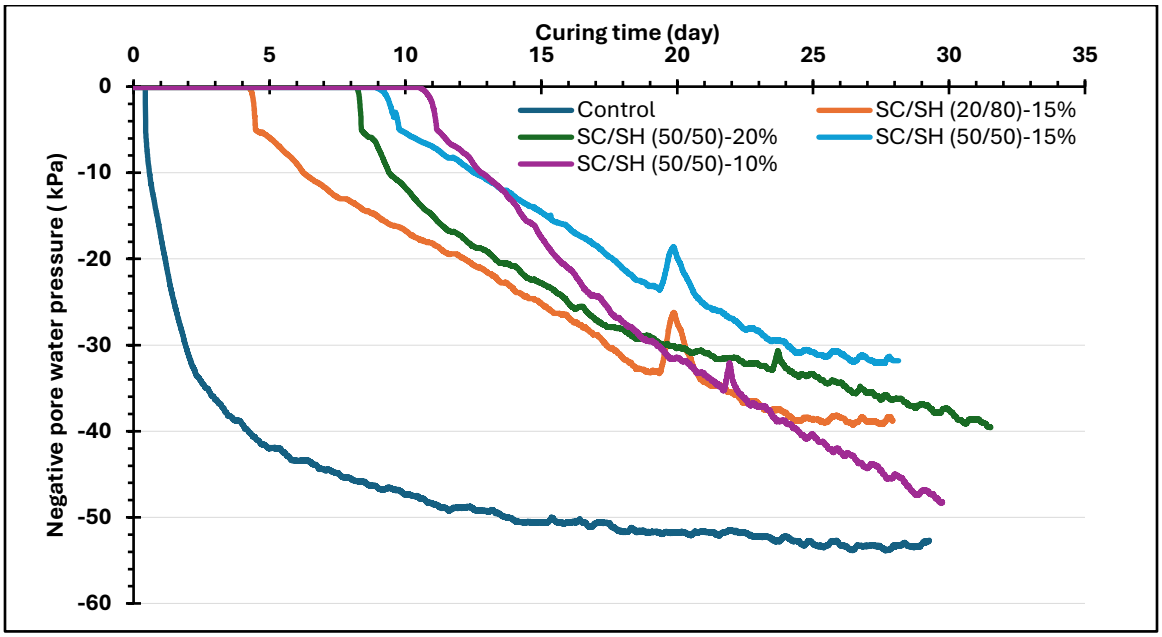

Figure 4.4. Evolution of matric suction (ψ), expressed as the absolute value of negative pore water pressure, in CPB mixtures over 28 days of curing.

4.3.1.4 Identification of hydration stages

The coupled EC–VWC–ψ responses collectively delineate a coherent sequence of hydration stages in slag-based CPB activated with blended sodium carbonate and sodium hydroxide.

Stage I: Ionization/Retardation

This initial stage is characterized by high EC values and nearly constant VWC, indicating elevated ionic concentration and limited water consumption. Slag dissolution remains restricted, particularly in carbonate-rich systems, due to buffering effects that delay alkalinity increase. Microstructural development and strength (see Figure 4.9) gain are minimal during this period.

Stage II: Acceleration/Gel Formation

The transition to this stage is marked by a rapid decrease in EC and a concurrent reduction in VWC, reflecting the precipitation of hydration products and incorporation of ions and water into solid phases. Hybrid activation with NaOH significantly shortens the duration of the ionization stage and promotes earlier onset of accelerated hydration (Dai et al., 2023). Extensive formation of C-(A)-S-H gels and associated phases establishes a continuous solid skeleton governing matrix densification and strength development (Walkley et al., 2021).

Stage III: Densification

Following the main gel precipitation phase, matric suction increases progressively, indicating ongoing pore refinement and reduction in hydraulic connectivity. Continued hydration and structural reorganization enhance matrix compactness, leading to sustained strength development at long curing times (Figure 4.9).

Overall, the coupled monitoring approach reveals that hydration kinetics in hybrid Na_2CO_3–NaOH activated slag CPB are governed by a transition from an ionization-dominated regime to an acceleration and densification regime. Balanced SC/SH ratios promote earlier gel formation, more efficient water consumption, and stronger pore refinement, ultimately driving superior mechanical performance. The integration of EC, VWC, and matric suction measurements thus provides a powerful framework for resolving hydration mechanisms under realistic CPB conditions.

4.3.2 Microstructural Evolution (XRD)

X-ray diffraction (XRD) analysis was conducted on cement paste specimens prepared without tailings and cured for 150 days to elucidate the phase assemblage associated with the hydration of OPC-based and hybrid Na_2CO_3–NaOH activated slag

binders. The use of paste samples enabled clearer identification of hydration products without interference from tailings minerals. The resulting diffraction patterns are presented in Figure 4.5.

4.3.2.1 Phase Assemblage of OPC and Hybrid-Activated Systems

The OPC control exhibits diffraction peaks characteristic of portlandite (CH) and residual clinker phases, together with a broad diffuse hump associated with poorly crystalline calcium silicate hydrate (C-S-H). Minor calcite peaks are also observed, likely resulting from partial carbonation during curing and sample preparation. This phase assemblage is typical of conventional Portland cement hydration, where the formation of C-S-H and CH governs mechanical performance (Taylor, 1997). In contrast, all Na_2CO_3–NaOH activated slag systems display markedly different diffraction signatures, confirming a fundamentally distinct hydration pathway. Portlandite is absent in all hybrid-activated mixtures, indicating that calcium released from slag dissolution is primarily incorporated into alternative hydration products rather than precipitating as CH. The diffraction patterns are dominated by a broad amorphous hump between approximately 25° and 35° 2θ, characteristic of poorly crystalline C-(A)-S-H gels that constitute the main binding phase in alkali-activated slag systems. In addition to the amorphous C-(A)-S-H matrix, distinct crystalline peaks corresponding to calcite are clearly identified in all hybrid systems, reflecting the active participation of carbonate species in the reaction process. Weak but discernible reflections attributed to hydrotalcite-like phases (Mg–Al layered double hydroxides) are also present, particularly in mixtures with balanced SC/SH ratios. The relative intensities of calcite and hydrotalcite-like phases are highest for the SC/SH (50/50)–10% mixture, suggesting more extensive reaction of carbonate species and enhanced stabilization of hydration products in this formulation. Mixtures with higher sodium carbonate content exhibit similar phase assemblages but with lower relative peak intensities, indicating slower reaction kinetics and less extensive slag dissolution.

4.3.2.2 Role of C-(A)-S-H Gel Formation

The broad amorphous hump observed in all hybrid-activated systems confirms that C-(A)-S-H gels constitute the dominant binding phase responsible for matrix cohesion and strength development. These gels form through the dissolution of calcium, silicon, and

aluminum species from slag particles under alkaline conditions and subsequently polymerize into a cross-linked amorphous network (Wang and Scrivener, 1995; Bernal et al., 2015a,b; Myers et al., 2013). Compared to OPC hydration, where C-S-H coexists with significant quantities of portlandite, the absence of CH in hybrid systems indicates more efficient utilization of calcium within the gel structure. This promotes the formation of a denser and more continuous solid skeleton, which directly contributes to matrix densification and sustained long-term strength gain. Similar microstructural densification trends associated with dominant C-(A)-S-H formation have been reported for carbonate- and hydroxide-activated slag binders (Bernal et al., 2015a,b; Walkley et al., 2021). The accelerated formation of C-(A)-S-H gels in balanced SC/SH systems is consistent with the coupled EC–VWC monitoring results, which demonstrate earlier deionization and more pronounced water consumption for these mixtures. The rapid decrease in ionic concentration and progressive binding of free water directly reflects enhanced slag dissolution and gel precipitation kinetics promoted by hybrid activation.

4.3.2.3 Role of Calcite Formation

Calcite is identified as a prominent crystalline phase in all Na_2CO_3–NaOH activated slag mixtures, reflecting the interaction between dissolved calcium species released from slag and carbonate ions supplied by sodium carbonate. Previous studies have shown that in carbonate-activated systems, calcium initially reacts with CO_3^{2-} species to form carbonate phases before extensive C-(A)-S-H gel precipitation occurs (Bernal et al., 2015a,b; Walkley et al., 2021). This early calcite formation plays a key role in regulating pore-solution chemistry by buffering alkalinity and controlling the availability of free calcium ions. Rather than acting solely as an inert byproduct, calcite contributes to microstructural refinement by occupying pore spaces and serving as nucleation sites for subsequent C-(A)-S-H precipitation. The presence of carbonate surfaces has been shown to enhance heterogeneous nucleation and growth of calcium silicate hydrate phases, thereby accelerating matrix consolidation (Lothenbach et al., 2008). This pore-filling effect promotes matrix densification and enhances the connectivity of hydration products. The higher calcite content observed in balanced SC/SH mixtures suggests more effective coupling between carbonate availability and slag dissolution. This mechanism facilitates a controlled transition from the ionization-dominated stage to accelerated gel formation,

consistent with the hydration kinetics revealed by EC and VWC monitoring. By simultaneously buffering pore-solution chemistry and promoting nucleation-driven densification, calcite formation plays a complementary role alongside C-(A)-S-H gels in establishing a compact and mechanically efficient hybrid-activated CPB matrix.

4.3.2.4 Role of Hydrotalcite-Like Phases

The presence of hydrotalcite-like phases in the hybrid-activated systems indicates the incorporation of magnesium and aluminum species into layered double hydroxide (LDH) structures formed as secondary reaction products during slag hydration (Wang and Scrivener, 1995; Bernal et al., 2011; Myers et al., 2013). These phases contribute to matrix densification by occupying pore spaces and enhancing microstructural continuity (Bernal and Provis, 2014; Walkley et al., 2021). In addition, their layered structure can regulate ionic concentrations within the pore solution by accommodating various anions, thereby contributing to long-term chemical stability (Zhu et al. 2017). The increased prominence of these phases in balanced SC/SH formulations further supports the observation that hybrid activation promotes more complete slag reaction and improved phase assemblage development.

4.3.2.5 Mechanistic Implications of Hybrid Activation

The XRD results collectively demonstrate that hybrid Na_2CO_3–NaOH activation fundamentally transforms the hydration chemistry of slag-based CPB relative to OPC-based systems. Instead of forming an AFt–CH dominated assemblage typical of Portland cement hydration, hybrid activation produces a microstructure composed of:

- An amorphous C-(A)-S-H gel network forming the primary binding phase;
- Crystalline calcite arising from carbonate participation;
- Stabilizing hydrotalcite-like LDH phases.

This composite phase assemblage promotes efficient pore filling, enhanced microstructural continuity, and sustained matrix densification. The synergistic effect of carbonate buffering and hydroxide-induced alkalinity increase governs the balance between early calcium carbonate formation and accelerated slag dissolution. Balanced

SC/SH ratios optimize this interplay, leading to faster gel precipitation, improved phase stabilization, and superior long-term performance.

These microstructural observations align closely with the hydration kinetics and physical property trends discussed in Sections 4.3.1 and 4.3.3. The accelerated deionization observed in EC monitoring, the pronounced water consumption captured by VWC measurements, and the strong suction development all reflect the progressive formation and densification of the hybrid-activated phase assemblage revealed by XRD. Overall, the XRD analysis confirms that Na_2CO_3–NaOH hybrid activation establishes a distinct and more efficient hydration pathway in slag-based CPB, underpinning the enhanced matrix densification and strength development observed in balanced formulations.

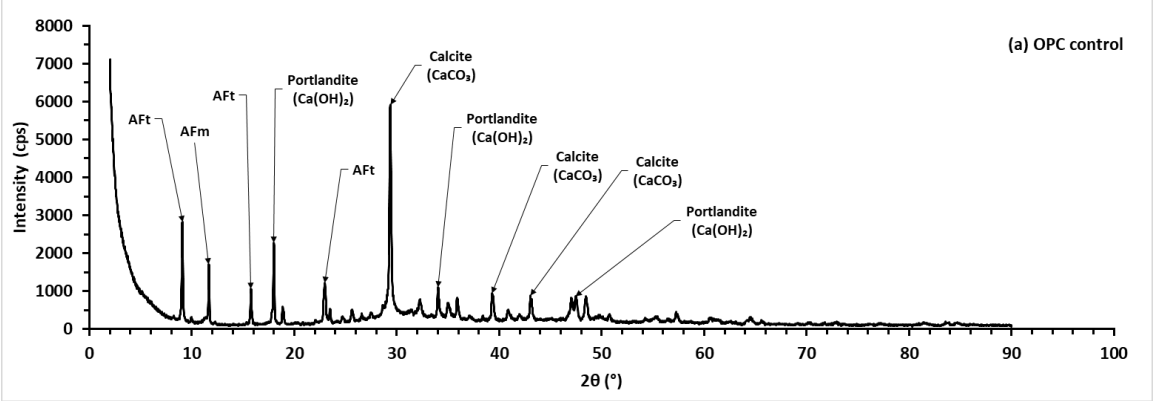

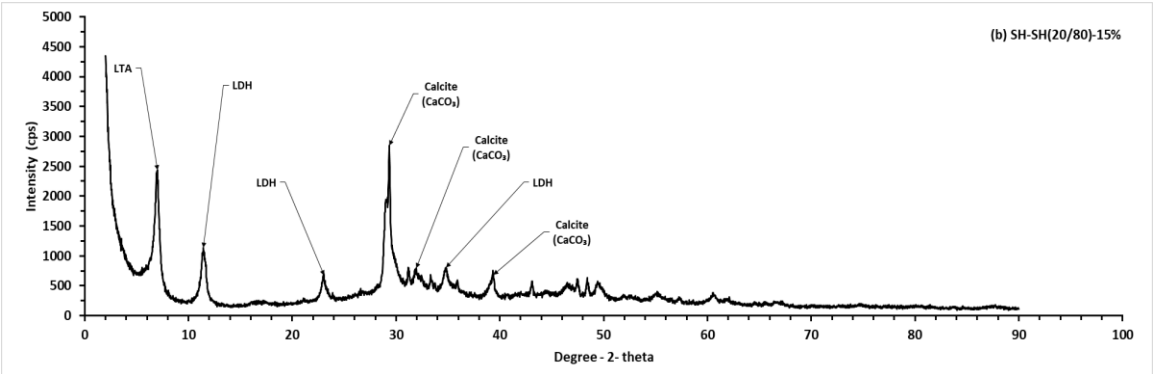

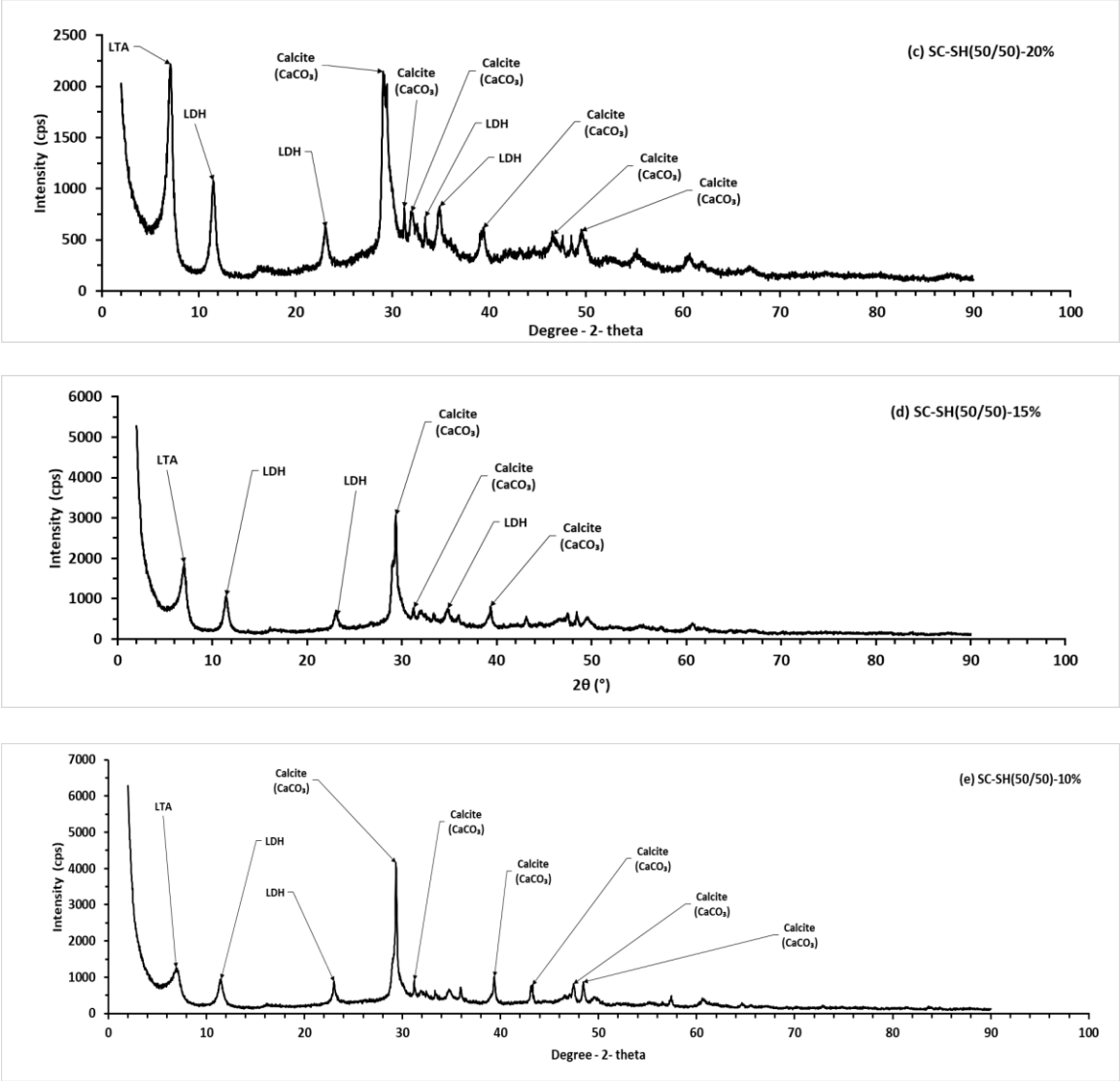

Figure 4.5. XRD patterns after 150 days: (a) OPC control; (b) SC/SH (20/80)-15%; (c) SC/SH (50/50)-20%; (d) SC/SH (50/50)-15%; (e) SC/SH (50/50)-10%. Main phases: calcite ($CaCO_3$), hydrotalcite (LDH), zeolite A (LTA). OPC reference shows AFt and CH.

4.3.3 Physical Property Evolution

The evolution of physical properties of the CPB mixtures was analyzed to characterize matrix densification and pore-structure refinement during curing. The parameters investigated include dry density (ρd), void ratio (e), porosity (n), and water content (w), measured at curing ages ranging from 1 to 150 days. These properties provide indirect yet robust indicators of hydration progress and microstructural development. The results are presented in Figures 4.6-4.8 and discussed below with emphasis on the influence of activator composition and curing time.

4.3.3.1 Dry density

The evolution of dry density with curing time is shown in Figure 4.6. For all CPB mixtures, dry density increases progressively throughout curing, indicating continuous densification of the backfill matrix associated with hydration reactions and precipitation of solid products. The OPC control consistently exhibits the lowest dry density values over the entire curing period. In contrast, the Na_2CO_3–NaOH activated slag mixtures display higher dry densities from early ages onward. Among the hybrid-activated systems, the SC/SH (50/50)–10% and SC/SH (50/50)–15% mixtures achieve the highest dry density values at long curing times, reflecting more efficient filling of interparticle voids. The enhanced dry density of the hybrid systems is attributed to the combined formation of amorphous C-(A)-S-H gels and secondary crystalline phases such as calcite and hydrotalcite-like compounds, which progressively occupy pore space and improve particle packing (Bernal et al., 2015; Walkley et al., 2021). The lower density observed in the OPC control, despite its relatively high strength, suggests that strength development in OPC-based CPB is governed primarily by the intrinsic stiffness of C-S-H rather than by bulk densification alone.

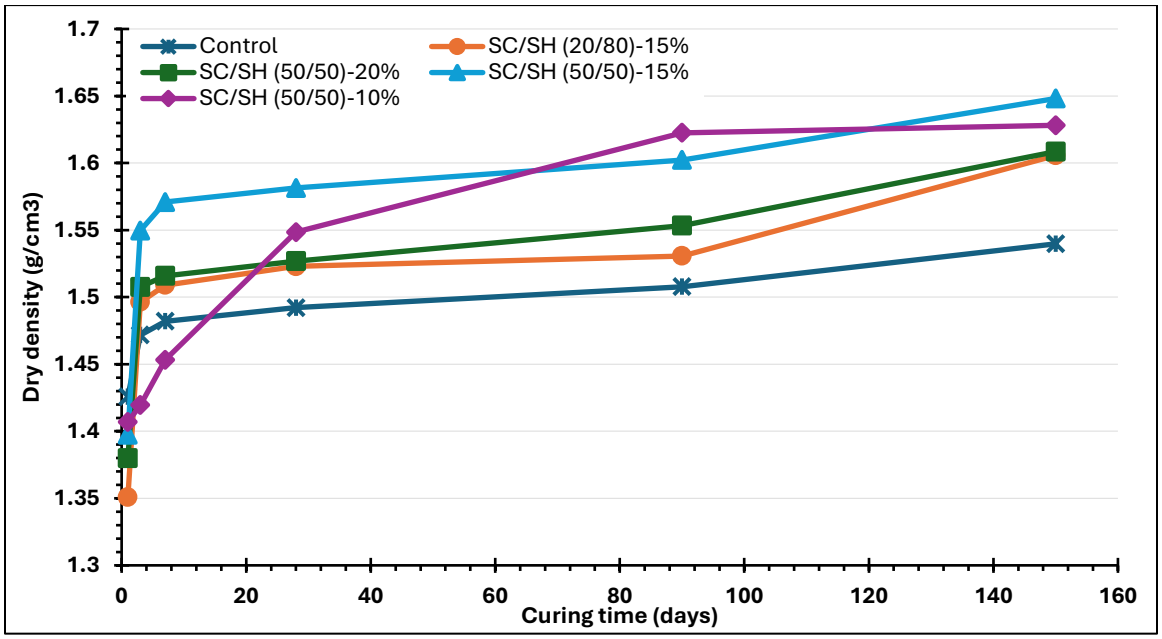

Figure 4.6. Evolution of dry density (ρd) of CPB mixtures with curing time.

4.3.3.2 Void ratio and porosity

The variations of void ratio and porosity with curing time are presented in Figures 4.7(a,b), respectively. All mixtures exhibit a pronounced reduction in both parameters during the first week of curing, followed by a more gradual decrease up to 150 days. This trend reflects rapid early formation of hydration products that occupy interparticle voids, followed by slower long-term pore refinement. Among the formulations, the hybrid-activated mixtures with balanced SC/SH ratios, particularly SC/SH (50/50)–10% and SC/SH (50/50)–15%, consistently display the lowest void ratio and porosity values throughout curing. In contrast, the OPC control remains the most porous mixture over the entire curing period. The more pronounced pore refinement in hybrid-activated systems is linked to sustained slag dissolution and continued precipitation of C-(A)-S-H gels and carbonate-bearing phases. These products progressively reduce pore connectivity and total pore volume, leading to a more compact internal structure. Mixtures with higher sodium carbonate content exhibit relatively higher void ratios and porosities, consistent with their delayed hydration kinetics and reduced extent of gel formation.

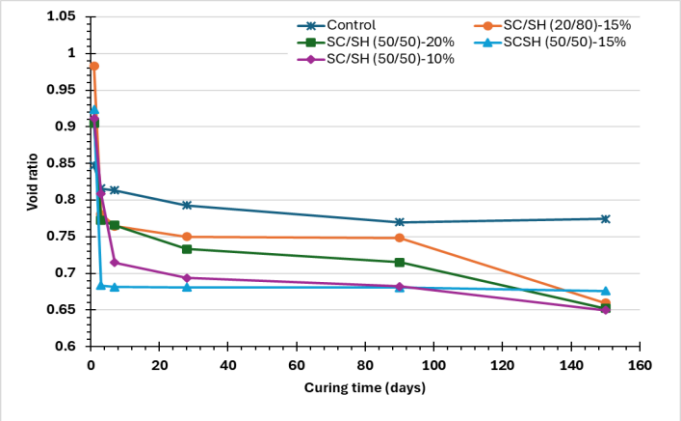

a. Variation of void ratio (e)

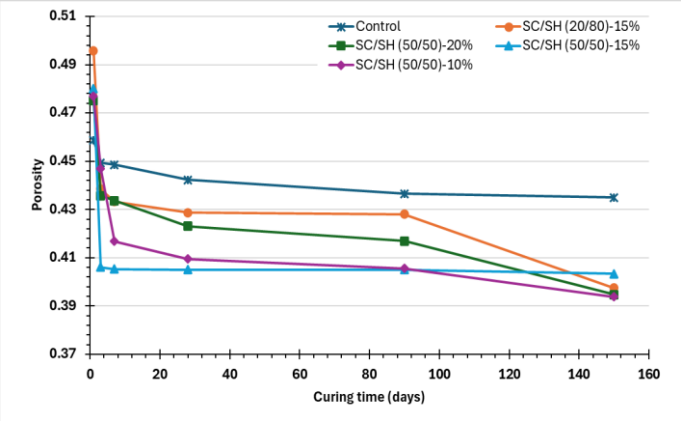

b. Variation of porosity (n)

Figure 4.7. Evolution of void ratio (e) and porosity (n) of CPB mixtures with curing time.

4.3.3.3 Water content

The evolution of water content with curing time is shown in Figure 4.8. For all mixtures, water content decreases steadily as curing progresses, reflecting both chemical consumption of water during hydration reactions and physical redistribution of pore water as the solid skeleton develops. The most pronounced reduction in water content is observed

for the SC/SH (50/50)–10% mixture, in agreement with its higher dry density and lower porosity. This behavior indicates more extensive incorporation of free water into hydration products and more efficient filling of pore spaces by reaction gels. In the Na_2CO_3–NaOH activated slag systems, water consumption is primarily associated with the formation of C-(A)-S-H gels and secondary phases that bind water within their structure (Bernal et al., 2015; Walkley et al., 2021). The OPC control exhibits a more limited decrease in water content, consistent with rapid early hydration followed by comparatively less long-term microstructural refinement.

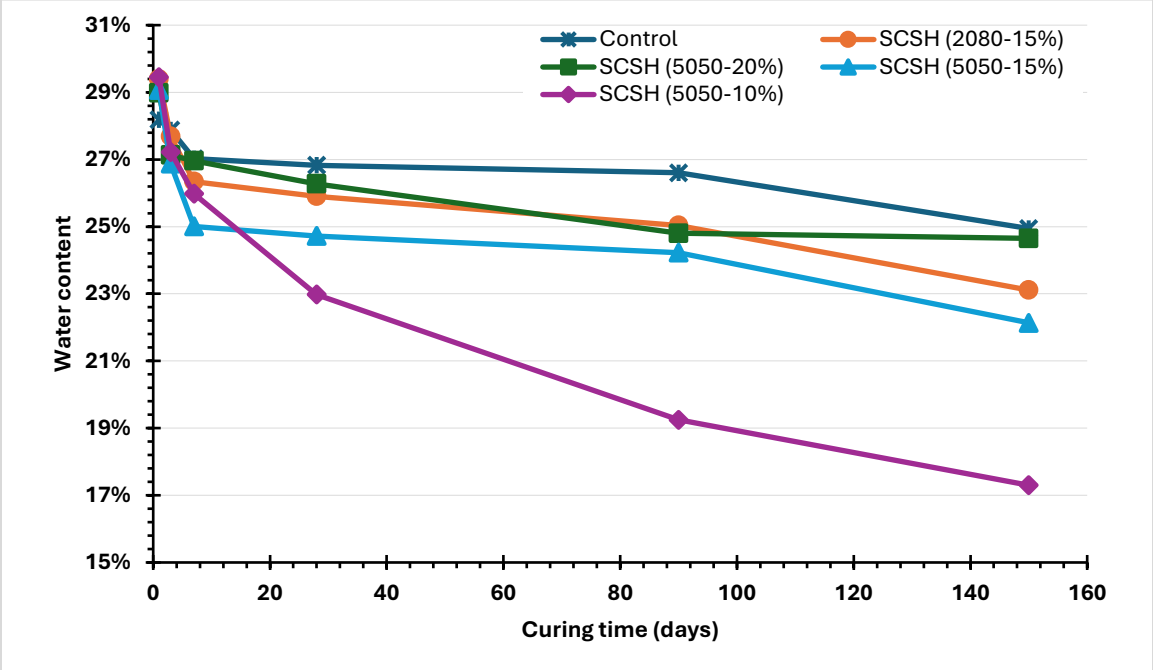

Figure 4.8. Evolution of water content (w) of CPB mixtures with curing time

4.3.3.4 Matrix Densification Trends and Influence of SC/SH Ratio

Taken together, the increase in dry density and the concurrent decreases in void ratio, porosity, and water content clearly demonstrate sustained matrix densification in all CPB mixtures with curing time. However, the extent and rate of densification are strongly influenced by activator chemistry. Hybrid Na_2CO_3–NaOH activated systems develop significantly denser matrices than the OPC control, confirming the effectiveness of hybrid activation in promoting long-term microstructural refinement under realistic CPB conditions. Within the hybrid systems, balanced SC/SH ratios yield the most compact structures, indicating an optimal interplay between carbonate buffering and hydroxide-

induced acceleration of slag dissolution. Mixtures with higher sodium carbonate content experience delayed hydration and less extensive pore filling, resulting in higher residual porosity and water content. Conversely, moderate hydroxide incorporation enhances slag dissolution and gel precipitation, promoting continuous densification.

These physical property trends align closely with the hydration kinetics discussed in Section 4.3.1 and the microstructural observations from XRD analysis in Section 4.3.2. Early transition to accelerated hydration, efficient water consumption, and extensive formation of C-(A)-S-H gels and secondary phases collectively drive the superior densification observed in balanced SC/SH formulations. Overall, the results confirm that matrix densification is a key mechanism governing performance in hybrid-activated slag CPB and that the SC/SH ratio plays a central role in controlling pore-structure evolution.

4.3.4 Strength Development (UCS)

The evolution of UCS of the CPB mixtures is presented in Figure 4.9. Strength development reflects the progressive hydration of binders, precipitation of binding phases, and the associated densification of the backfill matrix. UCS was measured at curing ages ranging from 1 to 210 days for all formulations to capture both early-age behavior and long-term performance.

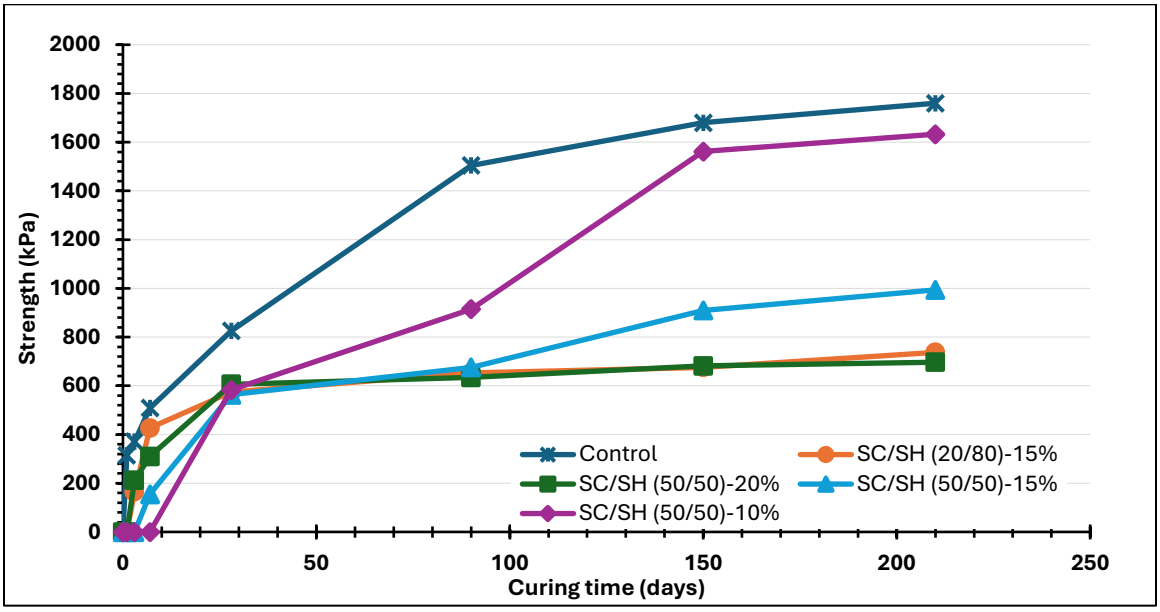

Figure 4.9. Evolution of unconfined compressive strength (UCS) of CPB mixtures with curing time.

4.3.4.1 Early-Age Retardation

At very early ages (1–7 days), all Na_2CO_3-activated slag mixtures exhibit negligible or very low UCS values compared to the OPC control. This behavior is attributed to the inherently slow early-age kinetics associated with sodium carbonate activation (Shi et al. 2003; Bernal et al., 2015a,b; Walkley et al., 2021). During this period, calcium released from slag dissolution preferentially reacts with carbonate species to form early carbonate phases, while the pore-solution alkalinity remains insufficient to promote extensive slag dissolution and C-(A)-S-H gel formation (Shi et al. 2003). Consequently, the formation of a continuous load-bearing solid skeleton is delayed, resulting in limited early strength development. In contrast, the OPC control shows significantly higher early UCS due to rapid hydration of clinker phases and early precipitation of C-S-H and portlandite, which rapidly establish mechanical integrity within the CPB matrix (Liu and Fall, 2022).

4.3.4.2 Acceleration with Hybrid Activation

Between 7 and 90 days of curing, a pronounced increase in UCS is observed for all hybrid Na_2CO_3–NaOH activated systems. The incorporation of sodium hydroxide increases pore-solution alkalinity, enhances slag dissolution, and accelerates the precipitation of C-(A)-S-H gels (Provis and Bernal, 2014; Bernal et al., 2015a,b; Dai et al., 2023). This hybrid activation mechanism effectively mitigates the retardation typically associated with sodium carbonate alone. The most significant strength gains during this period are recorded for the SC/SH (50/50)–10% and SC/SH (50/50)–15% mixtures, which reach UCS values of approximately 1.0–1.2 MPa at 90 days. In comparison, the SC/SH (20/80)–15% and SC/SH (50/50)–20% mixtures exhibit more moderate strength increases, indicating less efficient activation under these conditions. The accelerated strength development observed in balanced SC/SH systems is consistent with the hydration kinetics revealed by coupled EC–VWC–ψ monitoring, which showed earlier transition to the deionization–acceleration stage and more efficient gel formation.

4.3.4.3 Long-Term Performance Comparison

From 90 to 210 days of curing, all CPB mixtures continue to gain strength, confirming that hydration and microstructural refinement persist over long curing periods.

The sustained strength increase reflects ongoing slag dissolution, continued precipitation of C-(A)-S-H gels, and progressive pore-structure densification (Wang and Scrivener, 1995). Among the hybrid-activated systems, the SC/SH (50/50)–10% mixture achieves the highest long-term UCS, reaching approximately 1.6 MPa at 210 days. This value approaches that of the OPC control, which reaches approximately 1.8 MPa over the same period. The comparable long-term performance demonstrates the effectiveness of hybrid activation in producing mechanically robust CPB while relying on a lower-carbon binder system. Mixtures with higher sodium carbonate content maintain lower long-term UCS values, consistent with their delayed hydration kinetics and higher residual porosity. Similarly, increasing the total activator dosage beyond optimal levels does not yield proportional strength gains, suggesting that excessive activator content may not translate into more efficient utilization of dissolved species.

4.3.4.4 Identification of Optimal Formulations

The combined UCS results clearly indicate that balanced SC/SH ratios at moderate activator dosages provide the most favorable performance in slag-based CPB. In particular, the SC/SH (50/50)–10% mixture emerges as the optimal formulation for the mixtures studied in this research, exhibiting:

- The fastest transition from early-age retardation to accelerated hydration.
- The highest long-term UCS among alkali-activated systems.
- Matrix densification consistent with low porosity and water content.
- Strong capillary response indicative of refined pore structure.

This optimal behavior results from an effective balance between carbonate buffering and hydroxide-induced alkalinity enhancement. Carbonate species regulate early reaction pathways and contribute to secondary phase formation, while hydroxide ions accelerate slag dissolution and gel precipitation (Bernal et al., 2015a,b; Walkley et al., 2021; Dai et al., 2023). Overall, the UCS evolution confirms that hybrid Na_2CO_3–NaOH activation enables slag-based CPB to overcome early-age retardation while achieving long-term strength levels comparable to OPC-based systems. The results further demonstrate that strength development is strongly coupled to hydration kinetics and matrix densification

processes, as captured by the coupled monitoring framework and physical property evolution.

4.4. Integrated Mechanistic Discussion

The combined analysis of hydration kinetics, microstructural evolution, physical property development, and mechanical performance provides a comprehensive framework to interpret the behavior of slag-based CPB activated with blended sodium carbonate and sodium hydroxide. Rather than evolving independently, the observed changes in electrical conductivity (EC), volumetric water content (VWC), matric suction (ψ), phase assemblage, matrix densification, and strength development represent interconnected manifestations of the same underlying physicochemical processes governing binder hydration and microstructure formation.

4.4.1 Coupling between Hydration Kinetics and Matrix Densification

The coupled EC–VWC–ψ monitoring reveals a clear relationship between hydration reactions and the progressive densification of the CPB matrix. The initial ionization stage, characterized by high EC and nearly constant VWC (Figures 4.2-4.3), reflects elevated ionic concentration in the pore solution and limited formation of solid hydration products. During this stage, physical properties and UCS evolve only marginally, indicating that the microstructure remains largely unconsolidated. As curing progresses, the transition to the deionization–acceleration stage is marked by a rapid decrease in EC and a simultaneous reduction in VWC, signifying precipitation of hydration products and incorporation of ions and water into solid phases. This transition corresponds directly to the onset of matrix densification observed through increasing dry density and decreasing void ratio and porosity (Figures 4.6-4.8). The subsequent increase in matric suction (Figure 4.4) reflects the mechanical consequences of this chemical evolution. As hydration products progressively occupy pore spaces and reduce hydraulic connectivity, capillary stresses intensify, indicating pore refinement and structural consolidation. The relationship EC ↓ + VWC ↓ + ψ ↑ thus provides a direct mechanistic link between chemical reactions and physical matrix development. This evolution marks a fundamental shift in system control from an ionic-dominated regime, governed primarily by pore-solution chemistry,

to a solid skeleton-controlled regime, where the interconnected network of hydration products governs transport properties, capillary behavior, and mechanical response.

4.4.2 Role of Blended SC–SH Activation Chemistry

The hybrid sodium carbonate–sodium hydroxide activation strategy plays a central role in regulating hydration kinetics and microstructural development. Sodium carbonate introduces a buffering effect in the pore solution, moderating the rise in alkalinity and promoting early formation of carbonate phases through interactions with dissolved calcium species (Walkley et al., 2021). This buffering action stabilizes early reaction pathways but inherently delays extensive slag dissolution and gel formation. In contrast, sodium hydroxide increases pore-solution alkalinity, enhances slag dissolution, and accelerates precipitation of C-(A)-S-H gels. The hydroxide-induced acceleration shortens the ionization stage and promotes earlier transition to the deionization–acceleration regime. Balanced SC/SH ratios optimize the interplay between these two mechanisms. Carbonate species regulate early chemical stability and contribute to secondary phase formation, while hydroxide ions ensure sufficient alkalinity for rapid slag activation. This balance leads to:

- Earlier onset of accelerated hydration
- More efficient gel precipitation
- Enhanced pore refinement and densification

Excessive carbonate content prolongs retardation, whereas overly high activator dosages do not yield proportional improvements in reaction efficiency, highlighting the importance of optimized hybrid chemistry.

4.4.3 Mechanisms Governing Strength Development

Strength development in hybrid-activated slag CPB is governed by the progressive formation and stabilization of a composite microstructure revealed by XRD analysis (Figure 4.5). Unlike OPC-based systems dominated by C-S-H and portlandite, hybrid activation produces a phase assemblage composed of:

- Amorphous C-(A)-S-H gels forming the primary load-bearing network
- Crystalline calcite resulting from carbonate participation

- Hydrotalcite-like layered double hydroxide phases contributing to stabilization

The amorphous C-(A)-S-H gel provides continuous binding and mechanical cohesion, while calcite and hydrotalcite-like phases contribute to pore filling and microstructural continuity (Bernal et al., 2011; Myers et al., 2013). The absence of portlandite indicates efficient calcium utilization within the gel matrix and secondary phases.

The coupling between hydration kinetics and phase formation explains the observed UCS evolution (Figure 4.9). Early-age retardation corresponds to limited gel formation during the ionization stage. Accelerated strength gain occurs once extensive C-(A)-S-H precipitation begins, coinciding with EC and VWC decreases. Sustained long-term strength development results from continued gel growth and pore refinement. Balanced SC/SH formulations promote the most efficient microstructure formation pathway, producing dense matrices with low porosity and high suction, which directly translate into superior long-term mechanical performance.

4.4.4 Implications for CPB Design

The integrated mechanistic framework established in this study has important implications for the design and optimization of CPB systems. First, hybrid Na_2CO_3–NaOH activation enables tailorable hydration kinetics, allowing engineers to regulate early-age reaction rates and long-term performance by adjusting SC/SH ratios and activator dosages. Second, the observed trade-off between early-age retardation and accelerated long-term densification highlights the need to balance pumpability and early mechanical support. Carbonate-rich systems offer extended workability windows desirable for long transport distances, while hydroxide-enhanced formulations provide faster structural build-up when early strength is required. Third, the ability of hybrid-activated slag CPB to achieve long-term UCS comparable to OPC-based systems while relying on lower-carbon binders demonstrates strong potential for sustainable backfilling operations. Optimized hybrid activation offers a pathway to reduce CO_2 emissions and binder costs without sacrificing performance. Finally, the coupled EC–VWC–ψ monitoring approach provides a powerful non-destructive tool for real-time assessment of hydration behavior under realistic CPB

conditions. This framework can support predictive control of backfill performance and guide binder formulation in both laboratory and field applications.

Overall, the integrated results demonstrate that the performance of slag-based CPB activated with blended sodium carbonate and sodium hydroxide is governed by the coupled evolution of pore-solution chemistry, hydration kinetics, phase assemblage development, and matrix densification. Balanced hybrid activation chemistry effectively synchronizes these processes, producing dense microstructures and strong long-term mechanical performance while enabling flexible control over early-age behavior. This mechanistic understanding provides a robust basis for the rational design of next-generation low-carbon binders for underground backfilling.

4.5. Conclusions

This study investigated the hydration mechanisms, microstructural evolution, physical property development, and strength performance of slag-based CPB activated with blended sodium carbonate (SC) and sodium hydroxide (SH) under realistic backfill conditions. Based on coupled monitoring, XRD analysis, and mechanical testing, the following conclusions can be drawn:

- Hybrid SC–SH activation fundamentally modifies hydration pathways compared to conventional OPC-based CPB, promoting the formation of a composite phase assemblage dominated by amorphous C-(A)-S-H gels, calcite, and hydrotalcite-like phases rather than portlandite-based systems. This altered chemistry enhances matrix densification and long-term performance while eliminating reliance on Portland cement hydration products, thereby enabling the development of fundamentally different low-carbon binder systems.
- Hydration kinetics follow a distinct two-stage mechanism consisting of an initial ionization/retardation stage characterized by high electrical conductivity and limited water consumption, followed by a deionization–acceleration stage marked by rapid gel precipitation, water binding, and progressive pore refinement. This controllable hydration behavior provides

a basis for optimizing binder efficiency and minimizing excess material use, supporting resource-efficient and sustainable binder design.

- The coupled EC–VWC–ψ monitoring framework effectively resolves hydration processes in CPB systems, providing direct insight into ionic activity, water consumption, and capillary-driven microstructural consolidation. The combined trends (EC ↓, VWC ↓, ψ ↑) offer a powerful mechanistic indicator of matrix densification and hydration progress, facilitating the rational optimization of binder formulations to achieve required performance with reduced material and energy inputs.
- Balanced SC/SH ratios at moderate activator dosages yield optimal performance, with the SC/SH (50/50)–10% formulation exhibiting the fastest transition to accelerated hydration, the most pronounced pore refinement, and the highest long-term UCS among alkali-activated systems. Excessive carbonate content prolongs early retardation, while overly high activator dosages do not provide proportional benefits, highlighting the importance of optimized activator usage to minimize chemical consumption and environmental footprint.
- Hybrid-activated slag CPB achieves long-term strength comparable to OPC-based systems while exhibiting superior matrix densification, demonstrating the effectiveness of hybrid activation in overcoming early-age retardation associated with sodium carbonate alone. This performance equivalence enables direct substitution of Portland cement in backfill applications, thereby offering substantial potential for reducing CO_2 emissions, lowering embodied energy, and decreasing the environmental impact of underground mining operations.
- The results highlight strong sustainability potential, as hybrid SC–SH activation enables the use of low-carbon slag-based binders while maintaining mechanical performance suitable for underground backfilling operations. By valorizing industrial by-products and reducing dependence on carbon-intensive Portland cement, this approach supports cleaner production in mining and construction sectors, promotes circular economy

principles, and contributes to the development of environmentally responsible underground infrastructure systems. Tailorable hydration kinetics further allow optimization for pumpability, setting control, and early support requirements.

Overall, the integrated mechanistic framework established in this study demonstrates that blended sodium carbonate–sodium hydroxide activation provides an efficient and flexible strategy for controlling hydration behavior, microstructure development, and strength evolution in slag-based CPB. The findings offer a robust scientific basis for the design of next-generation sustainable backfill binders with tunable performance characteristics and demonstrate a viable pathway toward reducing the carbon footprint, improving resource efficiency, and advancing cleaner production practices in mining and geotechnical engineering applications.

Despite the comprehensive mechanistic insights provided, this study is limited by the use of qualitative XRD for microstructural characterization, a single tailings type, and a relatively short duration of coupled hydration monitoring. Future research should incorporate advanced imaging techniques, quantitative phase analysis, a wider range of tailings materials, and extended monitoring periods to further resolve microstructural evolution and long-term performance of hybrid-activated CPB systems, as well as to quantify environmental benefits such as CO_2 reduction potential, lifecycle environmental impact, and sustainability performance under field conditions.

4.6 References

Alsalman A, Assi LN, Kareem RS, Carter K, Ziehl P 2021. Energy and CO2 emission assessments of alkali-activated concrete and Ordinary Portland Cement concrete: A comparative analysis of different grades of concrete. *Cleaner Environmental Systems*, *3*, 100047.

Andrew RM. 2019. Global CO_2 emissions from cement production, 1928–2018. *Earth System Science Data*, 11, 1675–1710.

Bakharev T, Sanjayan JG, Cheng YB. 2002. Sulfate attack on alkali-activated slag concrete. *Cement and Concrete Research*, 32, 211–216.

Benzaazoua M, Fall, M, Belem T, 2004. A contribution to understanding the hardening process of cemented pastefill. *Minerals Engineering*, 17, 141–152.

Bernal SA, Provis JL. 2014. Geopolymers and related alkali-activated materials. *Annual Review of Materials Research*, 44, 299–327.

Bernal SA, Provis JL, Rose V., De Gutierrez, R.M., 2011. Evolution of binder structure in sodium silicate-activated slag-metakaolin blends. *Cement and Concrete Composites*, *33*(1), 46-54.

Bernal SA, Provis JL, Myers RJ, San Nicolas R, van Deventer JSJ. 2015. Role of carbonates in the chemical evolution of sodium carbonate-activated slag binders. *Materials and Structures*, 48, 517–529.

Bernal SA, Nicolas RS, van Deventer JS, Provis JL 2016. Alkali-activated slag cements produced with a blended sodium carbonate/sodium silicate activator. *Advances in Cement Research*, *28*(4), 262-273.

Chottemada PG, Kar A, Kara De Maeijer P 2023. Environmental impact analysis of alkali-activated concrete with fiber reinforcement. *Infrastructures*, *8*(4), 68.

Cui L, Fall M 2017. Multiphysics model for consolidation behavior of cemented paste backfill. *International Journal of Geomechanics*, *17*(3), 04016077.

Dai X, Ren Q, Aydin S, Yardimci MY, De Schutter, G 2023. Accelerating the reaction process of sodium carbonate-activated slag mixtures with the incorporation of a small addition of sodium hydroxide/sodium silicate. *Cement and Concrete Composites*, *141*, 105118.

Duxson P, Provis JL, Lukey GC, van Deventer JS 2007. The role of inorganic polymer technology in the development of 'green concrete'. *Cement and concrete research*, *37*(12), pp.1590-1597.

Fall M, Benzaazoua M, Saa EG 2008. Mix proportioning of underground cemented tailings backfill. *Tunnelling and Underground Space Technology, 23(1), 80-90*.

Fall M, Célestin JC, Pokharel M, Touré M 2010. A contribution to understanding the effects of curing temperature on the mechanical properties of mine cemented tailings backfill. *Engineering Geology*, *114*(3-4), 397-413.

Fernández-Jiménez A, Puertas F 2003. Effect of activator mix on the hydration and strength behaviour of alkali-activated slag cements. *Advances in Cement Research*, *15*(3), 129-136.

Fredlund DG, Rahardjo H. 1993. *Soil Mechanics for Unsaturated Soils*. John Wiley & Sons, New York.

Grabinsky M, Simms P 2006. Self-desiccation of cemented paste backfill and implications for mine design. In *Paste 2006: Proceedings of the Ninth International Seminar on Paste and Thickened Tailings* (pp. 323-332). Australian Centre for Geomechanics.

Liu, S., and M. Fall. 2022. "Fresh and hardened properties of cemented paste backfill: Links to mixing time." *Construction and Building Materials*, 324: 126688.

Lothenbach B, Le Saout G, Gallucci E, Scrivener KL. 2008. Influence of limestone on the hydration of Portland cements. *Cement and Concrete Research*, 38, 848–860.

Marathe S, Sheshadri A, Nikolaiev V 2025. Life cycle assessment of sustainable air-cured alkali-activated concrete for permeable pavements using agro-industrial wastes. *Scientific Reports*, *15*(1), p.22012.

Myers RJ, Bernal SA, San Nicolas R, Provis JL 2013. Generalized structural description of calcium–sodium aluminosilicate hydrate gels: the cross-linked substituted tobermorite model. *Langmuir*, *29*(17), 5294-5306.

Provis JL, Bernal SA. 2014. Geopolymers and related alkali-activated materials. *Annual Review of Materials Research*, 44, 299–327.

Shi C, Roy D, Krivenko P 2003. *Alkali-Activated Cements and Concretes*. CRC Press, London.

Tian X, Fall M. 2021. Non-isothermal evolution of mechanical properties, pore structure and self-desiccation of cemented paste backfill. *Construction and Building Materials*, 297, 123657.

Taylor HF. 1997. *Cement Chemistry*. 2nd ed. Thomas Telford, London.

Walkley B, Ke X, Provis JL, Bernal SA 2021. Activator anion influences the nanostructure of alkali-activated slag cements. *The Journal of Physical Chemistry C*, *125*(37), 20727-20739.

Wang SD, Scrivener KL. 1995. Hydration products of alkali-activated slag cement. *Cement and Concrete Research*, 25, 561–571.

Wu D, Fall M, Cai SJ 2014. Numerical modelling of thermally and hydraulically coupled processes in hydrating cemented tailings backfill columns. *International Journal of Mining, Reclamation and Environment*, *28*(3), 173-199.

Xiapeng P, Fall M, Haruna S 2019. Sulphate induced changes of rheological properties of cemented paste backfill. *Minerals Engineering*, *141*, 105849.

Yang KH, Song JK, Song KI 2013. Assessment of CO2 reduction of alkali-activated concrete. *Journal of Cleaner Production*, *39*, 265-272.

Yilmaz E, Belem T, Bussière B, Mbonimpa M, Benzaazoua M 2015a. Curing time effect on consolidation behaviour of cemented paste backfill containing different cement types and contents. *Construction and Building Materials*, *75*, 99-111.

Yilmaz E, Belem T, Benzaazoua M 2015b. Specimen size effect on strength behavior of cemented paste backfills subjected to different placement conditions. *Engineering Geology*, *185*, 52-62.

Zhu XH, Kang XJ, Yang K, Yang CH. 2017. Effect of graphene oxide on mechanical properties and formation of layered double hydroxides (LDHs) in alkali-activated slag cement. *Construction and Building Materials*, 132, 290–295.

Chapter 5: Technical Paper 2: Fresh properties of cemented paste backfill with slag activated by a blend of sodium carbonate and sodium hydroxide

Soya Bathily, Mamadou Fall, Abdurrahman Suleiman Mohammed

Author Contributions

Soya Bathily: Formal analysis, Investigation, Methodology, Visualization, Writing – original draft. Mamadou Fall: Conceptualization, Methodology, Project administration, Resources, Supervision, Funding Acquisition; Writing – review & editing. Abdurrahman Suleiman: Analysis, Methodology, Writing – review & editing.

(Submitted for publication)

Abstract

This study investigates the fresh-state and early-age properties of cemented paste backfill (CPB) incorporating slag activated by blended sodium carbonate (SC) and sodium hydroxide (SH) (alkali-activated ternary CPB, AA-TC-CPB). The effects of activator composition and dosage on rheological behavior, early hydration, and setting characteristics were examined using yield stress and viscosity measurements, X-ray diffraction (XRD), zeta potential analysis, and continuous monitoring of electrical conductivity (EC) and volumetric water content (VWC). The results show that SC/SH co-activation significantly alters early hydration kinetics and paste structuration compared with Portland cement-based CPB. Hydroxide-rich activation enhances slag dissolution and accelerates the formation of C-(A)-S-H and hydrotalcite-like phases, leading to faster rheological build-up. In contrast, balanced SC/SH systems delay early structuration, resulting in lower yield stress and viscosity at early ages but extended setting times. Mixtures activated with an SC/SH ratio of 50/50 provide a favourable compromise between pumpability and controlled setting, whereas under-activated systems exhibit limited early reaction and delayed structural development. Overall, the results demonstrate that sodium carbonate-sodium hydroxide co-activation offers a tunable approach to control the fresh

properties and early-age behavior of slag-based CPB, enabling optimisation of workability and setting performance for underground backfilling applications.

Keywords: Cemented paste backfill; Alkali-activated slag; Sodium carbonate; Sodium hydroxide; Fresh properties; Rheology; Setting time

5.1 Introduction

The mining industry plays an important role in global economic development by providing essential raw materials for construction, energy production, and technological advancement. However, mining activities generate enormous quantities of tailings, which are typically stored in surface tailings storage facilities (TSFs). These storage methods pose serious environmental risks, including soil and groundwater contamination, landscape degradation, and, in extreme cases, catastrophic tailings dam failures (Wu et al. 2014; Jiang and Fall, 2017). These challenges highlight the urgent need for safer and more sustainable approaches to tailings management in the mining sector.

CPB has emerged as an effective solution to reduce the environmental footprint of tailings disposal while improving underground mine stability. CPB consists of dewatered tailings mixed with a hydraulic binder and water to produce a pumpable paste that is placed in underground voids (Cui and Fall, 2017, 2018; Fang et al. 2020). The performance of CPB is strongly governed by its fresh-state properties, such as workability, flow ability (controlled by yield stress and viscosity), thixotropy, and setting time, which control both pipeline transport and structural stability after placement (Klein and Simon, 2006; Sagade and Fall 2024).

Ordinary Portland cement (OPC) is one the most widely used binders in CPB applications due to its availability and predictable strength development. Nevertheless, its extensive use raises both technical and environmental concerns when applied at the scale required in underground mining. The production of OPC is associated with high greenhouse gas emissions, estimated at approximately 0.9 t of CO_2 per ton of cement,

which significantly increases the environmental footprint of backfilling operations (Jiang and Fall, 2017; Scrivener et al., 2018). In addition, the high heat released during OPC hydration may induce thermal cracking in massive backfill pours, while low underground temperatures can markedly slow hydration kinetics and delay early strength development. The use of OPC can represent up to 75% of the cost of CPB (Fall et al. 2010). These limitations have stimulated growing interest in alternative binder systems better adapted to the operational and environmental constraints of CPB.

Among these alternatives, alkali-activated binders based on ground granulated blast-furnace slag (GGBFS) have attracted increasing attention. GGBFS is an industrial by-product with latent hydraulic reactivity that can be activated using alkaline solutions to form cementitious reaction products, primarily calcium-aluminosilicate-hydrate (C-(A)-S-H) gels (Bernal et al. 2013a). The nature of the activator strongly influences dissolution kinetics, hydrate assemblage, and early-age behavior. Sodium hydroxide (NaOH) is a highly effective activator that promotes rapid slag dissolution and strength development but may increase viscosity and reduce workability. In contrast, sodium carbonate (Na_2CO_3) is a milder activator that generally enhances workability while delaying setting and early strength gain (Brough and Atkinson, 2002; Ke et al., 2016; Jiao et al. 2018)

Previous studies have shown that combining different activators can provide greater control over early-age behavior. Puertas et al. (2003) reported that multi-activator systems allow fine-tuning of hydration kinetics and rheological properties in alkali-activated materials. More recently, Dai et al. (2023) demonstrated that modifying carbonate-activated slag binders through supplementary activation strategies can enhance hydration kinetics, improve setting behavior, and increase early strength development in CPB systems. Despite these advances, most investigations have primarily focused on strength and general performance characteristics, while the coupled mechanisms governing early-age rheological structuration, electrochemical evolution, and hydration-driven microstructural development in hybrid NaOH–Na_2CO_3 activated CPB systems remain insufficiently understood.

Fresh-state properties are critical to CPB performance in the field. Workability or flow ability ensures efficient pumping, viscosity governs energy demand and segregation,

thixotropy controls structural recovery after placement, and setting time dictates safe excavation schedules and operational efficiency (Klein and Simon, 2006; Xiapeng et al. 2019; Sagade and Fall, 2024). Alkali activators exert a strong influence on these properties: NaOH tends to increase viscosity and accelerate setting, whereas Na_2CO_3 extends workability and improves pumpability but delays strength development (Brough and Atkinson, 2002; Xiao et al., 2020). Hybrid NaOH-Na_2CO_3 systems have therefore been proposed as a means of balancing reactivity and workability. However, their behavior remains insufficiently documented under CPB-specific conditions, particularly with respect to fresh-state rheology, early-age structuration, and operational constraints.

Moreover, existing studies often examine fresh-state rheology, electrochemical characteristics, or early-age microstructural evolution separately. As a result, the coupled mechanisms by which activator chemistry controls the early ionic environment, particle interactions, hydrate formation, and time-dependent structuration in alkali-activated CPB systems are not yet fully established. In particular, the role of carbonate-hydroxide co-activation in balancing dispersion, structural build-up, and setting behavior in slag-based CPB remains insufficiently quantified.

Accordingly, this study investigates the fresh-state and early-age behavior of CPB incorporating slag activated by blended sodium carbonate and sodium hydroxide. A combined experimental approach involving rheological measurements, X-ray diffraction, zeta potential analysis, and continuous monitoring of electrical conductivity and volumetric water content is employed to elucidate the influence of activator composition and dosage on early paste structuration and setting behavior. The results aim to provide practical insights for optimising the workability and early performance of alkali-activated CPB systems for underground mining applications.

5.2 Experimental program

5.2.1 Materials and mixture proportioning

5.2.1.1 Materials

The grain size distribution, physical properties, and mineralogical composition of the silica tailings (ST) used in this study are presented in Fig. 5.1 and Tables 5.1 and 5.2.

The particle size distribution of ST is similar to the average grain size distribution reported for tailings from nine different mines in eastern Canada.

Table 5.1: Physical and grain-size characteristics of the silica tailings (ST) used in the CPB mixtures.

Element	G_s	D_{10}	D_{30}	D_{50}	D_{60}
Unit	-	µm	µm	µm	µm
ST	2.7	1.9	9.0	22.5	31.5
Average of 9 types of tailings	-	1.8	9.1	20.0	30.8

ST: silica tailings; Gs: specific gravity; D10, D30, D50, D60: characteristic particle diameters

Table 5.2: Mineralogical composition of the silica tailings (ST) determined by X-ray diffraction (wt.%).

	Mineral											
Tailings	Quartz	Albite	Dolomite	Calcite	Chlorite	Magnetite	Pyrite	Talc	Pyrrhotite	Spinel	Others	Total
ST (wt.%)	99.8	-	-	-	-	-	-	-	-	-	0.2	100.0

ST: silica tailings; wt.: weight.

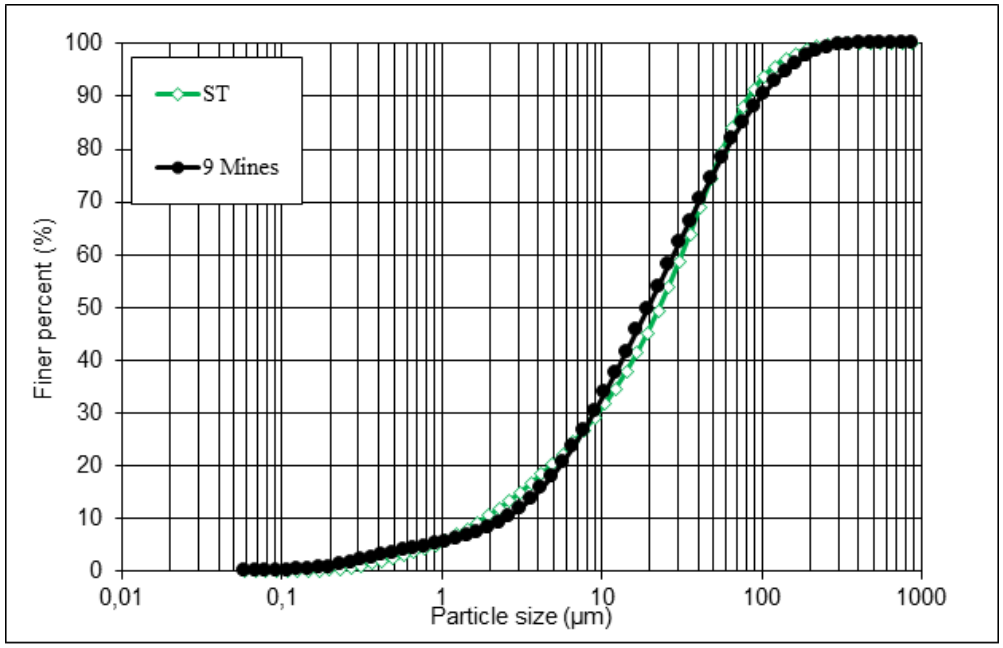

Figure 5.2: Grain size distribution of the silica tailings (ST) as well as average grain size distribution of tailings from nine mines in Eastern Canada

5.2.1.2 Binder and water

The binders used in this study consisted of ordinary Portland cement (PCI, Type I) and ground granulated blast-furnace slag (GGBFS). Portland cement was used as a reference binder, while slag was employed in the alkali-activated systems. Sodium carbonate (Na_2CO_3, purity >98%) and sodium hydroxide (NaOH, purity >98%) were used as alkaline activators for slag-based mixtures. All activators were added in solid anhydrous form, and their dosages were defined relative to the mass of slag. Mixing water consisted of tap water and was used without any chemical modification. Because the activators were introduced as solids, no correction to the mixing water content was required. The chemical composition and selected physical properties of Portland cement and slag are summarized in Table 5.3.

Table 5.3: Chemical composition and physical properties of Portland cement type I and ground granulated blast-furnace slag (GGBFS).

Binder	MgO (wt.%)	CaO (wt. %)	SiO_2 (wt.%)	Al_2O_3 (wt.%)	Fe_2O_3 (wt.%)	SO_3 (wt.%)	Rel. Density (%)	Specific surface (m^2/g)
PCI	2.65	62.82	18.03	4.53	2.70	3.82	3.15	1.3
Slag	10.98	41.14	34.23	9.54	-	3.87	2.90	2.2

wt.%: weight percent; PCI: Portland cement type I.

5.2.1.3 Specimen preparation

The mix proportions of the CPB mixtures prepared for rheological, setting time, and zeta potential tests are summarised in Table 5.4. The compositions of CPB mixtures instrumented for monitoring volumetric water content and electrical conductivity are also presented in Table 5.4. In addition, cement paste mixtures without tailings prepared for microstructural analyses are listed in Table 5.5. All raw materials were weighed to the nearest 0.1 g prior to batching.

Table 5.4: Mix design of CPB samples used for rheological, setting time, and zeta potential tests as well as for monitoring volumetric water content (VWC) and electrical conductivity (EC).

Sample	**PC (%)**	**Slag (%)**	**Activator content (%)**	**SC/SH ratio***	**W/B***
Control	4.5	0	0	-	7.4
SC/SH (50/50)-15%	0	4.5	15	50/50	7.4
SC/SH (20/80)-15%	0	4.5	15	20/80	7.4
SC/SH (50/50)-20%	0	4.5	20	50/50	7.4
SC/SH (50/50)-10%	0	4.5	10	50/50	7.4

*W/B: water-to-binder ratio; SC/SH = mass of SC/mass of SH (SC: Sodium Carbonate; SH: Sodium Hydroxide)

The required quantities of binders (Portland cement Type I and/or ground granulated blast-furnace slag), silica tailings, alkaline activators (sodium carbonate and sodium hydroxide), and mixing water were proportioned according to the mix designs. Mixing was carried out using a household food mixer for approximately 10 min to obtain homogeneous CPB mixtures. A constant water-to-binder mass ratio (W/B) of 7.4 was used for all CPB batches. This relatively high W/B ratio is typical of CPB practice, where excess water is required to ensure pumpability and pipeline transport over long distances. For cement paste mixtures prepared without tailings, the same procedure was followed, except that silica tailings were omitted. Sodium carbonate and sodium hydroxide were added as anhydrous solids; therefore, no correction to the mixing water content was required.

Table 5.5: Composition of cement paste mixtures prepared for XRD analysis after 4 h of curing.*

Sample	PC (g)	Slag (g)	Activator (%)	SC/SH ratio*	W/B
Control	100	0	0	-	1
SC/SH (50/50)-15%	0	100	15	50/50	1
SC/SH (20/80)-15%	0	100	15	20/80	1
SC/SH (50/50)-20%	0	100	20	50/50	1
SC/SH (50/50)-10%	0	100	10	50/50	1

*All pastes prepared with W/B = 1. Sodium carbonate (SC) and sodium hydroxide (SH) were added as anhydrous solids

Fresh CPB was poured into rigid plastic cylindrical molds in a single lift. During casting, the paste was gently stirred and the molds were tapped to release entrapped air; no external vibration was applied. Three specimen sizes were used depending on the test type: cylinders with a diameter of 100 mm and a height of 100 mm for rheological testing, cylinders with a diameter of 50 mm and a height of 100 mm for microstructural analyses, and cylinders with a diameter of 100 mm and a height of 200 mm for monitoring experiments. After casting, the molds were immediately sealed to prevent moisture loss.

All specimens were cured at 20 °C under sealed conditions. A total of fifteen cylinders (50 × 100 mm) were prepared for microstructural analyses, corresponding to three specimens per CPB mixture, including additional control samples. In addition, five large cylinders (100 × 200 mm) were cast for monitoring experiments.

For cement paste specimens intended for X-ray diffraction analysis, samples were oven-dried at 45 °C for four days at the selected curing age, then sealed in airtight plastic bags until testing to limit moisture exchange and carbonation. All specimens, molds, and instrumented samples were labelled with unique identifiers, and sensor calibration and seal integrity were verified prior to testing to ensure data reliability.

5.2.2 Test methods

5.2.2.1 Rheological tests

The fresh-state rheological behavior of the CPB mixtures was characterized through viscosity and yield stress measurements. Apparent viscosity was measured using a Brookfield digital viscometer (DV-E model) equipped with an RV6 spindle. Prior to testing, the samples were gently shaken for approximately 1 min to ensure homogeneity. The spindle was carefully immersed at the centre of the sample to avoid air entrapment, and the material was allowed to stabilise for approximately 30 s before measurement. Viscosity readings were recorded twice, at 30 s and 40 s, under a constant rotational speed of 50 revolutions per minute (rpm), and the average value was reported. All measurements were performed in accordance with the manufacturer's guidelines. Additional details regarding the use of this device for CPB viscosity measurements can be found in Haruna and Fall (2020).

The yield stress of CPB mixtures was determined using a Wykeham-Farrance vane shear apparatus. The device was equipped with a four-blade vane with a height of 2.5 cm and a diameter of 2.5 cm, driven at a constant rotational speed of 0.18 rpm and connected to a calibrated torsional spring. Tests were conducted at curing times of 0 min, 30 min, 1 h, 2 h, and 4 h, following the procedure described in ASTM D4648/D4648M-13. Prior to each test, the sample was gently stirred and homogenised for 1 min using a spatula to simulate shear conditions experienced during CPB transportation and to minimise particle settlement. During testing, the vane was rotated slowly while recording the torque-time response. The yield stress (τ_γ) was calculated from the maximum measured torque using the following expression recommended in ASTM D4648:

$$\tau_y = \frac{2T_m}{\pi D^3}\left(\frac{1}{3} + \frac{H}{D}\right)$$

Where τ_y is the yield stress (Pa), T_m is the maximum measured torque (N·m), and H and D, are the vane height and diameter (m), respectively. To improve measurement accuracy, each test was repeated at least twice, and the average value was reported.

5.2.2.2 Setting time measurements

The initial and final setting times of the CPB mixtures were determined using a Vicat apparatus in accordance with ASTM C191-13. Cylindrical specimens with a diameter of 100 mm and a height of 40 mm were prepared for the tests. Setting time measurements were based on the resistance of the mixture to needle penetration. The initial setting time was defined as the time at which the Vicat needle penetrated to a depth of 25 mm from the bottom of the specimen. The final setting time was defined as the time at which the needle, equipped with an annular collar, failed to leave any visible impression on the surface of the specimen. All tests were conducted under controlled laboratory conditions, and at least two measurements were performed for each mixture to ensure repeatability.

5.2.2.3 Microstructural analyses

X-ray diffraction (XRD) analysis was performed to identify the crystalline phases present in cement paste samples prepared with Portland cement (PC) and slag activated with sodium carbonate (Na_2CO_3) and sodium hydroxide (NaOH). After curing, the specimens were oven-dried at 45 °C for 4 days to stop hydration reactions, then ground and sieved through a 40 μm sieve prior to analysis. XRD measurements were carried out using an X-ray diffractometer equipped with Cu Kα radiation (λ = 1.5406 Å), operated at an accelerating voltage of 40 kV and a current of 40 mA. Diffraction patterns were collected over a 2θ range of 2°-90° with a step size of 0.02°. Phase identification was performed by comparing the characteristic diffraction peaks with reference data reported in the literature.

5.2.2.4 Zeta potential measurements

Zeta potential measurements were conducted to assess the surface charge and interparticle interactions of CPB suspensions. Suspensions were prepared by dispersing CPB samples in distilled water at a solid-to-liquid ratio of 0.05 g per 50 g of water. Measurements were carried out using a Zetasizer Nano series instrument (Malvern Instruments Ltd.) equipped with phase analysis light scattering (PALS) technology to determine electrophoretic mobility. The instrument software automatically converted electrophoretic mobility values into zeta potential based on standard electrokinetic models.

Each specimen was measured six times, and the average value was reported to ensure reproducibility and accuracy.

5.2.2.5 Electrical conductivity (EC) and volumetric water content (VWC) monitoring of the specimens

The electrical conductivity (EC) and volumetric water content (VWC) of CPB specimens were continuously monitored using a 5TE sensor (Decagon Devices, Inc.) connected to an Em50 data logger. The sensor provides a measurement range of 0-23 dS/m for EC and 0-1 m^3/m^3 for VWC, with an accuracy of ±0.1 dS/m. The sensor was positioned at the geometric centre of each specimen to minimise boundary effects. Monitoring was performed on both Portland cement-based and slag-based CPB mixtures activated with sodium carbonate (Na_2CO_3) and sodium hydroxide (NaOH). The 5TE sensor determines EC by applying an alternating electrical current between two electrodes, while VWC is estimated from the dielectric permittivity of the material. EC and VWC data were automatically recorded by the data logger at 5 minutes intervals throughout the first 24 h of curing. Duplicate measurements were conducted for each mixture, and mean values were reported to ensure measurement reliability.

5.3. Results and discussions

5.3.1 Evolution of the rheological properties of alkali-activated ternary CPB, AA-TC-CPB

5.3.1.1 Yield Stress Evolution

Figure 5.2 shows the time-dependent evolution of yield stress for AA-TC-CPB mixtures, highlighting distinct rheological responses governed primarily by activator chemistry and dosage. All mixtures exhibit an increase in yield stress with curing time, indicating progressive paste structuration; however, both the magnitude and kinetics of yield stress development differ markedly between the Portland cement-based control and alkali-activated systems.

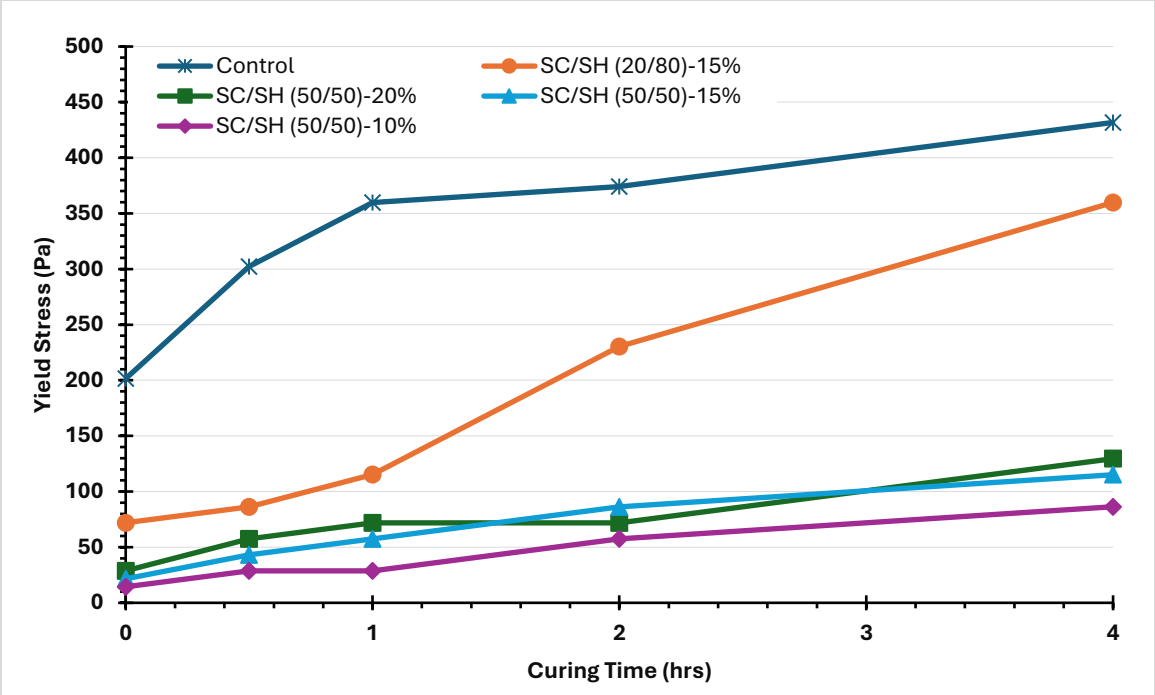

Figure 5.2. Time-dependent evolution of yield stress for CPB prepared with Slag activated by sodium carbonate (SC) and sodium hydroxide (SH) and for CPB with Portland cement.

The PCI control exhibits the highest initial and overall yield stress, increasing from approximately 200 Pa at 0 h to about 450 Pa after 4 h. This rapid build-up is attributed to early flocculation and hydration of Portland cement clinker phases, leading to the formation of a dense particle network dominated by early C-S-H precipitation in the absence of competing alkaline reactions (Taylor, 1977).

In contrast, the SC/SH (20/80)-15% mixture shows a pronounced early-age increase in yield stress, rising from approximately 70 Pa to 360 Pa within 4 h. This behavior is attributed to the hydroxide-rich activation environment, which promotes rapid slag dissolution and accelerated formation of early hydration products, resulting in a steadily densifying network (Li and Sun, 2000). Although the yield stress remains lower than that of the PCI control over the monitored period, the faster kinetics indicate more efficient early-age activation among the alkali-activated systems.

CPB mixtures with balanced activator ratios, such as SC/SH (50/50), exhibit slower structural build-up, reaching yield stress values of approximately 70-120 Pa after 4 h depending on activator dosage. The presence of sodium carbonate buffers pore solution chemistry and promotes transient carbonate precipitation, which temporarily limits ionic

mobility and delays nucleation and growth of C-(A)-S-H gels (Li and Sun, 2000). Consequently, despite similar activator contents, carbonate-rich formulations display reduced early-age yield stress compared to hydroxide-dominated systems. This reduced early-age yield stress is advantageous for CPB transport, as it enhances flowability and pumpability during placement operations.

Overall, these results demonstrate that activator chemistry exerts a stronger influence on early-age structuration kinetics than on absolute yield stress levels. While the PCI control achieves the highest yield stress due to rapid Portland cement hydration, hydroxide-rich activation (SC/SH = 20/80) provides the fastest structural build-up among alkali-activated systems. In contrast, carbonate-containing blends, although exhibiting slower structuration, provide enhanced workability retention and lower early-age yield stress, which can be advantageous for CPB applications requiring extended pumpability and handling time prior to setting.

5.3.1.2 Viscosity Evolution

Figure 5.3 illustrates the time-dependent evolution of viscosity for AA-TC-CPBs. The results include a Portland cement-based control mixture and four alkali-activated formulations with different SC/SH ratios and total activator contents.

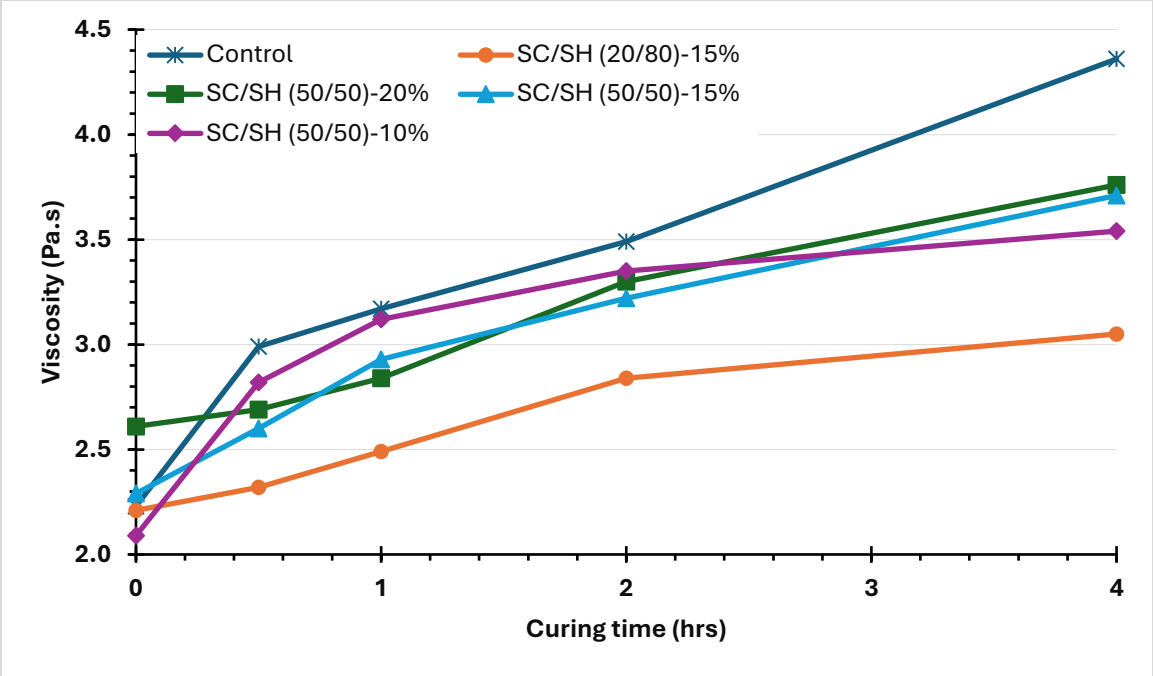

Figure 5.3. Time-dependent evolution of viscosity for CPB prepared with Slag activated by sodium carbonate (SC) and sodium hydroxide (SH) and for CPB with Portland cement.

All mixtures exhibit a progressive increase in viscosity with curing time, reflecting the gradual structural build-up of the paste as hydration and activation reactions proceed (Kou et al. (2020). The PCI control shows the highest viscosity values throughout the monitored period, reaching approximately 4.3 Pa·s after 4 h, consistent with rapid Portland cement hydration and continuous flocculation of cementitious phases.

At early ages (0-1 h), all activated systems experience a rapid rise in viscosity. The SC/SH (50/50)-10% mixture displays the steepest initial increase, which can be attributed to partial slag dissolution and the early formation of C-(A)-S-H gels under moderately alkaline conditions (Wang and Scrivener, 1995). In contrast, the SC/SH (20/80)-15% mixture, dominated by sodium hydroxide activation, exhibits the lowest viscosity values and the slowest rate of increase. This behavior suggests a more dispersed particle network at early ages, resulting from the dispersive effect of hydroxide ions, which enhances electrostatic repulsion between particles and delays the establishment of a cohesive microstructure. This interpretation is consistent with the well-established role of hydroxide ions (OH^-) in promoting slag dissolution through the breakdown of the glassy amorphous

aluminosilicate network of slag particles. High alkalinity (high pH) provided by (OH^-) accelerates the dissolution of slag, which initially promotes dispersion (Dai et al., 2022).

After approximately 1 h of curing, the rate of viscosity increase stabilises for most alkali-activated systems, indicating a balance between dispersion and progressive structuration. The PCI control, however, continues to thicken significantly, consistent with sustained hydration and flocculation processes. The gradual and steady viscosity growth observed in the SC/SH (50/50) series indicates that the presence of carbonate ions limits ionic mobility and delays gel connectivity, leading to a smoother rheological evolution compared with the Portland cement system.

Overall, the viscosity evolution of AA-TC-CPBs mixtures demonstrates that activator chemistry governs the competition between dispersion and structuration at early ages. Hydroxide-rich formulations promote lower initial viscosity and enhanced dispersion, whereas carbonate-containing blends favour slower structural build-up and improved workability retention. A balanced SC/SH ratio therefore appears effective in reducing initial viscosity and enhancing pumpability, while still allowing gradual network formation and adequate stability after placement.

5.3.1.3 XRD Analysis of Cemented Pastes

X-ray diffraction (XRD) analyses were performed on cement pastes prepared with Portland cement (control) and on slag activated by sodium carbonate (SC) and sodium hydroxide (SH) after 4 h of curing, in order to identify early-age reaction products and relate the microstructural development to the rheological behavior discussed in Sections 5.3.1.1 and 5.3.1.2. The mix compositions used for the XRD analyses are summarized in Table 5.5, and the corresponding diffraction patterns are presented in Figure 5.4.

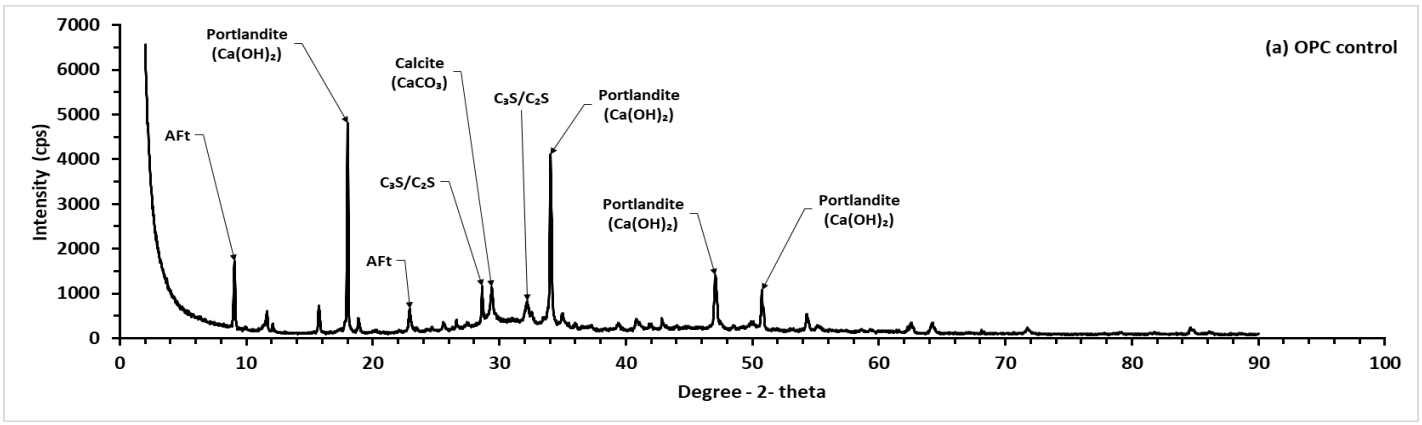
(a) OPC control
Portlandite (Ca(OH)₂)
Calcite (CaCO₃)
C₃S/C₂S
Portlandite (Ca(OH)₂)
AFt
C₃S/C₂S
Portlandite (Ca(OH)₂)
Portlandite (Ca(OH)₂)
AFt
Intensity (cps)
Degree - 2- theta

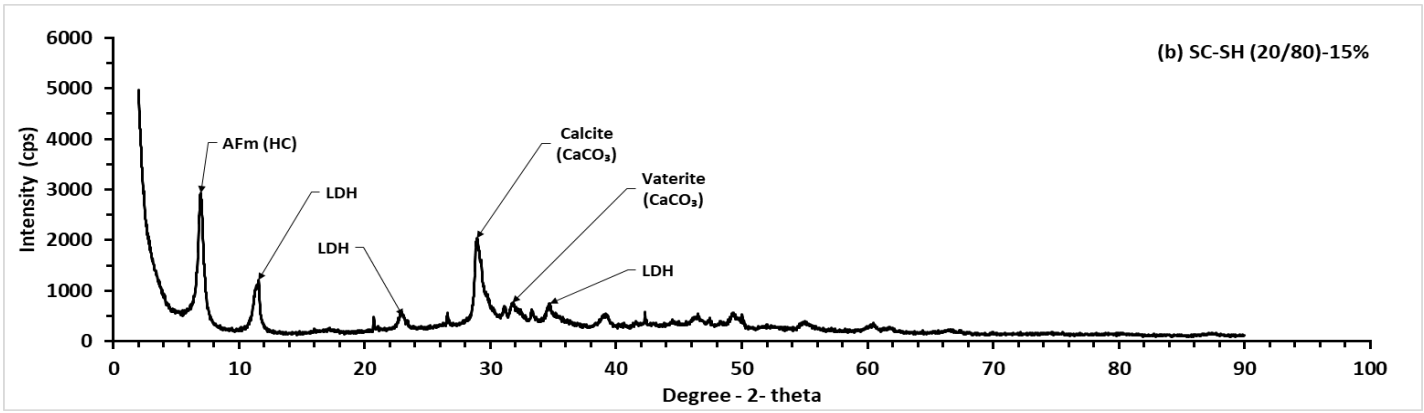
(b) SC-SH (20/80)-15%
AFm (HC)
Calcite (CaCO₃)
LDH
Vaterite (CaCO₃)
LDH
LDH
Intensity (cps)
Degree - 2- theta

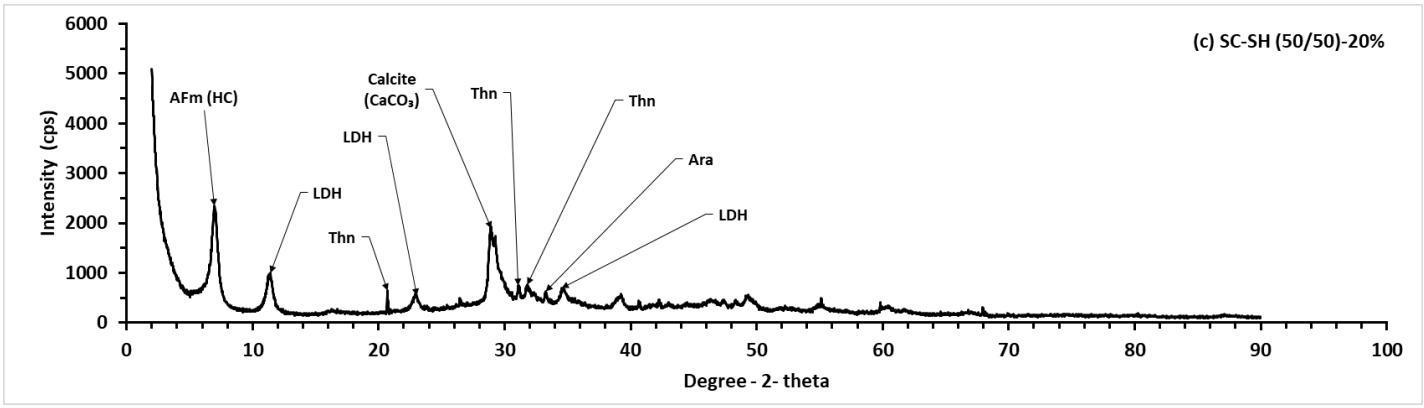
(c) SC-SH (50/50)-20%
AFm (HC)
Calcite (CaCO₃)
Thn
Thn
LDH
Ara
LDH
Thn
Intensity (cps)
Degree - 2- theta

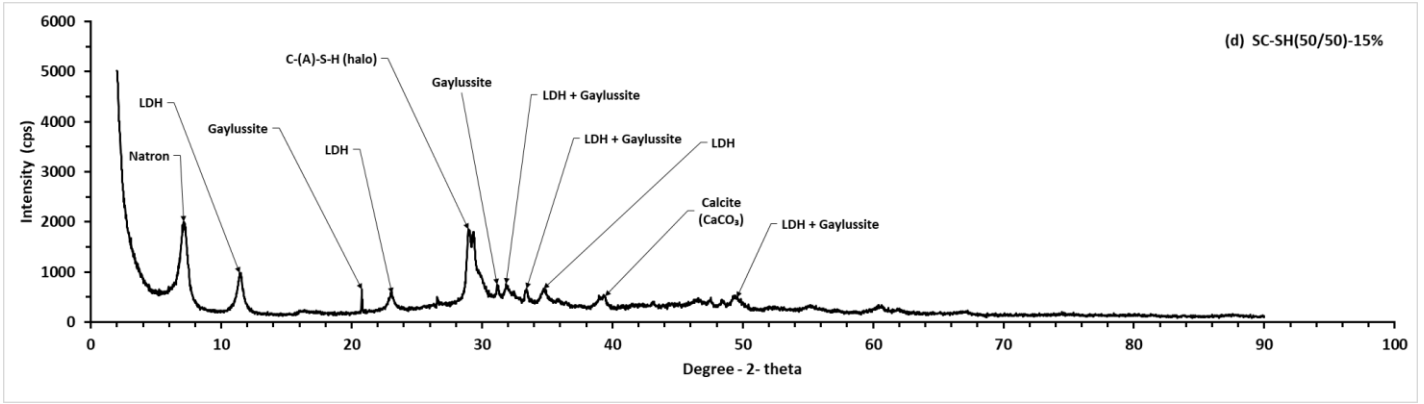
(d) SC-SH(50/50)-15%
C-(A)-S-H (halo)
Gaylussite
LDH
LDH + Gaylussite
Gaylussite
LDH + Gaylussite
LDH
Natron
LDH
Calcite (CaCO₃)
LDH + Gaylussite
Intensity (cps)
Degree - 2- theta

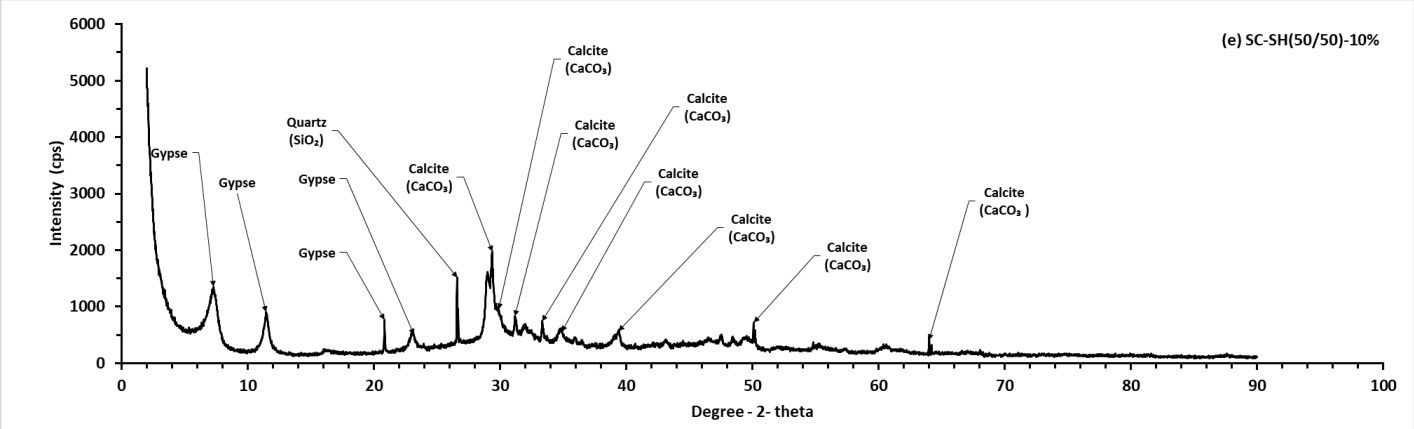

Figure 5.4. XRD patterns of cement pastes prepared with ternary binder after 4 h of curing: (a) OPC control, (b) SC-SH (20/80)-15 %, (c) SC-SH (50/50)-20 %, (d) SC-SH (50/50)-15 %, (e) SC-SH (50/50)-10 %.

The XRD pattern of the Portland cement-based control paste is characterized by intense portlandite ($Ca(OH)_2$) reflections at approximately 18°, 34°, and 47°, together with ettringite (AFt) and minor calcite peaks. This phase assemblage is typical of early-age OPC hydration, where rapid clinker hydration leads to the formation of crystalline calcium hydroxide, while silicate hydration remains incomplete at this curing age (Taylor, 1997; Scrivener et al., 2016).

In contrast, all SC/SH-activated systems are devoid of portlandite reflections, indicating a clear departure from OPC-type hydration mechanisms. Instead, the activated pastes exhibit diffraction features associated with carbonate-bearing phases and layered hydrates. Hydroxide-rich systems, particularly SC/SH (20/80)-15%, show pronounced reflections attributed to AFm hemicarbonate and hydrotalcite-like layered double hydroxides (LDH), together with calcite and vaterite. This phase assemblage reflects rapid slag dissolution under strongly alkaline conditions and preferential incorporation of carbonate species into AFm- and LDH-type structures rather than the formation of portlandite (Bernal et al., 2013b; Provis and van Deventer, 2014).

Mixtures with balanced activator ratios, such as SC/SH (50/50)-15% and SC/SH (50/50)-20%, display a combination of AFm-type phases, LDH reflections, and sodium carbonate-related phases, indicating simultaneous precipitation of layered hydrates and carbonate phases at higher activator dosages. The presence of a broad amorphous hump centred around 29° suggests the early formation of C-(A)-S-H gel, which is consistent with

progressive slag dissolution and the development of a cohesive binding network at early ages (Shi et al., 2011).

Conversely, the SC/SH (50/50)-10% mixture is dominated by crystalline calcite, gypsum, and persistent quartz reflections, with limited evidence of LDH or AFm phase development. The persistence of intense quartz peaks is consistent with previous studies reporting that quartz behaves as a largely inert filler during early-age alkali activation, particularly under moderate alkalinity and low activator dosage (Provis and van Deventer, 2014; Bernal et al., 2013b). At early curing stages, quartz does not actively participate in hydration reactions but reflects incomplete dissolution of the amorphous slag fraction, which delays the formation of C-(A)-S-H gel and limits early-age microstructural development (Shi et al., 2015). Such delayed reaction kinetics have been associated with weaker early-age structuration and reduced rheological build-up in alkali-activated systems with low activation capacity (Palacios et al., 2019; Sagade and Fall, 2024).

Overall, the XRD results demonstrate that SC/SH co-activation redirects the early reaction pathway from portlandite-rich OPC hydration toward the formation of carbonate-containing AFm phases, hydrotalcite-like LDH, and amorphous C-(A)-S-H gel. These microstructural features provide a mechanistic explanation for the early-age rheological behavior of AA-TC-CPBs mixtures, where rapid precipitation of layered hydrates and amorphous gels contributes to yield stress and viscosity build-up, while under-activated systems dominated by inert crystalline phases exhibit delayed structuration and reduced early-age cohesion (Sagade and Fall, 2024; Jiang and Fall, 2017).

5.3.1.4 Zeta Potential Results

Zeta potential measurements were performed on CPB mixtures prepared with Slag activated by sodium carbonate (SC) and sodium hydroxide (SH) and with Portland cement (control) after 4 h of curing. The objective was to evaluate the surface charge of suspended particles and assess the electrostatic stability of AA-TC-CPBs systems. The mix compositions used for these measurements are presented in Table 5.3, and the corresponding measurement results are presented in Figure 5.5.

Figure 5.5 shows that all CPB suspensions exhibit a net negative surface charge at 4 h of curing. The Portland cement-based control presents a moderately negative zeta

potential (−24.82 mV), which is typical of OPC suspensions where, Ca^{2+} ions partially screen the intrinsic negative charge of silicate and aluminate surfaces (Hunter, 1981; Lowke and Gehlen,2017). In contrast, all SC/SH-activated systems display significantly more negative zeta potential values, ranging from −33.77 mV to −36.70 mV, exceeding the commonly accepted colloidal stability threshold ($|Z| \geq 30$ mV). These values indicate enhanced electrostatic repulsion and improved particle dispersion compared to the Portland cement system, which is consistent with the reduced yield stress and viscosity observed in the rheological measurements discussed earlier.

At a constant total activator content (15%), the SC/SH (50/50) formulation exhibits a more negative zeta potential than the hydroxide-rich SC/SH (20/80) system, which is consistent with the lower yield stress values observed for the SC/SH (50/50) mixture compared to the SC/SH (20/80) mixture (Figure 5.2). This behavior suggests that the relative availability of OH^- (from NaOH) and CO_3^{2-} (from Na_2CO_3) governs the competition between surface deprotonation and anion adsorption. Hydroxide ions promote deprotonation of surface M-OH groups (M = Si, Al, Mg), increasing the negative surface charge, whereas carbonate species may adsorb or partially neutralize charged sites through the formation of carbonate-containing surface complexes, slightly reducing the magnitude of the zeta potential in carbonate-rich systems (Fernández-Jiménez and Palomo, 2005).

The electrokinetic response is consistent with the microstructural observations discussed in Section 5.3.1.3. Mixtures exhibiting more abundant hydrotalcite-like layered double hydroxides and AFm-type phases at early ages, particularly SC/SH (50/50)-15% and SC/SH (50/50)-20%, also show the most negative zeta potential values. This reflects enhanced slag dissolution and the presence of highly charged surfaces in the pore solution, promoting stable particle dispersion and delaying early flocculation (Sagade and Fall, 2024).

Overall, the zeta potential results confirm that SC/SH activation significantly modifies the electrostatic environment of slag-bearing CPB suspensions, providing greater colloidal stabilization during the early hours of hydration. This enhanced electrostatic repulsion explains the moderate viscosity levels and controlled yield stress evolution

observed in Sections 5.3.1.1 and 5.3.1.2, establishing a clear link between electrochemical surface properties and the macroscopic rheological behavior of AA-TC-CPB mixtures.

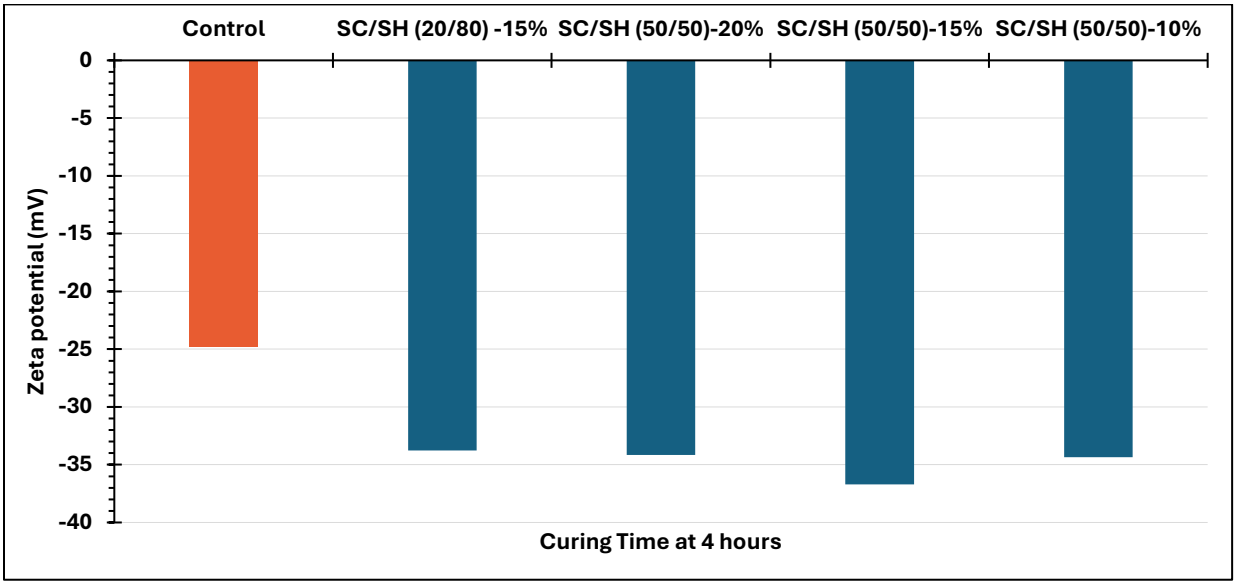

Figure 5.5. Zeta potential of AA-TC-CPB and Portland cement-CPB mixtures after 4 h of curing.

5.3.1.5 Electrical Conductivity Monitoring Results

Electrical conductivity (EC) of the pore solution was continuously monitored over the first 24 h of curing to assess ionic mobility and early hydration and activation reactions occurring within CPB mixtures prepared with ternary cement blends (McCarter et al., 1999; Huang et al., 2022). Electrical conductivity measurements provide a sensitive indicator of the dissolution of precursor phases and the subsequent formation of early reaction products (Snyder et al., 2003; Gevaudan et al., 2024). The mix compositions used for EC monitoring are listed in Table 5.3, and the corresponding results are displayed in Figure 5.6.

Figure 5.6 shows the evolution of electrical conductivity for all CPB mixtures during the first day of curing. A clear separation is observed between the Portland cement-based control and the SC/SH-activated systems (Zhu et al., 2018). In all mixtures, EC rises sharply immediately after mixing, reflecting the rapid release of ionic species into the pore solution, before approaching a quasi-steady state as hydration and activation products

precipitate and progressively consume dissolved ions (Heikal et al., 2014; Fang et al., 2023).

The Portland cement control exhibits a transient EC peak of approximately 4 mS/cm within the first hour, followed by a gradual decrease toward about 2 mS/cm at 1 day. This behavior is consistent with ordinary Portland cement hydration, where early dissolution of clinker phases releases Ca^{2+}, OH^{-}, and SO_4^{2-} ions, which are subsequently incorporated into hydration products such as ettringite and portlandite, reducing the ionic strength of the pore solution over time (Snyder et al., 2003; Lothenbach et al., 2011).

In contrast, all SC/SH-activated CPB systems maintain substantially higher EC levels throughout the monitoring period. The hydroxide-rich SC/SH (20/80)-15% mixture exhibits the highest EC values, rising rapidly to approximately 14-15 mS/cm and stabilising around 12-13 mS/cm after a slight decline. This behavior reflects the high initial availability of Na^{+} and OH^{-} ions supplied by the activators, which sustains a highly conductive pore solution during early-age slag dissolution and activation (Shi et al., 2011; Heikal et al., 2014).

Mixtures with balanced activator compositions (SC/SH = 50/50) exhibit intermediate EC plateaus that scale with total activator dosage, with values of approximately 11 mS/cm for 20%, 10 mS/cm for 15%, and 8 mS/cm for 10% activator content. The sharp initial EC increase observed in all activated systems reflects immediate ion availability from NaOH and Na_2CO_3 dissolution, while the subsequent plateau indicates the establishment of a dynamic equilibrium between continued slag dissolution and the precipitation of layered hydrates and C-(A)-S-H gel, which progressively regulate ionic transport in the pore solution (Zhu et al., 2018; Heikal et al., 2014).

At 1 day of curing, the EC hierarchy follows the order: SC/SH (20/80)-15% > SC/SH (50/50)-20% > SC/SH (50/50)-15% > SC/SH (50/50)-10% > Control. This ranking directly reflects the combined influence of activator chemistry and dosage on pore solution alkalinity and ionic strength. Hydroxide-dominant activation sustains the most conductive environment, whereas balanced SC/SH systems provide a moderated ionic regime that favours controlled activation kinetics (Shi et al., 2011; Fang et al., 2023).

Overall, the EC results confirm that SC/SH activation strongly governs the early ionic environment of AA-TC-CPB mixtures. Higher EC levels are associated with faster early-age activation and microstructural development, which is consistent with the more rapid yield stress and viscosity build-up discussed in Sections 5.3.1.1 and 5.3.1.2. Conversely, lower EC levels in under-activated systems correspond to delayed reaction kinetics and reduced early-age structuration, highlighting the critical role of pore solution chemistry in controlling the fresh-state behavior of alkali-activated CPB mixtures (Snyder et al., 2003; Zhu et al., 2018).

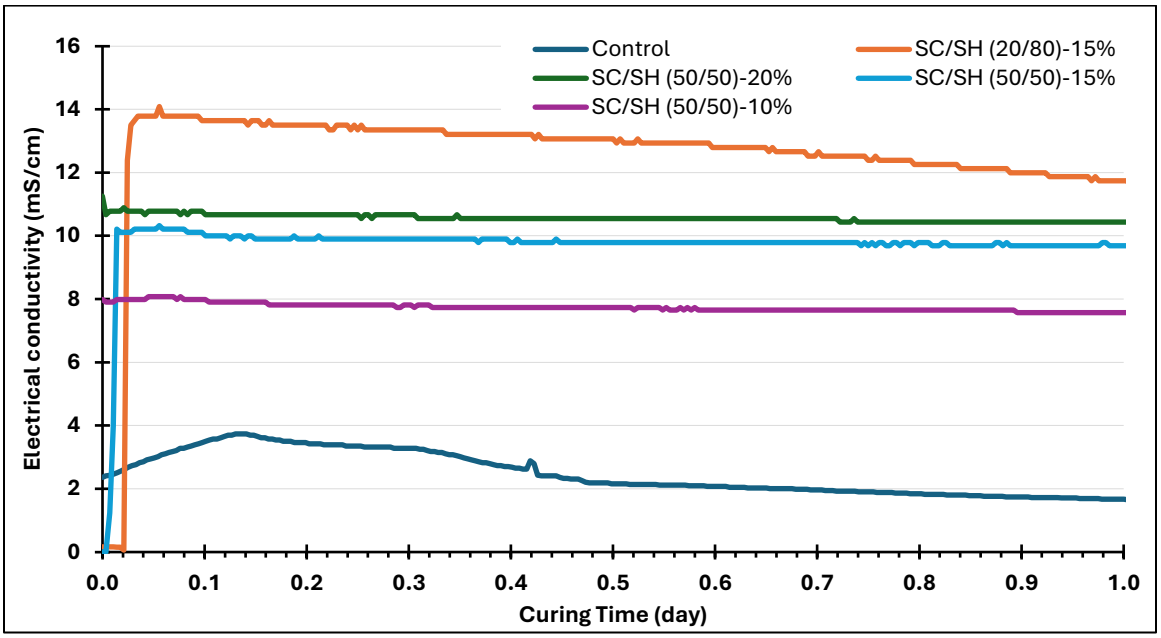

Figure 5.6. Electrical conductivity of AA-TC-CPBs and Portland cement CPB mixtures during the first 24 h of curing.

5.3.1.6 Volumetric Water Content (VWC) Monitoring Results

The volumetric water content (VWC) of CPB mixtures was continuously monitored during the first 24 h of curing to evaluate early-age water availability and consumption as a function of activator chemistry and dosage. The mix compositions used for these measurements are presented in Table 5.4, and the corresponding results are shown in Figure 5.7.

Figure 5.7 shows the evolution of VWC for the Portland cement-based control and the SC/SH-activated systems up to 1 day of curing. Although VWC remains comparatively stable in all mixtures, indicating that most mixing water is retained within the paste during

the early hydration period, clear differences are observed in both absolute values and temporal trends depending on binder formulation.

The Portland cement control exhibits the lowest VWC values and a gradual decrease from approximately 0.45 to 0.35 m^3/m^3 over 1 day. This continuous reduction reflects the progressive consumption of free water during the formation of early hydration products, such as portlandite and ettringite, and is consistent with the rapid stiffening behavior typically observed in OPC-based systems at early ages (Lothenbach et al., 2011; Haruna and Fall, 2020).

In contrast, all SC/SH-activated binders maintain higher and more stable VWC values, ranging approximately between 0.57 and 0.66 m^3/m^3. The hydroxide-rich formulation, SC/SH (20/80)-15%, consistently exhibits the highest VWC throughout the monitoring period, suggesting delayed water consumption and the persistence of a larger free-water fraction within the pore network prior to extensive gel formation. This behavior is consistent with delayed binding of water during the early stages of slag activation under strongly alkaline conditions (Bernal et al., 2014; Ke et al., 2016).

Mixtures with balanced activator compositions, particularly SC/SH (50/50)-20%, display slightly lower VWC values and a modest downward trend over time. This behavior indicates enhanced slag dissolution and earlier formation of C-(A)-S-H and hydrotalcite-like phases, which progressively incorporate water into the developing microstructure. Lower activator dosages, such as SC/SH (50/50)-10%, show comparatively higher VWC retention, reflecting reduced reaction kinetics and delayed microstructural development at early ages (Ke et al., 2016; Bernal et al., 2013b).

Overall, VWC monitoring demonstrates that co-activation with sodium carbonate and sodium hydroxide plays a critical role in controlling early-age water dynamics in CPB-TC mixtures. Hydroxide-dominant systems retain more free water during the first hours of curing, whereas balanced SC/SH formulations promote moderate water consumption alongside controlled paste structuration. These trends are fully consistent with the electrical conductivity evolution discussed in Section 5.3.1.5 and the rheological behavior reported in Sections 5.3.1.1 and 5.3.1.2, highlighting the close coupling between water availability,

ionic activity, and early-age structural build-up in alkali-activated CPB systems (Zhu et al., 2018; Bernal et al., 2013b).

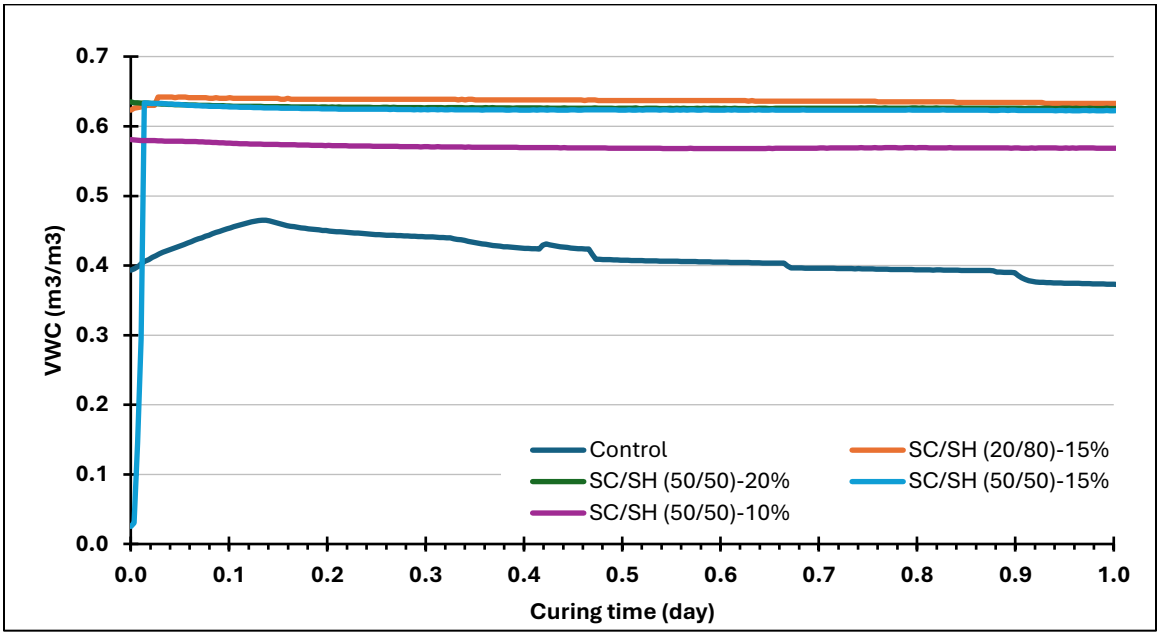

Figure 5.7. Volumetric water content (VWC) of AA-TC-CPBs and Portland cement-CPB mixtures during the first 24 h of curing.

5.3.2 Development of initial and final setting times of AA-TC-CPBs

The initial and final setting times of AA-TC-CPBs and Portland cement-CPB mixtures were determined to evaluate the influence of activator chemistry and dosage on early-age stiffening behavior and hydration kinetics. The mix compositions used for these tests are presented in Table 5.4, while the corresponding results are shown in Figure 5.8.

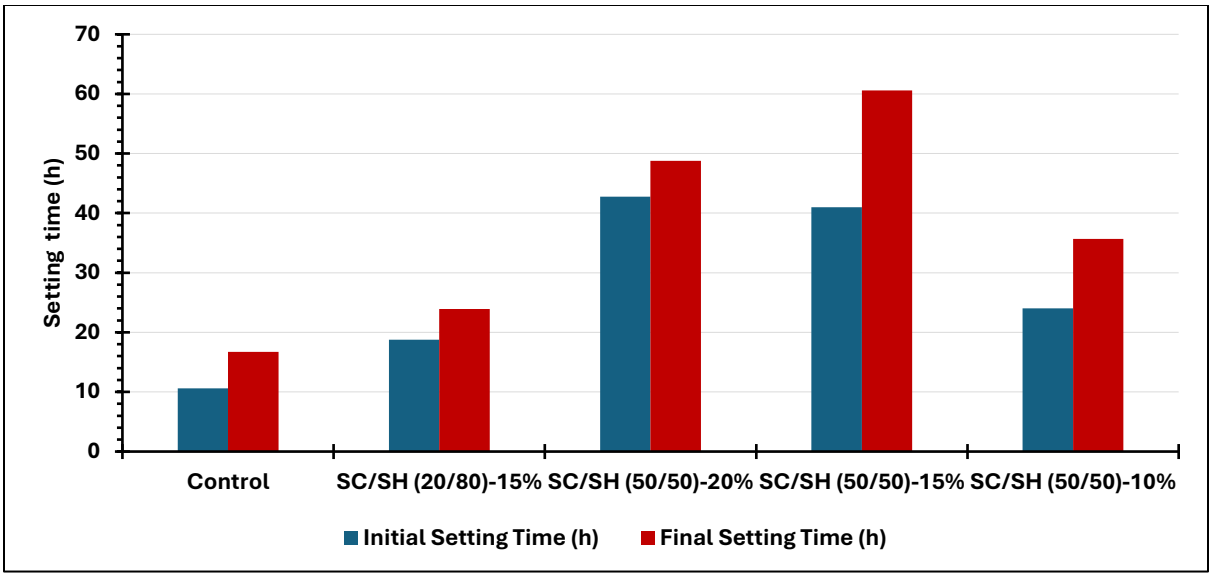

Figure 5.8. Initial and final setting times of AA-TC-CPBs and Portland cement-CPB mixtures

Figure 5.8 shows that both initial and final setting times are strongly governed by activator composition and dosage. Relative to the Portland cement-based reference, all SC/SH-activated mixtures exhibit significantly longer setting times, confirming that co-activation of slag with sodium carbonate and sodium hydroxide delays early paste structuration compared to ordinary Portland cement systems (Bernal et al., 2015; Ke et al., 2016).

The Portland cement control reaches initial and final setting at approximately 10 h and 17 h, respectively, which is consistent with typical OPC-based cemented paste backfill behavior and the rapid precipitation of ettringite and portlandite at early ages (Bullard et al., 2011; Sagade and Fall, 2024). These hydration products promote early network formation and rapid loss of workability.

Among the alkali-activated systems, the hydroxide-rich formulation SC/SH (20/80)-15% exhibits a moderate delay, with initial and final setting occurring at approximately 18 h and 25 h, respectively. This behavior reflects enhanced ionic activity and slag dissolution under high alkalinity, which accelerates early reactions relative to carbonate-rich systems but remains slower than OPC hydration (Li and Sun, 2000)

In contrast, mixtures with balanced activator compositions display the longest setting times. The SC/SH (50/50)-10% mixture reaches initial and final setting at approximately 22 h and 35 h, while SC/SH (50/50)-20% sets at around 42-43 h (initial) and 48-50 h (final). The SC/SH (50/50)-15% formulation exhibits the longest setting times, reaching initial and final set at approximately 40-41 h and around 60 h, respectively. This hierarchy indicates that the simultaneous presence of carbonate and hydroxide ions, combined with overall activator dosage, exerts a dominant control on the rate at which dissolved species are incorporated into solid reaction products (Bernal et al., 2015; Ke et al., 2016).

Mechanistically, carbonate-bearing formulations are characterized by buffered alkalinity, which lowers the initial pH and slows slag dissolution compared to hydroxide-rich systems (Bernal, 2016). In addition, the formation of transient carbonate phases (e.g., gaylussite and vaterite, Section 5.3.1.3) can temporarily immobilise Ca- and Na-bearing species, delaying the precipitation and percolation of C-(A)-S-H and LDH networks (Bernal et al., 2015; Ke et al., 2016). In the SC/SH (50/50) systems, sufficient OH^- availability sustains ionic activity (Section 5.3.1.5); however, in the presence of carbonate, complexation and ion pairing promote slower conversion of dissolved species into a continuous binding network, resulting in prolonged initial and final setting times.

Comparison with the monitoring results in Sections 5.3.1.5 and 5.3.1.6 further supports these interpretations. Mixtures exhibiting later setting times also show sustained electrical conductivity and near-constant volumetric water content at early ages, indicating delayed consumption of free ions and water as hydrates progressively form. The pronounced delay in final setting observed for SC/SH (50/50)-15% is therefore consistent with slow hydrate percolation under mixed-alkali activation conditions (Zhu et al., 2018; Bernal et al., 2013b).

Overall, co-activation with SC and SH enables tailorable setting behavior in AA-TC-CPB mixtures. Hydroxide-rich systems provide moderate delays while maintaining relatively rapid structuration, whereas balanced SC/SH formulations, particularly at 15-20% activator dosage, produce the longest setting periods. These mixtures offer extended placement windows while preserving controlled early-age structuration, which is

advantageous for underground backfilling operations requiring both pumpability and delayed stiffening.

5.4 Conclusions

This study investigated the early-age behavior of CPB prepared with ternary binder blends in which slag was co-activated using sodium carbonate (SC) and sodium hydroxide (SH). By combining rheological measurements, microstructural analyses, and electrochemical monitoring, the results demonstrate that activator chemistry and dosage govern both the kinetics and mechanisms of early paste structuration.

Hydroxide-rich systems (SC/SH = 20/80) promote rapid slag dissolution and early ionic availability, leading to faster build-up of yield stress and viscosity, as reflected by elevated electrical conductivity during the first hours of curing. In contrast, balanced co-activation (SC/SH = 50/50) delays early structuration, extends setting times, and provides improved workability and while maintaining controlled rheological evolution, particularly at intermediate activator dosages (15-20%). Under-activated mixtures, especially low-dosage carbonate-rich systems, exhibit limited slag dissolution, dominance of crystalline carbonate and sulfate phases, and slower reaction kinetics.

XRD results confirm that SC/SH co-activation fundamentally alters the early hydration pathway compared to Portland cement, suppressing portlandite formation and favouring the precipitation of carbonate-bearing AFm phases and hydrotalcite-like layered double hydroxides alongside an amorphous C-(A)-S-H gel. These microstructural features explain the electrochemical signatures observed during early curing and the corresponding rheological response of the CPB mixtures. Electrical conductivity and volumetric water content monitoring further show that later-setting systems retain a larger reservoir of pore solution ions and free water at early ages, whereas faster-structuring systems rapidly consume ions as hydration and precipitation proceed.

Overall, the results demonstrate that SC/SH co-activation offers a tunable strategy to balance pumpability, early stability, and setting behavior in slag-based CPB. Hydroxide-rich formulations are better suited for applications requiring rapid early strength development, while balanced SC/SH systems provide extended placement windows and

improved handling without compromising early structural integrity. These findings provide practical guidance for designing low-carbon CPB binders and highlight the potential of carbonate-hydroxide co-activation as a viable alternative to conventional Portland cement systems in underground backfilling operations.

5.5 References

Bernal SA. 2016. Advances in near-neutral salts activation of blast furnace slags. *RILEM Technical Letters*, 1, 39–44.

Bernal, S.A., Provis, J.L., Fernández-Jiménez, A., Krivenko, P.V., Kavalerova, E., Palacios, M., Shi, C., 2013a. Binder chemistry–high-calcium alkali-activated materials. In Alkali activated materials: state-of-the-art report, RILEM TC 224-AAM (pp. 59-91). Dordrecht: Springer Netherlands.

Bernal, S.A., Provis, J.L., Walkley, B., San Nicolas, R., Gehman, J.D., Brice, D.G., Kilcullen, A.R., Duxson, P. and van Deventer, J.S., 2013b. Gel nanostructure in alkali-activated binders based on slag and fly ash, and effects of accelerated carbonation. *Cement and Concrete Research*, *53*, 127-144.

Bernal, S.A., Provis, J.L., Myers, R.J., San Nicolas, R., van Deventer, J.S., 2015. Role of carbonates in the chemical evolution of sodium carbonate-activated slag binders. *Materials and Structures*, *48*(3), 517-529.

Brough AR, Atkinson A. 2002. Sodium silicate-based, alkali-activated slag mortars: Part I. Strength, hydration and microstructure. *Cement and Concrete Research*, 32, 865–879.

Bullard, J.W., Jennings, H.M., Livingston, R.A., Nonat, A., Scherer, G.W., Schweitzer, J.S., Scrivener, K.L., Thomas, J.J., 2011. Mechanisms of cement hydration. *Cement and concrete research*, *41*(12), 1208-1223.

Cui, L., Fall, M., 2018. Multiphysics modeling and simulation of strength development and distribution in cemented tailings backfill structures. *International Journal of Concrete Structures and Materials*, *12*(1), p.25.

Cui L, Fall M 2017. Multiphysics model for consolidation behavior of cemented paste backfill. *International Journal of Geomechanics*, *17*(3), 04016077.

Dai X, Gu X, Zheng J, Zhao L, Zhou L., Jiang H. 2023. Carbonate-activated binder modified by supplementary materials for mine backfill and the associated heavy metal immobilization effects. *International Journal of Minerals, Metallurgy and Materials*, *30*(8), 1548-1559.

Dai, X., Ren, L., Gu, X., Yilmaz, E., Fang, K., Jiang, H., 2022. Strength analysis and optimization of alkali activated slag backfills through response surface methodology. *Frontiers in Materials*, *9*, p.844608.

Fall, M., Célestin, J.C., Pokharel, M., Touré, M., 2010. A contribution to understanding the effects of curing temperature on the mechanical properties of mine cemented tailings backfill. *Engineering Geology*, *114*(3-4), pp.397-413.

Fang, Y., Zhuang, K., Zheng, D., Guo, W., 2023. The influence of alkali content on the hydration of the slag-based geopolymer: relationships between resistivity, setting, and strength development. *Polymers*, *15*(3), p.518.

Fang, K., Cui, L., Fall, M., 2020. A coupled chemo-elastic cohesive zone model for backfill-rock interface. *Computers and Geotechnics*, *125*, p.103666.

Fernández-Jiménez, A., Palomo, Á., 2005. Composition and microstructure of alkali activated fly ash binder: Effect of the activator. *Cement and concrete research*, *35*(10), 1984-1992.

Fernández-Jiménez A, Puertas F 2003. Effect of activator mix on the hydration and strength behaviour of alkali-activated slag cements. *Advances in Cement Research*, *15*(3), 129-136.

Gevaudan, J.P., Timounay, Y., Mayrhofer, L., Zarshenas, M., Moseler, M., 2024. How does the pore solution chemistry influence the passivation of reinforced alkali-and salt-activated slag materials?. *Journal of the American Ceramic Society*, *107*(3), 1625-1635.

Haruna, S., Fall, M., 2020. Time-and temperature-dependent rheological properties of cemented paste backfill that contains superplasticizer. *Powder Technology*, *360*, 731-740.

Heikal, M., Nassar, M.Y., El-Sayed, G., Ibrahim, S.M., 2014. Physico-chemical, mechanical, microstructure and durability characteristics of alkali activated Egyptian slag. *Construction and Building Materials*, *69*, 60-72.

Huang, L., Tang, L., Löfgren, I., Olsson, N., Yang, Z., 2022. Real-time monitoring the electrical properties of pastes to map the hydration induced microstructure change in cement-based materials. *Cement and Concrete Composites*, *132*, 104639.

Hunter RJ. 1981. *Zeta Potential in Colloid Science*. Academic Press, London.

Jiang, H., Fall, M., 2017. Yield stress and strength of saline cemented tailings in sub-zero environments: Portland cement paste backfill. *International Journal of Mineral Processing*, *160*, 68-75.

Jiao, Z., Wang, Y., Zheng, W., Huang, W., 2018. Effect of dosage of sodium carbonate on the strength and drying shrinkage of sodium hydroxide based alkali-activated slag paste. *Construction and Building Materials*, *179*, 11-24.

Ke X, Bernal SA, Provis JL. 2016. Controlling the reaction kinetics of sodium carbonate-activated slag cements using calcined layered double hydroxides. *Cement and Concrete Research*, 81, 24–37.

Klein K, Simon D. 2006. Effect of specimen composition on the strength development in cemented paste backfill. *Canadian Geotechnical Journal*, 43(3), 310–324.

Kou, Y., Jiang, H., Ren, L., Yilmaz, E.,Li, Y., 2020. Rheological properties of cemented paste backfill with alkali-activated slag. *Minerals*, *10*(3), 288.

Li, Y., Sun, Y., 2000. Preliminary study on combined-alkali–slag paste materials. *Cement and concrete research*, *30*(6), 963-966.

Lothenbach B, Scrivener K, Hooton RD. 2011. Supplementary cementitious materials. *Cement and Concrete Research*, 41, 1244–1256.

Lowke D, Gehlen C. 2017. The zeta potential of cement and additions in cementitious suspensions with high solid fraction. *Cement and Concrete Research*, 95, 195–204.

McCarter WJ, Chrisp TM, Starrs G. 1999. The early hydration of alkali-activated slag: developments in monitoring techniques. *Cement and Concrete Composites*, 21(4), 277-283.

Palacios, M., Alonso, M.M., Varga, C., Puertas, F., 2019. Influence of the alkaline solution and temperature on the rheology and reactivity of alkali-activated fly ash pastes. *Cement and Concrete Composites*, *95*, 277-284.

Provis JL, van Deventer JSJ. 2014. *Alkali-Activated Materials: State-of-the-Art Report, RILEM TC 224-AAM*. Springer, Dordrecht.

Sagade A, Fall M. 2024. Study of fresh properties of cemented paste backfill material with ternary cement blends. *Construction and Building Materials*, 411, 134287.

Scrivener KL, Snellings R, Lothenbach B. 2016. *A Practical Guide to Microstructural Analysis of Cementitious Materials*. CRC Press, Boca Raton.

Scrivener, K.L., John, V.M., Gartner, E.M., 2018. Eco-efficient cements: Potential economically viable solutions for a low-CO2 cement-based materials industry. *Cement and Concrete Research*, *114*, pp.2-26.

Shi C, Jiménez AF, Palomo A. 2011. New cements for the 21st century: the pursuit of an alternative to Portland cement. *Cement and Concrete Research*, 41, 750–763.

Snyder, K.A., Feng, X., Keen, B.D. and Mason, T.O., 2003. Estimating the electrical conductivity of cement paste pore solutions from OH−, K+ and Na+ concentrations. *Cement and Concrete Research*, *33*(6), 793-798.

Taylor HF. 1997. *Cement Chemistry*. 2nd ed. Thomas Telford, London.

Wang SD, Scrivener KL. 1995. Hydration products of alkali-activated slag cement. *Cement and Concrete Research*, 25, 561–571.

Wu D, Fall M, Cai SJ 2014. Numerical modelling of thermally and hydraulically coupled processes in hydrating cemented tailings backfill columns. *International Journal of Mining, Reclamation and Environment*, *28*(3), 173-199.

Xiao B, Fall M, Roshani A. 2020. Towards understanding the rheological properties of slag-cemented paste backfill. *International Journal of Mining, Reclamation and Environment*, 35(4), 268-290.

Xiapeng P, Fall M, Haruna S. 2019. Sulphate induced changes of rheological properties of cemented paste backfill. *Minerals Engineering*, *141*, 105849.

Zhu, X., Zhang, Z., Yang, K., Magee, B., Wang, Y., Yu, L., Nanukuttan, S., Li, Q., Mu, S., Yang, C., Basheer, M., 2018. Characterisation of pore structure development of alkali-activated slag cement during early hydration using electrical responses. *Cement and Concrete Composites*, *89*, 139-149.

Chapter 6: Synthesis of the Findings and Discussion

6.1 Introduction

This chapter provides an integrated synthesis of the experimental findings presented in Chapters 4 and 5, with the objective of consolidating the mechanical, physical, rheological, and microstructural insights obtained throughout this thesis. While the preceding chapters examined hardened and fresh-state properties separately, the present chapter brings these results together to establish coherent links between activation chemistry, early-age kinetics, microstructural development, and macroscopic performance of CPB formulated with alkali-activated slag binders.

Chapter 4 (Hardened properties) demonstrated that hybrid Na_2CO_3-NaOH (SC/SH) activation governs slag dissolution, gel precipitation, and long-term strength development. Results showed that mixtures with balanced activator ratios, especially SC/SH (50/50) at 10-15%, exhibited the most efficient hydration kinetics, characterized by rapid EC and VWC declines, high matric suction at late age, and refined pore structures dominated by C-(A)-S-H, hydrotalcite-like phases, and carbonate phases. These mixtures achieved the highest long-term UCS (≈1.6 MPa at 210 days), closely approaching the OPC control, confirming that hybrid activation can produce durable CPB as a low-carbon alternative with significantly reduced clinker content.

Chapter 5 (Fresh properties) showed that activator chemistry strongly influences early-age behavior relevant to transport and placement. Na_2CO_3-NaOH activation modified yield stress, viscosity, EC, and setting performance. Balanced SC/SH systems produced moderate initial viscosities, controlled structuration, and suitable setting times, while hydroxide-rich mixtures increased early stiffening and carbonate-rich mixtures prolonged workability. XRD, zeta potential, and EC monitoring confirmed that early behavior is driven by rapid ion release, carbonate buffering, and early formation of LDH and carbonate phases that shape interparticle interactions and rheological evolution.

Together, these two chapters highlight the continuity between fresh-state behavior during mixing and placement, and the subsequent mechanical performance once the backfill has hardened. The evolution of ionic activity, water consumption, pore refinement,

and phase assemblage are closely linked to both early rheology and long-term strength. A unified interpretation of these coupled processes is therefore required to guide rational mix design.

Accordingly, this chapter synthesizes the experimental evidence to (i) establish causal relationships between fresh-state kinetics and strength development, (ii) identify the key parameters controlling CPB performance across time scales, and (iii) translate the laboratory findings into practical implications for backfill design. The chapter also highlights the novel scientific contributions of this thesis and discusses the main limitations of the work, providing context for future research directions.

6.2 Synthesis and Integrated Interpretation of Fresh and Strength Results

6.2.1 Role of activator chemistry on early-age kinetics and fresh-state behavior

The fresh-state behavior of slag-based CPB systems is primarily governed by the chemistry of the alkaline activators, which controls early ionic reactivity, dispersion, and structural build-up. Results from Chapter 5 demonstrate that the relative proportions of sodium hydroxide and sodium carbonate strongly influence pore-solution chemistry and, consequently, rheology and setting behavior.

Hydroxide-rich systems (SC/SH (20/80)) generate a highly alkaline pore solution characterized by elevated electrical conductivity, promoting rapid slag dissolution and early nucleation of binding phases (Kou et al., 2020). These conditions lead to a steady increase in yield stress and viscosity during the first hours after mixing. The resulting fresh-state response is marked by faster structuration and shorter setting times, indicating a relatively rapid transition from a dispersed suspension to a mechanically coherent network.

In contrast, balanced SC/SH systems (50/50) exhibit buffered alkalinity due to the presence of carbonate species, which delays early reaction kinetics and nucleation of C-(A)-S-H gels (Li and Sun, 2000). The more negative zeta potential observed in these systems reflects enhanced colloidal stabilization and reduced interparticle attraction (Hunter, 1981; Lowke and Gehlen, 2017). This moderation of pore chemistry is evidenced by lower initial yield stress and viscosity, sustained EC plateaus, and nearly constant

volumetric water content during the first day. Carbonate-bearing formulations therefore remain more dispersed for longer periods, providing extended workable time and improved pumpability prior to setting. These observations highlight that activator chemistry offers a direct means of tuning early-age kinetics and fresh-state performance in CPB (Bernal, 2016; Jiao et al., 2018).

6.2.2 Transition from early structuration to hydrate development and pore refinement

Although fresh-state responses differ markedly at early ages, microstructural evidence indicates that adequately activated systems progressively converge toward similar hydration pathways. XRD results presented in Chapters 4 and 5 show that SC/SH activation suppresses the formation of portlandite and instead promotes early development of layered hydrates, including AFm hemicarbonate and hydrotalcite-like LDH, together with amorphous C-(A)-S-H gels (Wang and Scrivener, 1995; Bernal et al., 2015).

The precipitation of these phases marks the transition from early physico-chemical structuration to sustained hydrate growth and pore refinement. As hydration proceeds, dissolved ions are progressively incorporated into solid products, leading to a decrease in electrical conductivity and gradual binding of pore water (Wang and Scrivener, 1995). This evolution is accompanied by increasing matric suction and dry density, reflecting the development of a denser and more connected solid skeleton.

Under-activated systems, particularly those with low total activator dosage, deviate from this trend. Persistent inert phases such as quartz and dominant crystalline carbonate and sulfate phases indicate limited slag dissolution and delayed formation of binding gels (Ke et al., 2016). These microstructural features explain the slower structuration observed at early ages and foreshadow less efficient densification at later stages.

6.2.3 Coupling between fresh-state behavior and long-term strength development

The synthesis of fresh-state and hardened-state results demonstrates that early-age kinetics exert a lasting influence on long-term CPB performance (Fall et al., 2010). Fresh-state behavior determines how and when the solid network first forms, while the nature of

this early framework governs subsequent hydrate development, pore refinement, and strength gain.

Mixtures exhibiting controlled early structuration, rather than abrupt stiffening, tend to achieve superior long-term performance. Balanced SC/SH formulations illustrate this behavior most clearly: although their early-age yield stress and strength are lower than those of hydroxide-rich or OPC-based systems, their moderated kinetics favor progressive hydrate formation and sustained pore refinement. As shown in Chapter 4, this leads to lower porosity, higher dry density, and continuous strength gain at later ages (Bernal et al., 2015).

Conversely, systems that either stiffen too rapidly or remain under-activated fail to optimize this coupling. Rapid early reactions may compromise workability, while insufficient activation limits both early structuration and later strength development. These results confirm that fresh-state properties and hardened performance are intrinsically linked through the kinetics of slag activation and hydrate evolution and must therefore be considered jointly in CPB mix design (Kou et al., 2020; Fall et al., 2010).

6.3 Practical Implications for CPB Design

The integrated findings of this thesis provide clear guidance for the design of CPB using slag activated by blended sodium carbonate (SC) and sodium hydroxide (SH). By linking fresh-state behavior to long-term mechanical performance, the results enable rational selection of activator chemistry and dosage to meet operational constraints while ensuring adequate strength development.

From a placement and transport perspective, activator chemistry can be used to tailor workability and pumpability. Hydroxide-rich formulations (SC/SH 20/80) promote faster early structuration, as reflected by higher early yield stress and shorter setting times (Kou et al., 2020). Such mixes are suitable when early stability is required soon after placement, for example to limit deformation or segregation in steep stopes. However, the associated reduction in workable time necessitates careful control of mixing, transport duration, and pipeline shear conditions to avoid premature stiffening.

Balanced SC/SH formulations (50/50) provide a wider placement window, which is advantageous for long pipeline transport and complex underground layouts (Klein and Simon, 2006; Sagade and Fall, 2024). Their moderated early kinetics result in lower initial yield stress, slower viscosity build-up, and significantly delayed setting. At appropriate activator dosages (15 to 20%), these systems retain sufficient early cohesion while preserving pumpability, making them well suited for operations where extended handling time is critical. From an operational standpoint, this behavior can translate into reduced pumping energy demand, shorter pumping cycles, and a lower risk of pipeline blockage, thereby minimizing downtime associated with pipe flushing or de-clogging and reducing overall backfilling costs.

Activator dosage emerges as a second key design parameter. Adequate alkali content is required to ensure effective slag dissolution and early formation of binding phases. Under-activation, particularly at low dosages in balanced SC/SH systems, leads to delayed structuration, persistence of inert phases, and limited strength gain. Conversely, excessive alkalinity may accelerate early reactions without proportionate long-term benefits. The results therefore indicate that moderate dosages, combined with balanced SC/SH ratios, offer the most robust compromise between early handling requirements and later mechanical performance (Bernal, 2016; Jiao et al., 2018). Such optimization contributes to improved operational reliability by limiting unplanned stoppages linked to rapid stiffening and excessive rheological buildup during pumping.

The coupling between fresh-state behavior and hardened properties also highlights the importance of early-age monitoring for mix validation. Measurements of electrical conductivity, volumetric water content, and rheological parameters provide rapid indicators of whether a given formulation is likely to achieve the desired balance between workability and strength (Wang and Scrivener, 1995; Kou et al., 2020). Such tools can be used during laboratory qualification or pilot-scale trials to screen candidate mixes before field implementation, reducing technical risk and unnecessary operational costs.

Overall, the findings demonstrate that SC/SH co-activation enables flexible CPB design adapted to site-specific constraints (Bernal, 2016; Jiao et al., 2018). By adjusting the SC/SH ratio and total activator dosage, practitioners can tune early rheology, setting

time, and strength development in a controlled manner, thereby optimizing pumping efficiency, limiting maintenance interventions, and reducing reliance on Portland cement while maintaining operational reliability in underground mining environments.

6.4 Novel Research Contributions of the Thesis

This thesis makes several original contributions to the understanding and design of CPB formulated with alkali-activated slag binders. By integrating fresh-state characterization with hardened-state performance and microstructural analysis, the work advances both scientific knowledge and practical methodology for low-cement and cement-free backfill systems.

A first original contribution lies in the systematic evaluation of hybrid sodium carbonate/sodium hydroxide (SC/SH) activation in CPB under conditions representative of underground mining. While previous studies have examined alkali-activated slag pastes or mortars (Brough and Atkinson, 2002; Xiao et al., 2020), this thesis extends the investigation to realistic CPB mixtures incorporating tailings, high water contents, and curing regimes relevant to field practice. The results clarify how SC/SH co-activation modifies early kinetics, hydrate assemblage, pore refinement, and long-term strength development in backfill systems, addressing a gap between binder-focused studies and applied CPB research.

A second novel contribution is the explicit linkage established between fresh-state behavior and hardened performance. Through combined rheological measurements, setting-time tests, electrochemical monitoring (EC, VWC, zeta potential), and strength testing, the thesis demonstrates that early-age ionic reactivity and structuration govern subsequent microstructural evolution and strength gain. This integrated perspective moves beyond treating fresh and hardened properties as independent design targets and instead frames CPB performance as a continuous, time-dependent process controlled by activation chemistry.

Third, the thesis provides new insight into the role of carbonate-containing activation in CPB. The results show that sodium carbonate does not merely retard reactions (Fernández-Jiménez and Puertas, 2003; Bernal et al., 2015), but actively shapes hydration

pathways through carbonate buffering and the early formation of AFm hemicarbonate and hydrotalcite-like layered double hydroxides. When combined with sodium hydroxide at appropriate ratios and dosages, carbonate-bearing systems achieve controlled early structuration, progressive pore refinement, and sustained strength development. This finding refines current understanding of carbonate activation mechanisms in slag-based backfills and highlights conditions under which carbonation-related retardation can be beneficial rather than detrimental.

Another original contribution is the application of multi-parameter monitoring to characterize early-age behavior in CPB. Continuous EC and VWC measurements, coupled with rheology and microstructural observations, provide a comprehensive picture of ion consumption, water redistribution, and network formation during the first hours and days (Wang and Scrivener, 1995; Kou et al., 2020). This approach offers a practical framework for diagnosing early hydration behavior and for predicting longer-term performance based on early indicators, which has direct relevance for mix qualification and optimization.

Finally, the thesis contributes practical design guidance for low-carbon CPB systems. By identifying specific SC/SH ratios and activator dosages that balance pumpability, setting time, and strength development, the work provides actionable recommendations that can inform laboratory mix design and pilot-scale testing. These contributions collectively support the broader objective of reducing reliance on Portland cement in underground backfilling while maintaining operational safety and performance.

6.5 Limitations

Despite the comprehensive experimental program and integrated analysis presented in this thesis, several limitations should be acknowledged when interpreting the results and extending them to field applications.

First, all experiments were conducted under controlled laboratory conditions at approximately room temperature and without external confinement. In underground mining environments, CPB is subjected to variable thermal regimes, in-situ stresses, drainage conditions, and interactions with mine water chemistry. These factors can influence early-age kinetics, water redistribution, and long-term strength development, and

may alter the relative performance of different SC/SH formulations compared with laboratory observations (Fall et al., 2010).

Second, the monitoring of electrochemical and hydraulic parameters (electrical conductivity, volumetric water content, and zeta potential) was focused on early ages. While these measurements provided valuable insight into initial kinetics and structuration, extending continuous monitoring to longer curing periods would allow a more complete characterization of ion consumption, water binding, and phase evolution over time, particularly for systems exhibiting delayed reactions (Bernal, 2016).

Third, microstructural characterization relied primarily on qualitative X-ray diffraction analyses at selected ages. Although this approach successfully identified key crystalline phases and reaction pathways, quantitative phase analysis (e.g., Rietveld refinement with internal standards) and complementary techniques such as SEM-EDS or solid-state NMR would provide deeper insight into phase proportions, gel chemistry, and spatial distribution of hydrates.

Fourth, the scope of activator chemistry was limited to sodium carbonate and sodium hydroxide blends. Other hybrid systems, such as combinations involving sodium silicate or sulfate-based activators (Duxson et al., 2007; Bernal and Provis, 2014), were not considered and may offer additional opportunities to tailor kinetics, rheology, and long-term performance. Similarly, the influence of chemical admixtures commonly used in CPB practice (Haruna and Fall, 2020) was not addressed.

Finally, although the mixtures were designed to be representative of CPB used in underground mining, the results have not yet been validated at pilot or field scale. Scale effects related to mixing, pumping distance, shear history, and placement geometry may influence fresh-state behavior and early structuration in practice.

These limitations point to several directions for future work, including extended multi-parameter monitoring, quantitative microstructural analysis, broader activator systems, and field-scale validation. Addressing these aspects would further strengthen the applicability of alkali-activated slag binders for sustainable cemented paste backfill systems.

6.6 References

Bernal, S. A. 2016. “Advances in near-neutral salts activation of blast furnace slags.” *RILEM Technical Letters*, 1: 39–44. RILEM.

Bernal, S. A., J. L. Provis, R. J. Myers, R. San Nicolas, and J. S. J. van Deventer. 2015. “Role of carbonates in the chemical evolution of sodium carbonate-activated slag binders.” *Materials and Structures*, 48 (3): 517–529.

Brough, A. R., and A. Atkinson. 2002. “Sodium silicate-based, alkali-activated slag mortars: Part I. Strength, hydration and microstructure.” *Cement and Concrete Research*, 32 (6): 865–879.

Duxson, P., J. L. Provis, G. C. Lukey, and J. S. J. van Deventer. 2007. “The role of inorganic polymer technology in the development of ‘green concrete.’” *Cement and Concrete Research*, 37 (12): 1590–1597.

Fall, M., J. C. Célestin, M. Pokharel, and M. Touré. 2010. “A contribution to understanding the effects of curing temperature on the mechanical properties of mine cemented tailings backfill.” *Engineering Geology*, 114 (3): 397–413.

Fernández-Jiménez, A., and F. Puertas. 2003. “Effect of activator mix on the hydration and strength behaviour of alkali-activated slag cements.” *Advances in Cement Research*, 15 (3): 129–136.

Haruna, S., and M. Fall. 2020. “Time- and temperature-dependent rheological properties of cemented paste backfill that contains superplasticizer.” *Powder Technology*, 360: 731–740.

Hunter, R. J. 1981. *Zeta Potential in Colloid Science*. London: Academic Press.

Jiao, Z., Y. Wang, W. Zheng, and W. Huang. 2018. “Effect of dosage of sodium carbonate on the strength and drying shrinkage of sodium hydroxide based alkali-activated slag paste.” *Construction and Building Materials*, 179: 11–24.

Ke, X., S. A. Bernal, and J. L. Provis. 2016. “Controlling the reaction kinetics of sodium carbonate-activated slag cements using calcined layered double hydroxides.” *Cement and Concrete Research*, 81: 24–37.

Klein, K., and D. Simon. 2006. “Effect of specimen composition on the strength development in cemented paste backfill.” *Canadian Geotechnical Journal*, 43 (3): 310–324. NRC Research Press.

Kou, Y., H. Jiang, L. Ren, E. Yilmaz, and Y. Li. 2020. “Rheological Properties of Cemented Paste Backfill with Alkali-Activated Slag.” *Minerals*, 10 (3): 288. Multidisciplinary Digital Publishing Institute.

Li, Y., and Y. Sun. 2000. “Preliminary study on combined-alkali–slag paste materials.” *Cement and Concrete Research*, 30 (6): 963–966.

Lowke, D., and C. Gehlen. 2017. “The zeta potential of cement and additions in cementitious suspensions with high solid fraction.” *Cement and Concrete Research*, 95: 195–204.

Provis, J. L., and S. A. Bernal. 2014. “Geopolymers and related alkali-activated materials.” *Annual Review of Materials Research*, 44: 299–327. Annual Reviews.

Sagade, A., and M. Fall. 2024. “Study of fresh properties of cemented paste backfill material with ternary cement blends.” *Construction and Building Materials*, 411: 134287.

Wang, S.-D., and K. L. Scrivener. 1995. “Hydration products of alkali activated slag cement.” *Cement and Concrete Research*, 25 (3): 561–571.

Xiao, B., M. Fall, and A. Roshani. 2020. “Towards understanding the rheological properties of slag-cemented paste backfill.” *International Journal of Mining, Reclamation and Environment*, 35 (4): 268–290. Taylor & Francis.

Chapter 7: Conclusions and Recommendations for Future Studies

7.1 Key Conclusions Aligned with the Objectives

The primary objective of this thesis was to investigate the feasibility and performance of cemented paste backfill (CPB) formulated with slag activated by blended sodium carbonate and sodium hydroxide, with particular emphasis on the coupling between fresh-state behavior, hydration mechanisms, and strength development under conditions relevant to underground mining.

The results demonstrate that hybrid SC/SH activation provides an effective means of controlling early-age kinetics and long-term performance in slag-based CPB. Activator chemistry emerged as the dominant parameter governing the transition from a pumpable suspension to a mechanically stable backfill. Hydroxide-rich formulations promoted rapid ionic activity, accelerated slag dissolution, and faster early structuration, leading to shorter setting times and higher early stiffness. In contrast, balanced SC/SH systems exhibited moderated early kinetics, extended workable time, and delayed setting, while still achieving sustained strength gain at later ages when the activator dosage was sufficient.

The integration of fresh-state characterization with hardened-state measurements confirmed that rheological evolution, setting behavior, and electrochemical responses are intrinsically linked to subsequent microstructural development and pore refinement. Early formation of layered hydrates and amorphous C-(A)-S-H gels governs water redistribution and densification, which in turn controls unconfined compressive strength development. Mixtures that exhibited controlled early structuration rather than abrupt stiffening achieved more favorable long-term performance, highlighting the importance of balancing early kinetics with progressive hydrate growth.

Overall, the findings validate the central hypothesis of this thesis: slag-based CPB activated by blended sodium carbonate and sodium hydroxide can deliver tunable fresh-state behavior and mechanical performance compatible with geotechnical design requirements, while reducing reliance on Portland cement. Balanced SC/SH formulations at moderate activator dosages were identified as the most robust compromise between pumpability, setting control, and strength development.

7.2 Recommendations for Future Research

While this thesis provides a comprehensive laboratory-based assessment of SC/SH-activated slag CPB, several avenues for future research are recommended to further advance understanding and facilitate practical implementation.

First, future studies should investigate the influence of temperature, in-situ stress, and drainage conditions on fresh-state kinetics and strength development. These factors are expected to significantly affect hydration rates and water redistribution in underground environments and may alter the relative performance of different SC/SH formulations.

Second, extending multi-parameter monitoring beyond early ages would provide deeper insight into long-term ion consumption, water binding, and phase evolution. Coupling electrical, hydraulic, and mechanical monitoring over extended curing periods would improve the predictive capability of early-age indicators for long-term performance.

Third, quantitative microstructural characterization techniques, such as Rietveld refinement of XRD data, SEM-EDS, or solid-state NMR, should be incorporated to better quantify hydrate assemblages and gel chemistry. Such analyses would strengthen the mechanistic links between activator chemistry, microstructure, and macroscopic properties.

Fourth, the scope of activator systems could be expanded to include other hybrid combinations, such as sodium carbonate-sodium silicate or sodium hydroxide-sulfate systems, as well as the interaction of SC/SH activation with chemical admixtures commonly used in CPB practice.

Finally, pilot-scale and field-scale trials are essential to validate laboratory findings. Future work should focus on pipeline transport, large-scale mixing, and in-situ curing under realistic underground conditions to assess operational robustness and long-term performance.